MATHEMATICAL MODELLING FOR ANALYSING FIRE SPREAD IN A REAL-TIME COUPLED ATMOSPHERIC WILDLAND FIRE

BY

ZHIRI, Abraham Baba
MTech/SPS/2018/8027

DEPARTMENT OF MATHEMATICS FEDERAL UNIVERSITY OF TECHNOLOGY MINNA

JULY, 2021

ABSTRACT

Wildland fire spread is one of the most challenging problems faced by reserved or unreserved vegetation in many developed and developing nations, because it can lead to serious environmental hazards in claiming lives, properties, animals and some other valuable treasures. This thesis establishes an approximate analytical solution that is capable of analysing fire spread in a real-time coupled atmospheric wildland fire, in determining the effect of temperature, oxygen concentration, volume fraction of dry organic substance, volume fraction of moisture and volume fraction of coke. The analytical solution is obtained via direct integration and eigenfunction expansion technique, which depicts the influence of the parameters involved in the system. The effect of change in parameters values such as Frank-Kamenetskii number, Radiation number, Peclet energy number, Peclet mass number, Activation energy number and Equilibrium wind velocity are presented graphically and discussed. The results obtained show that Frank-Kamenetskii number reduces the temperature. Radiation number and Peclet energy number reduces the temperature, oxygen concentration and volume fraction of coke while they enhances volume fractions of dry organic substance and moisture. Activation energy number reduces the temperature and volume fraction of coke while it enhances volume fractions of dry organic substance and moisture. Also, Peclet mass number and Equilibrium wind velocity both enhance oxygen concentration. The inference drawn from this is that an increase in Radiation number will remove heat from the burning scene. Similarly, reducing wind velocity will limit the oxygen contact with fuel. With continuous supply of heat, the ignition of additional fuel will continue as long as there is enough oxygen present. Thus, it is obvious that these three elements (heat, fuel and oxygen) must be present before combustion can occur. Varying anyone of the elements will vary the intensity or otherwise of the fire. Armed with this knowledge, the fire fighters are better equipped to manage fire.

TABLE OF CONTENTS

LIST OF FIGURES

CHAPTER ONE

1.0 INTRODUCTION

1.1 Background to the Study

The term _wildfire‘ which also means wildland fire, rural fire or forest fire refers to an unplanned, unwanted or uncontrolled fire in an area of combustible vegetation occurring most likely in rural areas (Scott and Glasspool, 2006).

Forest fire ignition could be as a result of; human action (intentional) in clearing of land, extreme/intensive drought, in rare cases thunderstorm (lightning) and hunter‘s burning bush in search of wild animals. For both human, extreme/intensive drought and lightning-caused fires, there is a geographical gradient of fire ignition, mainly due to variations in climate and fuel composition but also to population density for instance. The timing of fires depends on their causes. In populated areas, the timing of human-caused fires is closely linked to human activities and peaks in the afternoon whereas, in remote areas, the timing of lightning-caused fires is more linked to weather conditions and the season, with most such fires occurring in summer. Better tools for modelling forest fire behaviour are important for managing fire suppression, planning controlled burns to reduce the fuels, as well as to help assess fire danger (Anne *et al.*, 2012).

Basically, there four types of fire models which are; surface fire, crown fire, spotting fire and ground fire. Surface fire models deals with the fire that burns the vegetation closed to the surface, such as brush, small trees, or herbaceous plants. Crown fire models are somewhat complementary to surface fire models and studied how the fire spreads over the canopy of trees in a given forest. Spotting fire models provides the equations to analyse those new fire caused by incandescent pieces of the main fire transported out of the main

fire perimeter. Finally, ground fire models focused their attention on those physical processes that occur in the substrate of the soil when a fire takes place (Carlos, 2014)

The greatest aim of any analysing system is to enable an end user to carry out useful and meaningful analysis. A useful analysis is one that helps the user achieve a particular aim. The field of wildland fire behaviour, aims primarily to stop the spread of the fire or to at least reduce its impact on life and property. The earliest efforts at wildland fire behaviour analysis concentrated on analysing the likely danger posed by a particular fire or set of conditions prior to the outbreak of a fire. These fire danger systems were used to assess the level of preparedness of suppression resources or to aid in the identification of the onset of bad fire weather for the purpose of calling total bans on intentionally lit fire (Perminov, 2018).

The forest fire are very complicated phenomena. At present, fire services can forecast the danger rating of or the specific weather elements relating to forest fire. There is need to understand and analyse forest fire initiation, behaviour and spread (Perminov, 2018).

It seems more promising to use methods of mathematical modeling that will allow taking into account the dynamics of this process in space and time.

1.2 Statement of the Research Problem

In global context, fire outbreak is becoming alarming due to intractable practice. Analysis of vegetation fire spread has been a challenge to researchers and managers for several decades, but in spite of the various models and fire behaviour forecasting systems that have been developed over the years as described by Sullivan (2009a, 2009b, 2009c), there is not yet a commonly accepted fire behaviour simulator that can be applied in operational conditions for large and complex fire. This is due to the complexity of the physical and

chemical processes that are involved in large-scale fire requiring a large number of input parameters that are not easy to obtain and physical models that are not yet fully developed. Physical models have been formulated mathematically and implemented in numerical codes like Grishin (1994), Albini (1996), Linn *et al.* (2002), Se´ro-Guillaume and Margerit (2002) and Mell *et al.* (2007). Nevertheless, practical applications of these models are not yet possible owing to large computational requirements and uncertainty regarding the description of key physical processes. Based on these scenarios, there is need for this study to broaden and sharpen the scope of what is already known about fire spread analysis and coupled atmospheric-wildland fire.

1.3 Significance of the Study

Wildland fire is one of the most complicated problems discovered worldwide and they cause a lot of havoc to biodiversity as well as local ecology. Fire spread is difficult to fight/combat in nature, yet it cannot be done away with, but can only be controlled, suppressed or managed. However, in a recent time, fire spread model gained more attention in order to enhance suppression rate. It is therefore important for us to widen our knowledge on wildland fire spread. Based on this, we present a mathematical model to analyse fire spread process, thus making the research significant.

1.4 Scope and Limitation

The thesis focuses on the mathematical model for analysing fire spread in a real-time coupled atmospheric-wildland fire. It is limited to approximate analytical simulation of the governing model equations.

1.5 Aim and Objectives

The aim of this research work is to establish an analytical solution that is capable of analysing fire spread in real-time coupled atmospheric-wildland fire.

The objectives of this study are to:

i. Formulate mathematical equations governing forest fire propagation.
ii. Obtain the analytical solution of the model using direct integration and eigenfunction expansion technique
iii. Provide the graphical representation of the solutions obtained.

1.6 Definition of Terms

Active crown fire: This occurs when the surface fire and crown fire are linked. Surface intensity is sufficient to ignite tree crowns, and fire spread and intensity in the tree crowns encourages surface fire spread and intensity.

Combustion: Is a flame speed which is the measured rate of expansion of the flame front in a combustible reaction.

Crown fire: This is a forest fire that spreads from treetop to treetop at great speed ahead of the ground fire.

Emissions: Is the production and discharge of gaseous substance into the atmosphere. **Fire:** Is a chemical reaction involving the bonding of oxygen with carbon or other fuel, with the production of heat and the presence of flame. **Firebrand:** Is a piece of burning wood.

Fire prediction: Is a way of forecasting the outbreak of fire.

Fire spread: Is the rate at which fire is propagated through radiation, convection and conduction.

Flame: A stream of burning vapour or gas, emitting light and heat.

Mass fire: Is a fire resulting from many simultaneous ignitions that generates a high level of energy output.

Modeling: Is the generation of a physical, conceptual or mathematical representation of a real phenomenon that is difficult to observe directly.

Peatbog fire: This is also known as underground or root fire, and it is a wildland fire caused by the burning of tree roots. This type of fire can burn for a great length of time, until its fuel is totally consumed or exhausted.

Running crown fire: Is the crown fire that covers the entire forest from the soil surface to the top of the tree crowns or passes through the trees and the underbrush, herbage and moss layer.

Solid fuel: Refers to various forms of solid material that can be burnt to release energy, providing heat and light through the process of combustion.

Surface fire: Is a forest fire that burns only the surface litter and undergrowth.

Suppression: Is an act of stoppage or reduction of fire spread.

Wildland fire: Is an unwanted or unplanned fire in an area of combustible vegetation.

Wind: Is the movement of atmospheric air usually caused by convection or differences in air pressure.

CHAPTER TWO

2.0 LITERATURE REVIEW

2.1 Forest Fire

A great deal of work has been done on the theoretical problem of how forest fire spread (Perminov, 2005). Forest fire models have been developed since 1940 to the present, but a lot of chemical and thermodynamic questions related to fire behaviour are still to be resolved. Forest fire are divided into underground (peatbog) fire, surface fire, active crown fire, running crown fire (also called independent crown fire), and mass fire (Grishin, 2002). The forest fire are a common occurrence in most parts of the world and they cause a lot of damage to biodiversity as well as to the local ecology. Wildland fire impact the lives of millions of people and cause major damage every year worldwide, yet they are a natural part of the cycle of nature. Better tools for modelling wildland fire behaviour are important for managing fire suppression, planning controlled burns to reduce the fuels, as well as to help assess fire danger. Fire models range from tools based on fire spread rate formulas, such as BehavePlus (Rothermel, 1972; Andrews, 2007). There have been several studies conducted on wildland fire to clarify and understand the consequences and then plans made to manage these vegetation fire.

Weber (1991) concentrated on physical wildland fire modelling and proposed a system by which models were described as physical, empirical or statistical, depending on whether they account for different modes of heat transfer, make no distinction between different heat transfer modes, or involve no physics at all. Pastor *et al*. (2003) proposed descriptions of theoretical, Empirical and semi-empirical, again depending on whether the model was based on purely physical understanding, of a statistical nature with no physical understanding, or a combination of both.

Clark *et al.* (1996a, b) concluded that, wildland fire is a complicated multiscale process, from the flame reaction zone on milimeter scale to the synoptic weather scale of hundreds of kilometers. Since direct numerical simulation of wildland fire is computationally intractable and detailed data are not available anyway, compromises in the choice of processes to be modelled, approximations, and parameterisation are essential. Fortunately, a practically important range of wildland fire behavior can be captured by the coupling of a mesoscale weather model with a simple 2-D fire spread model.

Clark *et al.* (1996a, b, 2004) found that weather has a major influence on wildland fire behavior; in particular, wind plays a dominant role in the fire spread. Conversely, fire influences the atmosphere through the heat and vapor fluxes from burning hydrocarbons and evaporation of fuel moisture. Fire heat output has a major effect on the atmosphere; the buoyancy created by the heat from the fire can cause tornadic strength winds, and the air motion and moisture from the fire can affect the atmosphere also away from the fire. It is well known that a large fire ―creates its own weather‖. The correct wildland fire shape and progress result from the two-way interaction between the fire and the atmosphere.

Grishin (1997) divided models into two classes, deterministic or stochastic-statistical. However, these schemes are rather limited given the combination of possible approaches and, given that describing a model as semi-empirical or semi-physical is a ‗glass half-full or half-empty' subjective issue, a more comprehensive and complete convection was required. Clark *et al.* (2004) noted that the horizontal wind right above the fireline may even be zero, and proposed to take the wind from a specified distance behind the fireline. Also, the strong heat flux from fire disturbs the logarithmic wind profile and the rate of spread as a function of wind at a specific altitude may not be a good approximation; rather, the fire spread may depend more strongly on the complete wind profile.

Mandel *et al.* (2009) combines the Weather Research and Forecasting Model (WRF) with the Air Refueling Wing (ARW) dynamical core Skamarock *et al.* (2008), with a semi-empirical fire spread model. It is intended to be faster than real time in order to deliver a good result of prediction and analysis.

2.2 Crown Fire

Crown fire is initiated by convective and radiative heat transfer from surface fire. However, convection is the main heat transfer mechanism. Crown fire are more difficult to control than surface fire. One of the first accepted methods for analysing crown fire was given by Rothermal (1991) and this semi-empirical model allows the collection of robust data regarding forest fire rates of spread as a function of fuel bulk and moisture, wind velocity and the terrain slope. However, these models use data for particular cases and do not give results for general fire conditions. Also, crown fire initiation and hazards have been studied and modelled in detail (Albini, 1985). Conditions for the start and spread of crown fire were studied by Van Wagner (1977). The discussion of the problems of modelling forest fire was provided by a group of co-workers at Tomsk University (Grishin, 1997).

The main results of these studies were presented by Grishin (1997) in his monograph. A mathematical model of forest fire obtained in this work is based on an analysis of known and original experimental data (Konev, 1977), and using concepts and methods from reactive media mechanics. The physical two-phase models used in (Morvan *et al.,* 2004) may be considered as a development and extension of the formulation proposed by Grishin (1997) and continuation of numerical modelling of wildfire initiation (Grishin and Perminov, 1998).

Currently, experimental research on the distribution of grass-roots and crown forest fire has been continued by Cruz *et al.* (2002). However, the investigation of crown fire initiation

has been limited mainly to cases without taking into account the interaction of crown forest fire with boundary layer of atmosphere. At present, a large amount of studies are focused on the firebrand generation and transport (Song *et al.,* 2017) at the same time there are many researches related to spread of forest fire because it is an important parameter used in the evaluation of hazards for fire safety applications. In the work of (Golner *et al.,* 2017) the problem of flame spread was revisited, with a particular emphasis on the effect of flow and geometry on concurrent flame spread over solid fuels. Despite the diversity of studies related to forest fire, there is currently no data on the dependence of the amount of combustion products emissions on forest characteristics and meteorological data. Typically, measurement data are used to estimate the volume of discarded combustion products, in particular, carbon oxides. As a rule, the calculations of Carbon dioxide (CO_2) release were based on the 2006 Intergovernmental Panel on Climate Change (IPCC) guidelines in the Agriculture, Forestry and Other Land Use (AFOLU) sector. For example, Geographic Information System (GIS) was applied as a key tool for implementing the spatial inventory of (CO_2) emissions and removals (Miphokasap, 2017). At the same time, Mickler *et al.* (2017) developed a method and approach to estimate above ground and below ground carbon emissions from a 2008 peatland wildfire by analyzing vegetation carbon losses from field surveys of biomass consumption which in turn, comes from the fire and soil carbon losses. In another approach, free-burning experimental fire were conducted in a wind tunnel to explore the role of ignition type and thus fire spread mode on the resulting emissions profile from combustion of fine Eucalyptus litter fuels (Surawski *et al*, 2015). However, these calculations can be used in estimating combustion product emissions for specific regions and in specific non-changing meteorological conditions. It seems more promising

to use methods of mathematical modelling that will allow taking into account the dynamics of this process in space and time.

2.3 Fire Spread Simulations

The ultimate aim of any fire spread simulation development is to produce a product that is practical, easy to implement and provide timely information on the progress of fire spread for wildland fire authorities. With the advent of cheap personal computing and the increased use of geographic information systems, the late 1980s and early 1990s saw a flourishing of methods to analyse and predict the spread of fire across the landscape (Beer, 1990). As the generally accepted methods of analysing the behaviour of wildland fire at that time were (and still are) one-dimensional models derived from empirical studies (Sullivan, 2007a), it was necessary to develop a method of converting the single dimension forward spread model into one that could spread the entire perimeter in two dimensions across a landscape. This involves two distinct processes: firstly, representing the fire in a manner suitable for simulation, and secondly, propagating that perimeter in a manner suitable for the perimeter‘s representation. Two approaches for the representation of the fire have been implemented in a number of softwares. The first treats the fire as a group of mainly contiguous independent cell that grows in number, described in the literature as a raster implementation. The second treats the fire perimeter as a closed curve of linked points, described in the literature as a vector implementation.

Mandel *et al.* (2008) analyzed a wildland fire model with data assimilation and used an ensemble ―Kalman‖ filter techniques with regularization to assimilate temperatures measured at selected points into running wildland fire simulations. It was recorded that, the assimilation technique is able to modify the simulations to track the measurements

correctly even if the assimilations were started with an erroneous ignition location that is quite far away from the correct one.

Lopes *et al.* (2017) addresses the problem of how wind should be taken into account in fire spread simulations, on the study of the effect of two-way coupling on the calculation of forest fire spread: model development. Their study was based on the software system Fire Station, which incorporates a surface fire spread model and a solver for the fluid flow (Navier–Stokes) equations. It was noted that, a two-way coupling method for fire behaviour prediction, where the buoyancy effects caused by the fire heat release are fully simulated. They concluded and described the underlying models for wind field and fire spread calculation.

2.4 Coupled Atmosphere-Wildland Fire Model

Barovik and Taranchuk (2010) used finite difference approximation method to study the mathematical modeling of running crown forest fires and observed that at any fixed equilibrium wind velocity, there is some critical moisture content value W > W* at which fire propagation stops due to the big losses of thermal energy on Combustible Forest Material (CFM) heating and drying. In practice, when fighting or localizing the combustion by spraying water, the conditions for fire extinction by moisture content parameter are artificially created. The obtained results of computations show that to create fire extinction conditions it is enough to increase the moisture content. Their model equations are

$$\frac{\partial \varphi_1}{\partial t} = \phi_{\varphi 1}(\varphi 1, T), \quad \frac{\partial \varphi_2}{\partial t} = \phi_{\varphi 2}(\varphi 2, T), \tag{2.1}$$

$$\frac{\partial \varphi_3}{\partial t} = \phi_{\varphi 3}(\varphi 1, \varphi 3, c1, c2, T), \quad \frac{\partial \varphi_4}{\partial t} = 0, \tag{2.2}$$

$$\frac{\partial c_1}{\partial t} + (V, gradc_1) - \frac{1}{\rho_5} div(\rho_5 D_T gradc_1) = \phi_{c1}(\varphi_1, \varphi_2, \varphi_3, c_1, c_2, T), \tag{2.3}$$

$$\frac{\partial c_2}{\partial t} + (V, gradc_2) - \frac{1}{\rho_5} div(\rho_5 D_T gradc_2) = \phi_{c2}(\varphi_1, \varphi_2, \varphi_3, c_1, c_2, T), \tag{2.4}$$

$$\frac{\partial T}{\partial t} + \frac{\rho_5 c_{p5}(V, gradT) - div(\lambda_T gradT)}{\rho_5 c_{p5} + \sum_{j=1}^{4} \rho_j \varphi_j c_{pj}} = \phi_T(\varphi_1, \varphi_2, \varphi_3, c_1, c_2, T), \tag{2.5}$$

where

$$\phi_{\varphi 1}(\varphi_1, T) = -\frac{R_1}{\rho_1}, \phi_{\varphi 2}(\varphi_2, T) = -\frac{R_2}{\rho_2}, \tag{2.6}$$

$$\phi_{\varphi 3}(\varphi_1, \varphi_2, \varphi_3, c_1, c_2, T) = \alpha_c \frac{R_1}{\rho_3} - \frac{M_c R_3}{(M_1 \rho_3)}, \tag{2.7}$$

$$\phi_{c1}(\varphi_1, \varphi_2, \varphi_3, c_1, c_2, T) = \frac{1}{\rho_5}\left(\kappa_{51} - c_1 Q - \frac{\alpha}{cp\,5\Delta h}(c_1 - c_{1\infty})\right), \tag{2.8}$$

$$\phi_{c2}(\varphi_1, \varphi_2, \varphi_3, c_1, c_2, T) = \frac{1}{\rho_5}\left(\kappa_{52} - c_2 Q - \frac{\alpha}{cp\,5\Delta h}(c_2 - c_{2\infty})\right), \tag{2.9}$$

$$\phi_T(\varphi_1, \varphi_2, \varphi_3, c_1, c_2, T) = \frac{q_5 R_5 - q_2 R_2 + q_3 R_3 - \frac{\alpha}{\Delta h}(T - T_\infty) - 4K_R \sigma T^4}{\rho_5 c_{p5} + \sum_{j=1}^{4} \rho_j \varphi_j c_{pj}}. \tag{2.10}$$

That is

$$
\begin{cases}
R_1 = k_{01}\rho\varphi_1 e^{\left(\frac{-E_1}{RT}\right)} \\
R_2 = k_{02}T^{\frac{1}{2}}\rho\varphi_2 e^{\left(\frac{-E_2}{RT}\right)} \\
R_3 = k_{03}s_\sigma\rho_5\varphi_3 c_1 e^{\left(\frac{-E_3}{RT}\right)} \\
R_{51} = -R_3 - 0.5R_5\frac{M_1}{M_2} \\
R_{52} = (1-\alpha_c)v_\Gamma R_1 - R_5
\end{cases}
\qquad (2.11)
$$

are the dependences describing the speed of CFM pyrolysis, drying, coke burning and chemical reactions in gas phase.

With initial and boundary conditions:

$$
\begin{cases}
T|_{t=0} = T_0(P),\ T(\pm\infty) = T_\infty; \\
c_1|_{t=0} = c_{10}(P),\ c_1(\pm\infty) = c_{1\infty}; \\
c_2|_{t=0} = c_{20}(P),\ c_2(\pm\infty) = c_{2\infty}; \\
c_3|_{t=0} = 1 - c_{10}(P) - c_{20}(P),\ c_3(\pm\infty) = 1 - c_{1\infty} - c_{2\infty}; \\
\varphi_1|_{t=0} = \varphi_{10}(P),\ \varphi_1(-\infty) = \varphi_{1K},\ \varphi_1(+\infty) = \varphi_{1H}; \\
\varphi_2|_{t=0} = \varphi_{20}(P),\ \varphi_2(-\infty) = \varphi_{2K},\ \varphi_2(+\infty) = \varphi_{2H}; \\
\varphi_3|_{t=0} = \varphi_{30}(P),\ \varphi_3(-\infty) = \varphi_{3K},\ \varphi_3(+\infty) = \varphi_{3H}; \\
\varphi_4|_{t=0} = 0.
\end{cases}
\qquad (2.12)
$$

Mandel *et al.* (2018) studied Coupled atmosphere-wildland fire modelling with WRF-Fire. They described the coupled atmosphere-fire model WRF-Fire, as they did not support canopy fire, although canopy fire collocated with ground fire is contained in Coupled Atmospheric Wildland Fire Environment (CAWFE). In a coupled model, however, the feedback on the fire is from the wind that is influenced by the fire.

Perminov (2018) worked on mathematical modeling of wildland fires initiation and spread using a coupled atmospheric-forest fire setting. The method of finite volume is used to

obtain discrete analogies. The boundary-value problem is solved numerically using the method of splitting according to physical processes. He estimated the amount of carbon dioxide and carbon monoxide emissions at crown forest fire spread.

Furthermore, the mathematical model gives an opportunity to describe the different conditions of crown forest fire spread taking into account different weather conditions, and state of forest combustible materials, which allows applying the given model for analysing and preventing fire. The results of calculation of the rate of crown forest fire are agreed with the laws of physics and experimental data (Grishin, 1997). Their model equations are

$$\frac{\partial \rho}{\partial t} + \frac{\partial}{\partial x_j}\left(\rho v_j\right) = Q, j = \overline{1, 3}, i = \overline{1, 3}; \quad (2.13)$$

$$\rho \frac{dv_i}{dt} = -\frac{\partial P}{\partial x_j} + \frac{\partial}{\partial x_j}\left(-\rho \overline{v_i' v_i'}\right) - \rho^{SC}{}_{d}{}^{v}{}_{i}\left|\vec{v}\right| - \rho g_i - Q v_i; \quad (2.14)$$

$$\rho c_p \frac{dT}{dt} = \frac{\partial}{\partial x_j}\left(-\rho c_p v_j' \overline{T'}\right) + q_5 R_5 - \alpha_v \left(T - T_s\right) + k_g \left(cU_R - 4\sigma T^4\right); \quad (2.15)$$

$$\rho \frac{dC_\alpha}{dt} = \frac{\partial}{\partial x_j}\left(-\overline{\rho v_i' c_\alpha'}\right) + R_{5\alpha} - Q c_\alpha, \alpha = 1, 2, 3; \quad (2.16)$$

$$\frac{\partial}{\partial x_j}\left(\frac{c}{3k}\frac{\partial U_R}{\partial x_j}\right) - kcU_R + 4k_s\sigma T^4 + 4k_q\sigma T^4 = 0; \quad (2.17)$$

$$k = k_g + k_s;$$

$$\sum_{i=1}^{4} \rho_i c_{pi} \varphi_i \frac{\partial T_s}{\partial t} = q_3 R_3 - q_2 R_2 - k_s \left(cU_R - 4\sigma T_s^4\right) + \alpha_v \left(T - T_s\right); \quad (2.18)$$

$$\rho_1 \frac{\partial \varphi_1}{\partial t} = -R, \rho_2 \frac{\partial \varphi_2}{\partial t} = -R, \rho_3 \frac{\partial \varphi_3}{\partial t} = \alpha R - \frac{M_c}{M_1} R, \rho_4 \frac{\partial \varphi_4}{\partial t} = 0; \quad (2.19)$$

$$\sum_{\alpha=1}^{4} c_\alpha = 1, P_e = \rho RT \sum_{\alpha=1}^{4} \frac{c_\alpha}{M_\alpha}, \bar{g} = (0, 0, -g). \quad (2.20)$$

Such that

$$\left.\begin{aligned} R_1 &= k_1 \rho \varphi_1 e^{\left(\frac{-E_1}{RT}\right)} \\ R_2 &= k_2 \rho T_2^{0.5} \varphi_{2s} e^{\left(\frac{-E_2}{RT}\right)} \\ R_3 &= k_3 \rho \varphi_3 s_\sigma c_1 e^{\left(\frac{-E_3}{RT}\right)} \\ R_5 &= k_5 M_2^{0.25} \left(\frac{c_2 M_1}{M_2}\right)^{\gamma} e^{\left(\frac{-E_5}{RT}\right)} \end{aligned}\right\} \quad (2.21)$$

With the initial values for volume of fractions of condensed phases that is determined using the expressions:

$$\varphi_{1e} = \frac{d(1 - v_z)}{\rho_1}, \varphi_{2e} = \frac{Wd}{\rho_2}, \varphi_{3e} = \frac{\alpha_c \varphi_{1e} \rho_1}{\rho_3} \quad . \quad (2.22)$$

Where

d is the bulk density for surface layer, v_z is the coefficient of ashes of forest fuel, W is the forest moisture content.

2.5 Summary of Review and Gap to Fill

In reviewing the above literatures, we observed that, several works have been carried out on wildland fire. Some authors worked on fire spread model without considering coupled atmospheric fire. Others concentrated on coupled atmospheric-wildland fire and ignored fire spread analysis that incorporates diffusion. In forest fire spread, diffusion is rarely negligible, and it is advisable to take it into account in analysis fire spread when fire outbreak takes place. Most authors simulated their models numerically. In view of the above, the present study is aimed at establishing an analytical solution capable of analysing

the volume fractions of dry organic substance, moisture, coke, oxygen concentration and temperature, by incorporating diffusion term in the process of fire spread in a real-time coupled atmospheric-wildland fire. This will be achieved via direct integration and eigenfunction expansion technique.

CHAPTER THREE

3.0 MATERIALS AND METHODS

3.1 Model Formulation

Following Perminov (2018), a wildfire model is formulated based on balance equations for energy and fuel, where the fuel loss due to burning corresponds to the fuel reaction rate. In formulating our model, the following assumptions were made;

i. the forest during a forest fire is considered as a multi-scale, multi-physics problem.

ii. the environment is considered to be a five-phase porous medium, consisting of dry organic substance (matter), water in liquid state (moisture), solid pyrolysis product (coke), ash and gas phase.

iii. the gas phase is assumed to consist of oxygen only.

iv. pressure is considered constant.

v. wind velocity in the forest canopy is assumed constant.

vi. ash is neglected.

vii. thermal equilibrium between the gas and solid phase is considered.

Based on the above assumptions, the equations governing forest fires propagation is given as:

Volume fraction of dry organic substance

$$\frac{\partial \varphi_s}{\partial t} = -k_1 \varphi_s e^{-\frac{E_1}{RT}}. \tag{3.1}$$

Volume fraction of moisture

$$\frac{\partial \varphi_m}{\partial t} = -k_2 \varphi_m T^2 e^{-\frac{E_2}{RT}}. \tag{3.2}$$

Volume fraction of coke

$$\rho_c \frac{\partial \varphi_c}{\partial t} = \alpha \; k \rho \varphi \; e^{-\frac{E}{RT}} - \frac{M_c}{M_1} k \; S \rho \quad \varphi C \; e^{-\frac{E_3}{RT}}. \tag{3.3}$$

Mass concentration of oxygen

$$\rho_g \left(\frac{\partial C}{\partial t} + v \frac{\partial C}{\partial x} \right) = \frac{\partial}{\partial x} \left(\rho_g \nu_T \frac{\partial C}{\partial x} \right) - \frac{\alpha}{c_{pg} \Delta h} \left(C_{ox} - C_{ox\infty} \right) - \left(1 - \alpha_c \right) k_1 \rho_s \varphi_s C_{ox} e^{-\frac{E}{RT}} - k_2 \rho_m T^{\frac{1}{2}} \varphi_m C_{ox} e^{\frac{-E}{RT}} \left(\frac{M_c}{M_1} c_{ox} \varphi_c c_{ox} e^{-k_3 S \sigma \rho_g} \right)^{1+} e^{\frac{-E}{RT}} \tag{3.4}$$

Energy balance equation

$$\left(\phi \rho_g C_{pg} + (1-\phi) \sum_{i=1}^{s+m+c} \rho_i c_{pi} \varphi_i \right) \frac{\partial T}{\partial t} + \rho_q C_{pq} v \frac{\partial T}{\partial x} = \frac{\partial}{\partial x} \left(\lambda_T \frac{\partial T}{\partial x} \right) - \frac{\alpha}{\Delta h} \left(T - T_\infty \right) - 4 K_R \sigma T^4 - k_2 \rho_m q_2 T^{\frac{1}{2}} \varphi_m e^{\frac{-E_2}{RT}} + k_3 S_\sigma \rho_q q_3 \varphi_c C_{ox} e^{\frac{-E_3}{RT}}. \tag{3.5}$$

The initial and boundary conditions are formulated as:

$$\varphi_s (x, 0) = \varphi_{so}, \; \varphi_m (x, 0) = \varphi_{mo}, \; \varphi_c (x, 0) = \varphi_{co}, \; C_{ox} (x, 0) = C_{ox_o}, \; C_{ox} (0, t) = C_{ox_\infty}, \; C_{ox} (\mathrm{L}, t) = C_{ox\infty}, \; T (x, 0) = T_o, \; T (0, t) = T_\infty, \; T (\mathrm{L}, t) = T_\infty. \tag{3.6}$$

Where

φ_s is the volume fraction of dry organic substance

φ_m is the volume fraction of moisture

φ_c is the volume fraction of coke

C_{ox} is the concentration of oxygen

T is the temperature (in Kelvin)

x is a coordinate in the system of coordinates connected with the centre of an initial fire (distance)

t is the time

T_∞ is the unperturbed ambient temperature

k_1, k_2, k_3 pre- exponential factors of chemical reactions

E_1, E_2, E_3 activation energy of chemical reactions

C is the concentration

R is the universal gas constant

S_σ is the specific surface of the condensed product of pyrolysis (coke)

v is the equilibrium wind velocity vector

U is the reference velocity

λ_T is the turbulent thermal conductivity

$C_{ox\infty}$ is the unperturbed density of concentration of oxygen

P_i , $i = (s, m, c)$ is the i^{-th} phase density, that is

ρ_s is the density of dry organic substance

ρ_m is the density of moisture

ρ_c is the density of coke

ρ_g is the density of gas phase (a mix of gases)

Δh is the crown height

M_c is the molecular mass of carbon

M_1 is the mass of combustible forest material (CFM)

C_{pg} is the thermal capacity of a gas phase

q_2 ⎫ ⎧ heat effects of processes of evaporation of
burning q_3 ⎭

D_T is the diffusion coefficient

α is the coefficient of heat exchange between the atmosphere and a forest canopy

α_c is the coke number of combustible forest material (CFM)

σ is the Stefan-BoltzMann constant

K_R is the Integrated absorptance

C_{pi} , $i = (s, m, c)$ is the i^{-th} phase of thermal capacity

s is the dry organic substance

m is the moisture

c is the coke

ox is the oxygen (O_2)

We make additional assumption that C_{pi} , P_i are constant and equal for all species. Although these assumptions could be relaxed in the future, they considerably simplify the equation. Again, we assume $\sum_{i=1}^{s+m+c} \rho_i C_{pi} \varphi_i = \rho_g C_{pg}$.

3.2 Non – dimensionalisation

Here we non-dimensionalise the equation (3.1)– (3.6) using the following dimensionless variables.

$$x' = \frac{x}{L},\ t' = \frac{Ut}{L},\ v' = \frac{v}{U},\ \psi_1 = \frac{\varphi_s}{\varphi_{so}},\ \psi_2 = \frac{\varphi_m}{\varphi_{mo}},\ \psi_3 = \frac{\varphi_c}{\varphi_{co}},\ \phi = \frac{C_{ox_o} - C_{ox}}{C_{ox_o} - C_{ox\infty}},$$
$$\in = \frac{RT_0}{E},\ \theta = \frac{E(T - T_o)}{RT_o},\ f = \frac{E_1}{E_3},\ r = \frac{E_2}{E_3}. \qquad (3.7)$$

So, equation (3.7) becomes

$$\left.\begin{array}{l} x = x'L, \quad \varphi_s = \varphi_{so}\psi_1, \quad \varphi_m = \varphi_{mo}\psi_2, \quad \varphi_c = \varphi_{co}\psi_3, \quad C_{ox} = [C_{ox_o} - C_{ox_\infty}]\phi + C_{ox_\infty} \\ T = T_0(1+\in\theta), \quad t = \dfrac{t'L}{U}, \quad v = v'U, \quad E_1 = fE_3, \quad E_2 = rE_3. \end{array}\right\} \quad (3.8)$$

Now we have,

$$\left.\begin{array}{l} \partial\varphi_s = \varphi_{so}\partial\psi_1, \quad \partial\varphi_m = \varphi_{mo}\partial\psi_2, \quad \partial\varphi_c = \varphi_{co}\partial\psi_3, \quad \partial C_{ox} = [C_{ox_o} - C_{ox_\infty}]\partial\phi \\ \partial T = \in T_o\partial\theta, \quad \partial t = \overset{L}{\quad}\partial t', \quad \partial x = L\partial x', \quad e^{\frac{-E_1}{RT}} = e^{\frac{-fE_3}{RT_o}\frac{f\theta}{1+\in\theta}}, \quad e^{\frac{-E_2}{RT}} = e^{\frac{-rE_3}{RT_o}\frac{r\theta}{1+\in\theta}} \\ e^{\frac{-E_3}{RT}} = e^{\frac{-E_3}{RT_o}\frac{\theta}{1+\in\theta}}. \end{array}\right\} \quad (3.9)$$

Then equation (3.1) becomes

$$\frac{U\varphi_{so}\partial\psi_1}{L\partial t'} = -k_1\varphi_{so}\psi_1 e^{\frac{-fE_3}{RT_o}\frac{f\theta}{1+\in\theta}}, \quad (3.10)$$

that is,

$$\frac{\partial\psi_1}{\partial t'} = \frac{-k_1 L\psi_1 e^{\frac{-fE_3}{RT_o}\frac{f\theta}{1+\in\theta}}}{U}, \quad (3.11)$$

dropping prime, we have

$$\frac{\partial\psi_1}{\partial t} = -a\psi_1 e^{\frac{f\theta}{1+\in\theta}}. \quad (3.12)$$

Where,

$$a = \frac{k_1 L e^{\frac{-fE_3}{RT_o}}}{U}. \quad (3.13)$$

Equation (3.2) becomes

$$\frac{U\varphi_{mo}\partial\psi_2}{L\partial t'} = -k_2\varphi_{mo}T_{o2}^{\frac{1}{}}(1+\in\theta)_2^{\frac{1}{}} e^{\frac{-rE_3}{RT_o}\psi_2}{}^{\frac{r\theta}{1+\in\theta}}, \quad (3.14)$$

that is,

$$\frac{\partial \psi_2}{\partial t'} = \frac{-k_2 T_0^{\frac{1}{2}} \left(1+\in\theta\right)^{\frac{1}{2}} L e^{\frac{-rE_3}{RT_o}} \psi_2 e^{\frac{r\theta}{1+\in\theta}}}{U}, \tag{3.15}$$

dropping prime, we have

$$\frac{\partial \psi_2}{\partial t} = -b\psi_2 \left(1+\in\theta\right)^{\frac{1}{2}} e^{\frac{r\theta}{1+\in\theta}}. \tag{3.16}$$

Where,

$$b = \frac{k T^{\frac{1}{2}} L e^{\frac{-rE_3}{RT_0}}}{U}. \tag{3.17}$$

Equation (3.3) becomes

$$\frac{U \rho_c \varphi_{c0} \partial \psi_3}{\partial t} = \alpha k \rho \varphi e^{\frac{-fE_3}{RT_o}} \psi e^{\frac{f\theta}{1+\in\theta}} - \left\{ \frac{M_c k S \rho \varphi}{M_1} \left[C - C \right] \phi + C \right) e^{\frac{-E}{RT_o}} \psi e^{\frac{\theta}{1+\in\theta}} \right\}, \tag{3.18}$$

that is,

$$\frac{\partial \psi_3}{\partial t'} = \frac{\alpha k \rho \varphi L e^{\frac{-fE_3}{RT_o}} \psi e^{\frac{f\theta}{1+\in\theta}}}{U \rho_c \varphi_{c0}} - \left\{ \frac{M_c k_3 S_\sigma \rho_g L \left(C_{0x0} - C_{ox\infty}\right)}{M_1 U \rho_c} \left[\phi + \frac{C}{C - C} \right] e^{\frac{-E_3}{RT_o}} \psi e^{\frac{\theta}{1+\in\sigma}} \right\}, \tag{3.19}$$

dropping prime, we obtain

$$\frac{\partial \psi_3}{\partial t} = \beta \psi_1 e^{\frac{f\theta}{1+\in\theta}} - \gamma \left(\phi + q\right) \psi_3 e^{\frac{\theta}{1+\in\theta}}. \tag{3.20}$$

Where,

$$\beta = \frac{\alpha_c \kappa_1 \rho_s \varphi_{so} L e^{\frac{-fE_3}{RT_o}}}{U \rho_c \varphi_{co}}$$

$$\gamma = \frac{M_c k_3 S_\sigma \rho_q L_{RT}}{M_1 U \rho_c} (C_{ox_o} - C_{ox_\infty}) e^{\frac{-E_3}{o}} \quad (3.21)$$

$$q = \frac{C_{ox_\infty}}{C_{ox_o} - C_{ox_\infty}}.$$

Equation (3.4) becomes

$$\rho_g \left(\frac{U \left[C_{ox_o} - C_{ox_\infty} \right] \partial\phi}{L \partial t'} + \frac{Uv' \left[C_{ox_o} - C_{ox_\infty} \right] \partial\phi}{L \partial x'} \right) = \frac{\partial}{L \partial x'} \left(\rho_{gT} D \left[C_{ox_o} - C_{ox_\infty} \right] \frac{\partial\phi}{L \partial x'} \right) -$$

$$\left(\frac{\alpha}{C_{pg} \Delta h} \left(\left[C_{ox_o} - C_{ox_\infty} \right] \phi + C_{ox_\infty} - C_{ox_\infty} \right) - 1 - \alpha_{(c)1} k_s \rho_{so} \varphi_{(C_{ox_o} - C_{ox_\infty})} \left(\frac{C_{ox_\infty}}{C_{ox_o} - C_{ox_\infty}} \right) \left(\frac{-fE}{RT_o} \right) \frac{f\theta}{e^{1+\in\theta}} \right) \right.$$

$$\left. -k_2 \rho_{mo}^{\frac{1}{2}} T^{\frac{1}{2}} \left(1+\in\theta \right)^{\frac{1}{2}} \varphi\psi C_{ox_o} - C_{ox_\infty} \left(\phi + \frac{C_{ox_\infty}}{C_{ox_o} - C_{ox_\infty}} \right) e^{\frac{E}{RT_o}} e^{\frac{1+\in\theta}{r\theta}} \right\},$$

$$-k_3 S_\sigma \rho_q \frac{M_c}{M_1} \left[C_{ox_o} - C_{ox_\infty} \right] \left(\phi + \frac{\frac{M_1}{M_c} + C_{ox_\infty}}{C_{ox_o} - C_{ox_\infty}} \right) \varphi_{co} \psi_3 \left(C_{ox_o} - C_{ox_\infty} \right) \left(\frac{C_{ox_\infty}}{C_{ox_o} - C_{ox_\infty}} \right) \left(\frac{-E}{e^{RT_o}} \frac{\theta}{e^{1+\in\theta}} \right) \quad (3.22)$$

that is,

$$\frac{\rho_g U\left[C_{ox_0}-C_{ox_\infty}\right]}{L}\left(\frac{\partial\phi}{\partial t'}+v'\frac{\partial\phi}{\partial x'}\right)=\frac{\rho_g}{L^2}\left(C_{ox_0}-C_{ox_\infty}\right)\frac{\partial}{\partial x'}\left(D_T\frac{\partial\phi}{\partial x'}\right)-$$

$$\frac{\alpha_c}{C_{pg}\Delta h\left(C_{ox_0}-C_{ox_\infty}\right)}\left(k_1\rho_s\varphi_{so}L\left(1-\alpha_c\right)\left(C_{ox_0}-C_{ox_\infty}\right)\left(\phi+\frac{C_{ox_\infty}}{C_{ox_0}-C_{ox_\infty}}\right)e^{\frac{-fE_3}{RT_o}}\cdot\frac{f\theta}{1+\epsilon\theta}\right.$$

$$-k_2\rho_s T^{\frac{1}{2}}\left(1+\epsilon\theta\right)^{\frac{1}{2}}\varphi_{mo}\psi_{mo}\left(C_{ox_0}-C_{ox_\infty}\right)\left(\phi+\frac{C_{ox_\infty}}{C_{ox_0}-C_{ox_\infty}}\right)e^{\frac{-rE_3}{RT_o}}e^{\frac{r\theta}{1+\epsilon\theta}}-$$

$$\left.k_3S_\sigma\rho_g\frac{M_c}{M_1}\left[C_{ox_0}-C_{ox_\infty}\right]\left[\phi+\frac{M_1+C_{ox_\infty}}{M_c\left(C_{ox_0}-C_{ox_\infty}\right)}\right]\varphi_{co}\psi_3\left(C_{ox_0}-C_{ox_\infty}\right)\left(\phi+\frac{C_{ox_\infty}}{C_{ox_0}-C_{ox_\infty}}\right)e^{\frac{-E_3}{RT_o}}e^{\frac{\theta}{1+\epsilon\theta}}\right) \quad (3.23)$$

So, it implies that,

$$\frac{\partial\phi}{\partial t'}+v'\frac{\partial\phi}{\partial x'}=\frac{\partial}{\partial x'}\left(D_T\frac{\partial\phi}{\partial x'}\right)-\frac{\alpha L}{C_{pg}\rho_g\Delta hU}\left(\phi-\left(\frac{e^{\frac{-fE_3}{RT_o}}}{\rho_g U}\left(\phi+\frac{C_{ox_\infty}}{C_{ox_0}-C_{ox_\infty}}\right)\psi_1 e^{\frac{f\theta}{1+\epsilon\theta}}\right)\right.\right.$$

$$\left.\left.-\frac{1}{2}\frac{\left(1+\epsilon\theta\right)^{\frac{1}{2}}}{\rho_g U}\left(\phi+\frac{C_{ox_\infty}}{C_{ox_0}-C_{ox_\infty}}\right)e^{\frac{-rE_3}{RT_o}}e^{\frac{r\theta}{1+\epsilon\theta}}-\right.\right.$$

$$\left.\left.\frac{k_3S_\sigma\rho_g\frac{M_c}{M_1}\left[C_{ox_0}-C_{ox_\infty}\right]L\varphi_{co}e^{\frac{-E_3}{RT_o}}\left(\phi+\frac{M_1+C_{ox_\infty}}{M_c\left(C_{ox_0}-C_{ox_\infty}\right)}\right)\left(\phi+\frac{C_{ox_\infty}}{C_{ox_0}-C_{ox_\infty}}\right)\psi_3 e^{\frac{\theta}{1+\epsilon\theta}}}{\rho_g U}\right)\right), \quad (3.24)$$

dropping prime, we have

$$\frac{\partial\phi}{\partial t}+v\frac{\partial\phi}{\partial x}=\frac{\partial}{\partial x}\left(D_1\frac{\partial\phi}{\partial x}\right)^{f\theta}-\beta_1\phi-\beta_2\psi_1\left(\phi+q\right)e^{1+\epsilon\theta}-\beta_3\left(1+\epsilon\theta\right)^{\frac{1}{2}}\psi_2\left(\phi+q\right)e^{1+\epsilon\theta}}^{\frac{r\theta}{}}$$

$$\left.-\beta_4\psi_3\left(\phi+p\right)\left(\phi+q\right)e^{\frac{\theta}{1+\epsilon\theta}}.\right| \quad (3.25)$$

Where,

$$
\left.
\begin{aligned}
D_1 &= \frac{D}{LU} = \frac{1}{P_{em}} \\
\beta_1 &= \frac{\alpha L}{C_{pg}\rho_g \Delta h U} \\
\beta_2 &= \frac{(1-\alpha)k_{c1}\rho_s \varphi_{so} L}{\rho_g U} e^{\frac{-fE_3}{RT_o}} \\
\beta_3 &= \frac{k_2 \rho_{mo} T_o^{\frac{1}{2}} \varphi_{mo} L e^{\frac{-rE_3}{RT_o}}}{\rho_g U} \\
\beta_4 &= \frac{k_3 S_\sigma \rho_g \frac{M_c}{M_1} \left[C_{ox_o} - C_{ox_\infty}\right] L \varphi_{co} e^{\frac{-E_3}{RT_o}}}{\rho_g U} \\
p &= \frac{\frac{M_1}{M_c} + C_{ox_\infty}}{C_{ox_o} - C_{ox_\infty}} \cdot \frac{\rho_{ox_o}}{\rho_{ox_\infty}}
\end{aligned}
\right\} \quad (3.26)
$$

We assume that the differences in temperature within the flow are such that T^4 can be expressed as a linear combination of the temperature; we expand T^4 in Taylor series about T_o as follows:

$$T^4 = T^4_o + 4T^3_o (T - T_o) + 6T^2_o (T - T_o)^2 + \ldots \quad (3.27)$$

and neglecting higher order terms beyond the first degree in $(T - T_o)$ we have

$$T^4 = -3T^4_o + 4T^3_o T \quad (3.28)$$

$$T^4 = -3T^4_o + 4T_o^4 (1 + \in \theta) \quad (3.29)$$

$$T^4 = -3T^4_o + 4T_o^4 + 4T_o^4 \in \theta \quad (3.30)$$

$$T^4 = T^4_o\left(1+4\in\theta\right). \tag{3.31}$$

Equation (3.5) becomes

$$\rho_g C_{pg}\left(\frac{\partial T}{\partial t}+v\frac{\partial T}{\partial x}\right)=\frac{\partial}{\partial x}\left(\lambda_T\frac{\partial T}{\partial x}\right)-\frac{\alpha}{\Delta h}\left(T-T_\infty\right)-4K_R\sigma T^4 \quad -k_2\rho_m q_2 T^{\frac{1}{2}}\varphi_m e^{\frac{-E_2}{RT}}, \tag{3.32}$$
$$+k_3 S_\sigma \rho_g q_3 \varphi_c C_{0x} e^{\frac{-E_3}{RT}}$$

that is,

$$\rho_g C_{pg}\left(\frac{U\in T\,\partial\theta}{L\partial t'}+\frac{Uv'\in T\,\partial\theta}{L\partial x'}\right)=\frac{\partial}{L\partial x'}\left(\lambda\frac{\in T\partial\theta}{L\partial x'}\right)-\frac{\alpha}{\Delta h}\left(T_o\left(1+\in\theta\right)-T_\infty\right)$$
$$-4K_R\sigma\left(T^4_o\left(1+4\in\theta\right)\right)-k_2\rho_m q_2\left(T_o^{\frac{1}{2}}\left(1+\in\theta\right)^{\frac{1}{2}}\varphi_{mo}e^{\frac{-rE}{RT_o}}\psi_2 e^{\frac{r\theta}{1+\in\theta}}\right) \tag{3.33}$$
$$+k_3 S_\sigma \rho_g q_3 \varphi_{co}\left(C_{ox_o}-C_{ox_\infty}\right)\left(\phi+\frac{C_{ox_\infty}}{C_{ox_o}-C_{ox_\infty}}\right)e^{\frac{-E_3}{RT_o\psi_3}}e^{\frac{\theta}{1+\in\theta}}.$$

It implies that,

$$\frac{\rho C_{pg} U\in T_o}{L}\left(\frac{\partial\theta}{\partial t'}+v'\frac{\partial\theta}{\partial x'}\right)=\frac{\partial}{L\partial x'}\left(\lambda\frac{\in T\partial\theta}{L\partial x'}\right)-\frac{\alpha}{\Delta h}\left(T_o\left(1+\in\theta\right)-T_\infty\right)$$
$$-4K_R\sigma\left(T^4_o\left(1+4\in\theta\right)\right)-k_2\rho_m q_2\left(T_o^{\frac{1}{2}}\left(1+\in\theta\right)^{\frac{1}{2}}\varphi_{mo}e^{\frac{-rE}{RT_o}}\psi_2 e^{\frac{r\theta}{1+\in\theta}}\right), \tag{3.34}$$
$$+k_3 S_\sigma \rho_g q_3 \varphi_{co}\left(C_{ox_o}-C_{ox_\infty}\right)\left(\phi+\frac{C_{ox_\infty}}{C_{ox_o}-C_{ox_\infty}}\right)e^{\frac{-E_3}{RT_o\psi_3}}e^{\frac{\theta}{1+\in\theta}}$$

that is,

$$\frac{\partial\theta}{\partial t'}+v'\frac{\partial\theta}{\partial x'}=\frac{\partial}{\partial x'}\left(\frac{\lambda_T}{L\rho_{g_{pg}}C_U}\frac{\partial\theta}{\partial x'}\right)-\frac{\alpha L}{\rho_{g_{pg}}C_U\Delta h}\left(\theta+\frac{T_o-T_\infty}{\in T_o}\right)$$

$$-\frac{4K_R\sigma L\left(T_o^3(1+4\in\theta)\right)}{\rho_q C_{pq}\in U}-\frac{k_2\rho_m q_2\left(T_o^{\frac{1}{2}}(1+\in\theta)^{\frac{1}{2}}L\varphi_{mo}e^{\frac{-rE}{RT_o}}\right)}{\rho_q C_{pq}\in T_oU}\psi_2 e^{\frac{r\theta}{1+\in\theta}},$$

$$+\frac{k_3 S_\sigma\rho_g q_3\varphi_{co}L\left(C_{ox_o}-C_{ox_\infty}\right)}{\rho_g C_{pg}\in T_oU}\left(\phi+\frac{C_{ox}}{C_{ox_o}-C_{ox_\infty}}\right)\psi_3 e^{\frac{-E_3}{RT_o}\frac{\theta}{1+\in\theta}}$$

dropping prime, we have

$$\frac{\partial\theta}{\partial t}+v\frac{\partial\theta}{\partial x}=\frac{\partial}{\partial x}\left(\lambda_1\frac{\partial\theta}{\partial x}\right)-\alpha_1(\theta+\gamma_1)-R_a(1+4\in\theta)-\delta\psi_2(1+\in\theta)^{\frac{1}{2}}e^{\frac{r\theta}{1+\in\theta}}$$

$$+\delta_1\psi_3(\phi+q)e^{\frac{\theta}{1+\in\theta}}.$$

Where,

$$\lambda_1=\frac{\lambda_T}{L\rho_g C_{pg}U}=\frac{1}{P_e}$$

$$\alpha_1=\frac{\alpha L}{\rho_g C_{pg}U\Delta h}$$

$$R_a=\frac{4K_R\sigma LT_o^3}{\rho_g C_{pg}\in U}$$

$$\delta=\frac{k_2\rho_m q_2 T_o^{\frac{1}{2}}L\varphi_{mo}e^{\frac{-rE_3}{RT_o}}}{\rho_q C_{pq}\in T_oU}$$

$$\delta_1=\frac{k_3 S_\sigma\rho_g q_3\varphi_{co}L\left(C_{ox_o}-C_{ox_\infty}\right)^{\frac{-E_3}{RT_o}}}{\rho_g C_{pg}\in T_oU^e}$$

$$q=\frac{C_{ox}}{C_{ox_o}-C_{ox_\infty}}$$

$$\gamma_1=\frac{T_o-T_\infty}{\in T_o}.$$

(3.35)

(3.36)

(3.37)

Equation (3.6) becomes

$$\left.\begin{array}{l}\varphi_s(x,0)=\varphi_{so}\psi_1(x',0)=\varphi_{so}\\ i.e\\ \psi_1(x',0)=1\end{array}\right\}, \tag{3.38}$$

dropping prime, we have

$$\psi_1(x,0)=1. \tag{3.39}$$

$$\left.\begin{array}{l}\varphi_m(x,0)=\varphi_{mo}\psi_2(x',0)=\varphi_{mo}\\ i.e\\ \psi_2(x',0)=1\end{array}\right\}, \tag{3.40}$$

dropping prime, we have

$$\psi_2(x,0)=1. \tag{3.41}$$

$$\left.\begin{array}{l}\varphi_c(x,0)=\varphi_{co}\psi_3(x',0)=\varphi_{co}\\ i.e\\ \psi_3(x',0)=1\end{array}\right\}, \tag{3.42}$$

dropping prime, we have

$$\psi_3(x,0)=1\ . \tag{3.43}$$

$$\left.\begin{array}{l}C_{0x}(x,0)=\left(C_{0x_0}-C_{ox_\infty}\right)\phi(x',0)+C_{ox_\infty}=C_{ox_0}\\ i.e\\ C_{ox_o}-C_{ox_\infty}\end{array}\right\}, \tag{3.44}$$

dropping prime, we have

$$\phi(x,0)=1. \tag{3.45}$$

$$C_{ox}(0,t) = (C_{ox_0} - C_{ox_\infty})\phi(0,t) + C_{ox_\infty} = C_{ox_\infty}$$

i.e

$$C_{ox_0} - C_{ox_\infty} \quad (3.46)$$

dropping prime, we have

$$\phi(0,t) = 0 . \quad (3.47)$$

$$C_{ox}(L,t) = (C_{ox_0} - C_{ox_\infty})\phi(1,t) + C_{ox_\infty} = C_{ox_\infty}$$

i.e

$$C_{ox_0} - C_{ox_\infty} \quad (3.48)$$

dropping prime, we have

$$\phi(1,t) = 0 . \quad (3.49)$$

$$T(x,0) = T_0(1+\in\theta(x',0)) = T_0$$

i.e

$$\theta(x',0) = 0 \quad (3.50)$$

dropping prime, we obtain

$$\theta(x,0) = 0 . \quad (3.51)$$

$$T(0,t) - T_\infty = (1+\in\theta(0,t')) - T_\infty$$

i.e

$$\theta(0,t') = \frac{T_\infty - T_0}{\in T_0} = \sigma_1 \quad (3.52)$$

dropping prime, we obtain

$$\theta(0, t) = \sigma_1 . \tag{3.53}$$

$$\left.\begin{array}{l} T(\mathrm{L}, t) = T_o\left(1+\in\theta(1, t')\right) = T_\infty \\ i.e \\ \theta(1, t') = \dfrac{T_\infty - T_o}{\in T_o} = \sigma_1 \end{array}\right\}, \tag{3.54}$$

dropping prime, we have

$$\theta(1, t) = \sigma_1 . \tag{3.55}$$

Therefore, the dimensionless equations and the initial and boundary conditions are:

$$\left.\begin{array}{l} \dfrac{\partial \psi_1}{\partial t} = -a\psi_1 e_1^{\frac{f\theta}{1+\in\theta}} \\ \psi_1(x, 0) = 1 \end{array}\right\}, \tag{3.56}$$

$$\left.\begin{array}{l} \dfrac{\partial \psi_2}{\partial t} = -b\psi_2\left(1+\in\theta\right)^{\frac{1}{2}} e^{\frac{r\theta}{1+\in\theta}} \\ \psi_2(x, 0) = 1 \end{array}\right\}, \tag{3.57}$$

$$\left.\begin{array}{l} \dfrac{\partial \psi_3}{\partial t} = \beta\psi_1 e^{\frac{f\theta}{1+\in\theta}} - \gamma\left(\phi+q\right)\psi_3 e^{\frac{\theta}{1+\in\theta}} \\ \psi_3(x, 0) = 1 \end{array}\right\}, \tag{3.58}$$

$$\left.\begin{array}{l} \dfrac{\partial \phi}{\partial t} + v\dfrac{\partial \phi}{\partial x} = \dfrac{\partial}{\partial x}\left(D_1 \dfrac{\partial \phi}{\partial x}\right) - \beta_1\phi - \beta_2\psi_1\left(\phi+q\right)e^{\frac{f\theta}{1+\in\theta}} \\ -\beta_3\left(1+\in\theta\right)^{\frac{1}{2}}\psi_2\left(\phi+q\right)e^{\frac{r\theta}{1+\in\theta}} - \beta_4\psi_3\left(\phi+p\right)\left(\phi+q\right)e^{\frac{\theta}{1+\in\theta}} \\ \phi(x, 0) = 1, \quad \phi(0, t) = 0, \quad \phi(1, t) = 0 \end{array}\right\}, \tag{3.59}$$

$$\frac{\partial\theta}{\partial t}+v\frac{\partial\theta}{\partial x}=\frac{\partial}{\partial x}\left(\lambda_1\frac{\partial\theta}{\partial x}\right)-\alpha_1(\theta+\gamma_1)-R_a(1+4\in\theta)-\delta\psi_2(1+\in\theta)^{\frac{1}{2}r\theta}e^{1+\in\theta}+\delta_1\psi_3(\phi+q)e^{\frac{\theta}{1+\in\theta}} \quad (3.60)$$

$$\theta(x,0)=0,\ \theta(0,t)=\sigma_1,\ \theta(1,t)=\sigma_1.$$

3.3 Analytical Solution

In the limit of $\in\to 0$, let $D_1=Cons\tan t,\ \lambda_1=cons\tan t$ and following Ayeni (1978), e^{θ} can be approximated as:

$$e^{\theta}\approx 1+e-2\theta \quad (3.61)$$

and let,

$$\beta_2=a_2v,\ \beta_1=a_1v,\ \beta_3=a_3v,\ \delta_2=a_4v,\ \delta_3=a_5v,\ \delta_4=a_6v,\ b=a_7v,\ \gamma=a_8v,\ \beta=a_9v, \quad (3.62)$$

and similarly let,

$$\begin{aligned}\psi_1&=\psi_{10}+v\psi_{11}+\ldots\\ \psi_2&=\psi_{20}+v\psi_{21}+\ldots\\ \psi_3&=\psi_{30}+v\psi_{31}+\ldots\\ \phi&=\phi_0+v\phi_1+\ldots\\ \theta&=\theta_0+v\theta_1+\ldots\end{aligned} \quad (3.63)$$

Using (3.61), (3.62) and (3.63) in (3.56)—(3.60) we obtain the following equations

$$\frac{\partial\psi_{10}}{\partial t}+v\frac{\partial\psi_{11}}{\partial t}=-a_6(\psi_{10}+v\psi_{11})(1+f(e-2)(\theta_0+v\theta_1)), \quad (3.64)$$

$$\frac{\partial\psi_{20}}{\partial t}+v\frac{\partial\psi_{21}}{\partial t}=-a_7(\psi_{20}+v\psi_{21})(1+\in(\theta_0+v\theta_1))^{\frac{1}{2}}(1+r(e-2)(\theta_0+v\theta_1)), \quad (3.65)$$

$$\frac{\partial\psi_{20}}{\partial t}+v\frac{\partial\psi_{21}}{\partial t}=-a_7v(\psi_{20}+v\psi_{21})\left(1+\frac{1}{2}\in(\theta_0+v\theta_1+\ldots)\right)(1+r(e-2)(\theta_0+v\theta_1)), \quad (3.66)$$

$$\frac{\partial \psi_{20}}{\partial t} \quad \frac{\partial \psi_{21}}{\partial t} \qquad \left(\left(\frac{1}{2}\right)\frac{1}{2}\right)\qquad (3.67)$$

$$\frac{\partial \psi}{\partial t} + v\frac{\partial \psi}{\partial t} = a\,v\,\psi + v\psi\,1 + f\,e-2\,\theta + v\theta - \},\qquad (3.68)$$

$$a\,v\,\phi + v\phi + q\,\psi + v\psi 1 + e - 2\,\theta + v\theta$$

$$\frac{\partial \phi}{\partial t} + v\frac{\partial \phi}{\partial t} + v\left|\frac{\partial \phi}{\partial x}\frac{\partial \phi}{\partial x}\right| = \nu_1\left|\frac{\partial^2 \phi}{\partial x^2} + v\frac{\partial^2 \phi}{\partial x^2}\right| - \beta_1\left(\phi_0 + v\phi_1\right)$$

$$-a\,v\,\psi + v\psi\,\phi + v\phi + q\,1 + f\,e-2\,\theta + v\theta \qquad (3.69)$$

$$-a_2\,v\left|\left(\frac{1}{2}\right)\frac{1}{2}\right|\left(1 + r\,(e-2)(\theta_o + v\theta_1)\right)$$

$$-a\,v\left|\left(\phi_0 + v\phi_1\right) + q\right|\left(1 + r\,(e-2)(\theta_o + v\theta_1)\right)$$

$$\frac{\partial \theta}{\partial t} + v\frac{\partial \theta}{\partial t} + v\left|\frac{\partial \theta}{\partial x}\frac{\partial \theta}{\partial x}\right| = \lambda_1\left|\frac{\partial^2 \theta}{\partial x^2} + v\frac{\partial^2 \theta}{\partial x^2}\right| - \alpha_1\left(\left(\theta_o + v\theta_1\right) + \gamma_1\right) \qquad (3.70)$$

$$-R\;1+4\in\theta + v\theta - a\,v\,\psi + v\psi \quad \frac{1}{2}\in\theta + \frac{1}{2}\,v\theta \quad \frac{1+r}{(\theta_o + v\theta_1)}\,(e-2)\cdot$$

$$+ a_5\,v\,(\psi_{30} + v\psi_{31})\left((\phi_o + v\phi_1) + q\right)\left(1 + (e-2)(\theta_o + v\theta_1)\right).$$

Collecting the like powers of v in equations (3.64), (3.67), (3.68), (3.69) and (3.70) we have

v^o :

$$\frac{\partial \psi_{10}}{\partial t} = 0 \quad , \qquad (3.71)$$

$$\psi_{10}(x,0) = 1$$

$$\frac{\partial \psi_{20}}{\partial t} = 0 \quad , \qquad (3.72)$$

$$\psi_{20}(x,0) = 1$$

$$\left.\begin{aligned}&\frac{\partial \psi_{30}}{\partial t} = 0\\ &\psi_{30}(x,0) = 1\end{aligned}\right\}, \tag{3.73}$$

$$\left.\begin{aligned}&\frac{\partial \phi_o}{\partial t} = D_1 \frac{\partial^2 \phi_o}{\partial x^2} - \beta_1 \phi_o\\ &\phi_o(x,0) = 1,\ \phi_o(0,t) = 0,\ \phi_o(1,t) = 0\end{aligned}\right\}, \tag{3.74}$$

$$\left.\begin{aligned}&\frac{\partial \theta_o}{\partial t} = \lambda_1 \frac{\partial^2 \theta_o}{\partial x^2} - (4R_a \in + \alpha_1)\theta_o - (R_a + \alpha_1 \gamma_1)\\ &\theta_o(x,0) = 0,\ \theta_o(0,t) = \sigma_1,\ \theta_o(1,t) = \sigma_1.\end{aligned}\right\} \tag{3.75}$$

Similarly we have;

v^1 :

$$\left.\begin{aligned}&\frac{\partial \psi_{11}}{\partial t} = -a_6 \psi_{10}\left(1 + f(e-2)\theta_0\right)\\ &\psi_{11}(x,0) = 0\end{aligned}\right\}, \tag{3.76}$$

$$\left.\begin{aligned}&\frac{\partial \psi_{21}}{\partial t} = -a_7 \psi_{20}\left(1 + \frac{1}{2} \in \theta_0\right)(1 + r(e-2)\theta_o)\\ &\psi_{21}(x,0) = 0\end{aligned}\right\}, \tag{3.77}$$

$$\left.\begin{aligned}&\frac{\partial \psi_{31}}{\partial t} = a_9 \psi_{10}\left(1 + f(e-2)\theta_0\right) - a_8(\phi_o + q)\psi_{30}\left(1 + (e-2)\theta_0\right)\\ &\psi_{31}(x,0) = 0\end{aligned}\right\}, \tag{3.78}$$

$$\left.\begin{aligned}&\frac{\partial \phi_1}{\partial t} = D_1 \frac{\partial^2 \phi_1}{\partial x^2} - \beta_1 \phi_1 - \frac{\partial \phi_o}{\partial x} - a_1 \psi_{10}(\phi_o + q)\left(1 + f(e-2)\theta_o\right)\\ &- a_2\left(1 + \frac{1}{2} \in \theta_o\right)\psi_{20}(\phi_o + q)(1 + r(e-2)\theta_o) - a_3 \psi_{30}(\phi_o + p)(\phi_o + q)(1 + (e-2)\theta_o)\\ &\phi_1(x,0) = 0,\ \phi_1(0,t) = 0,\ \phi_1(1,t) = 0\end{aligned}\right\}, \tag{3.79}$$

$$\left.\begin{aligned}
&\frac{\partial\theta}{\partial t} = \lambda_1 \frac{\partial_2\theta}{\partial x^2} - (\alpha_1 + 4R_a\in)\theta_1 - \frac{\partial\theta_o}{\partial x} - a_4\psi_{20}\left(1 + \frac{1}{2}\in\theta_o + \ldots\right)\left(1 + r(e-2)\theta_o\right)\\
&+ a_5\psi_{30}(\phi_o + q)\left(1 + (e-2)\theta_o\right),\\
&\theta_1(x,0) = 0,\ \theta_1(0,t) = 0,\ \theta_1(1,t) = 0.
\end{aligned}\right\} \quad (3.80)$$

Solving equations (3.71), (3.72) and (3.73) via direct integration and applying the initial conditions we obtain respectively;

$$\psi_{10}(x,t) = 1, \quad (3.81)$$

$$\psi_{20}(x,t) = 1, \quad (3.82)$$

$$\psi_{30}(x,t) = 1. \quad (3.83)$$

We solve equations (3.74) and (3.75) using eigenfunction expansion technique. Now, we consider the problem (Myint-U and Debanth, 1987) and compare with equation (3.74)

$$\left.\begin{aligned}
&\frac{\partial u}{\partial t} = k\frac{\partial_2 u}{\partial x^2} + \alpha u + F(x,t),\\
&u(x,0) = f(x), \quad u(0,t) = 0, \quad u(L,t) = 0
\end{aligned}\right\}, \quad (3.84)$$

we assume

$$u(x,t) = \sum_{n=1}^{\infty} u_n(t)\sin\frac{n\pi}{L}x. \quad (3.85)$$

Where,

$$u_n(t) = \int_0^t e^{\left(\alpha - k\left(\frac{n\pi}{L}\right)^2\right)(t-\tau)} F_n(\tau)\,d\tau + b_n e^{\left(\alpha - k\left(\frac{n\pi}{L}\right)^2\right)t}, \quad (3.86)$$

$$F_n(t) = \frac{2}{L}\int_0^L F(x,t)\sin\frac{n\pi}{L}x\,dx, \quad (3.87)$$

$$b_n = \frac{2}{L}\int_0^L f(x)\sin\frac{n\pi}{L}x\,dx. \quad (3.88)$$

From equation (3.74), we have

$$u = \phi_o ,\ \ f(x) = 1, L = 1,\ \ k = D_1 ,\ \ \alpha = -\beta_1,\ \ F(x, t) = 0. \tag{3.89}$$

Thus,

$$b_n = 2\int_0^1 \sin n\pi x dx, \tag{3.90}$$

$$b_n = -\frac{2}{n\pi}\left[\cos n\pi x\right]_0^1 dx, \tag{3.91}$$

$$b_n = \frac{2}{n\pi}\left\lceil 1 - (-1)^n \right\rceil. \tag{3.92}$$

Also, since $F(x, t) = 0$ we have that,

$$F_n(t) = 0 . \tag{3.93}$$

Using (3.92) *and* (3.93) *in* (3.86) we obtain;

$$\phi_{on}(t) = \frac{2}{n\pi}\left\lceil 1 - (-1)^n \right\rceil e^{-c_1 t}, \tag{3.94}$$

where;

$$c_1 = \left(\beta_1 + D_1 (n\pi)^2\right). \tag{3.95}$$

Using (3.94) in (3.85) it becomes

$$\phi_o(x, t) = \sum_{n=1}^{\infty} A e^{-c_1 t} \sin n\pi x , \tag{3.96}$$

where;

$$A = \frac{2\left\lceil 1 - (-1)^n \right\rceil}{n\pi}, \tag{3.97}$$

then,

$$\frac{\partial \phi_0}{\partial x} = \sum_{n=1}^{\infty} n\pi A e^{-c_1 t} \cos n\pi x. \qquad (3.98)$$

Now, to solve (3.75), we need to transform the boundary conditions from non-homogeneous problem to homogeneous one. In doing this, we first find a function $\mu(x, t)$ which satisfies the boundary conditions. We note that;

$$\mu(x, t) = \alpha(t) + \frac{x}{L}(\beta(t) - \alpha(t)). \qquad (3.99)$$

Equation (3.99) does the trick of transformation. We then, make the change of variables as follows;

$$\theta_o(x, t) = H(x, t) + \mu(x, \qquad (3.100)$$

t). From equation (3.75) we have

$$\alpha(t) = \sigma_1 t^o, \ \beta(t) = \sigma_1 t^o, \ L = 1. \qquad (3.101)$$

Then,

Using (3.101) in (3.99) we obtain

$$\mu(x, t) = \sigma_1 t^o + x(\sigma_1 - \sigma_1) t^o, \qquad (3.102)$$

$$\mu(x, t) = \sigma_1 t^o. \qquad (3.103)$$

That is, differentiating (3.100) with respect to t we have

$$\frac{\partial \theta}{\partial t}^o = \frac{\partial H}{\partial t} + \frac{\partial \mu}{\partial t}. \qquad (3.104)$$

But

$$\frac{\partial \mu}{\partial t} = 0, \ \frac{\partial \mu}{\partial x} = 0, \ \frac{\partial_2 \mu}{\partial x^2} = 0. \qquad (3.105)$$

$$\frac{\partial \mu}{} = 0$$

We then substitute ∂t from (3.105) into (3.104) and it becomes

$$\frac{\partial \theta_o}{\partial t} = \frac{\partial H}{\partial t}. \qquad 3.106$$

$$\frac{\partial^2 \mu}{} = 0$$

Similarly, differentiating (3.100) withrespect to x twice and substitute ∂x^2 from (3.105) we obtain

$$\frac{\partial \theta_o}{\partial x} = \frac{\partial H}{\partial x} + \frac{\partial \mu}{\partial x} = \frac{\partial H}{\partial x}, \qquad 3.107$$

$$\frac{\partial^2 \theta}{\partial x^2} = \frac{\partial^2 H}{\partial x^2}. \qquad (3.108)$$

We then transform the term $-(4R_a \in +\alpha_1)\theta_o$ in (3.75) using (3.100), which implies that;

$$\left.\begin{aligned} -(4R_a \in +\alpha_1)\theta_o &= -(4R_a \in +\alpha_1)(H(x,t)+\mu(x,t)), \\ -(4R_a \in +\alpha_1)\theta_o &= -(4R_a \in +\alpha_1)H(x,t) - \sigma_1(4R_a \in +\alpha_1). \end{aligned}\right\} \qquad (3.109)$$

Next, we transform the boundary conditions

$$\left.\begin{aligned} &\theta_o(x,0) = H(x,0)+\mu(x,0) = 0, \\ &H(x,0)+\sigma_1.0^{0} = 0, \\ &so, \quad H(x,0) = -\sigma_1. \end{aligned}\right\} \qquad (3.110)$$

$$\left.\begin{aligned} &\theta_o(0,t) = H(0,t)+\mu(0,t) = \sigma_1, \\ &H(0,t)+\sigma_1 = \sigma_1, \\ &so, \quad H(0,t) = 0. \end{aligned}\right\} \qquad (3.111)$$

$$\left.\begin{aligned} &\theta_o(1,t) = H(1,t)+\mu(1,t) = \sigma_1, \\ &H(1,t)+\sigma_1 = \sigma_1, \\ &so, H(1,t) = 0. \end{aligned}\right\} \qquad (3.112)$$

Hence, using (3.106), (3.108), (3.109) with the boundary conditions (3.110), (3.111) and (3.112) in (3.75) we obtain,

$$\left.\begin{aligned} \frac{\partial H}{\partial t} &= \lambda_1 \frac{\partial^2 H}{\partial x^2} - (4R_a \in +\alpha_1)H - (\sigma_1(4R_a \in +\alpha_1) + (R_a + \alpha_1\gamma_1)) \\ H(x,0) &= -\sigma_1,\ \mathrm{H}(0,t) = 0,\ \mathrm{H}(1,t) = 0 \end{aligned}\right\} \quad (3.113)$$

So,

$$\left.\begin{aligned} \frac{\partial H}{\partial t} &= \lambda_1 \frac{\partial^2 H}{\partial x^2} - b_1 H - b_2 \\ H(x,0) &= -\sigma_1,\ \mathrm{H}(0,t) = 0,\ \mathrm{H}(1,t) = 0 \end{aligned}\right\}, \quad (3.114)$$

where

$$\left.\begin{aligned} b_1 &= (4R_a \in +\alpha_1) \\ b_2 &= (\sigma_1(4R_a \in +\alpha_1) + (R_a + \alpha_1\gamma_1)) \end{aligned}\right\}. \quad (3.115)$$

That is,

Comparing (3.114) with (3.84)—(88) we have the following;

$$u = H,\ k = \lambda_1,\ \alpha = -b_1, F(x,t) = -b_2,\ f(x) = -\sigma_1,\ L = 1. \quad (3.116)$$

$$b_n = -2\sigma_1 \int_0^1 \sin n\pi x dx, \quad (3.117)$$

$$b_n = \frac{2}{n}\frac{\sigma}{\pi}\left[\cos n\pi x\right]_0^1, \quad (3.118)$$

$$b_n = \frac{2}{n}\frac{\sigma}{\pi}\left[(-1)^n - 1\right]. \quad (3.119)$$

Also,

$$F_n(t) = -2b_2 \int_0^1 \sin n\pi x dx, \quad (3.120)$$

$$F_n(t) = \frac{2}{n}\frac{b}{\pi^2}\left[\cos n\pi x\right]_0^1, \quad (3.121)$$

$$F_n(t) = \frac{2}{n}\frac{b}{\pi^2}\left[(-1)^n - 1\right]. \quad (3.122)$$

Using (3.119) and (3.122) in (3.86) we have,

$$H_n(t) = \frac{2b_2}{n\pi}\left[(-1)^n - 1\right]\int_0^t e^{-\left(b_1 + \lambda_1 (n\pi)^2\right)(t-\tau)}\, d\tau + b_n e^{-\left(b_1 + \lambda_1 (n\pi)^2\right)t}, \tag{3.123}$$

$$H_n(t) = \frac{2b_2\left[(-1)^n - 1\right]e^{-c_2 t}}{n\pi}\int_0^t e^{c_2 \tau}\, d\tau + b_n e^{-c_2 t}, \tag{3.124}$$

where;

$$c_2 = \left(b_1 + \lambda_1 (n\pi)^2\right), \tag{3.125}$$

$$H_n(t) = \frac{2b_2\left[(-1)^n - 1\right]}{n\pi c_2} e^{-c_2 t}\left[e^{c_2 \tau}\right]_0^t + b_n e^{-c_2 t}. \tag{3.126}$$

So,

$$H_n(t) = \frac{2b_2\left[(-1)^n - 1\right]}{n\pi c_2} e^{-c_2 t}\left[e^{c_2 t} - 1\right] + b_n e^{-c_2 t}, \tag{3.127}$$

that is,

$$H_n(t) = \frac{2b_2\left[(-1)^n - 1\right]}{n\pi c_2}\left[1 - e^{-c_2 t}\right] + b_n e^{-c_2 t}. \tag{3.128}$$

Using (3.128) in (3.85) we obtain,

$$H(x,t) = \sum_{n=1}^{\infty}\left(A_1 + \left(b_n - A_1\right)e^{-c_2 t}\right)\sin n\pi x, \tag{3.129}$$

where

$$A_1 = \frac{2b_2\left[(-1)^n - 1\right]}{n\pi c_2}. \tag{3.130}$$

Therefore, using (3.103) and (3.129) in (3.100) we have,

$$\theta_o(x,t) = \sigma_1 + \sum_{n=1}^{\infty}\left(A_1 + (b_n - A_1)e^{-c_2 t}\right)\sin n\pi x, \tag{3.131}$$

that is;

$$\frac{\partial \theta_o}{\partial x} = \sum_{n=1}^{\infty} n\pi\left(A_1 + (b_n - A_1)e^{-c_2 t}\right)\cos n\pi x. \tag{3.132}$$

Using (3.81) and (3.131) in (3.76) we obtain,

$$\frac{\partial \psi_{11}}{\partial t} = -a_6\left(1 + f(e-2)\left(\sigma_1 + \sum_{n=1}^{\infty}\left(A_1 + (b_n - A_1)e^{-c_2 t}\right)\sin n\pi x\right)\right). \tag{3.133}$$

So, integrating (3.133), we have

$$\psi_{11}(x,t) = -a_6\left(t + f(e-2)\left(\sigma_1 t + \sum_{n=1}^{\infty}\left(A t - \left(\frac{b_n - A_1}{c_2}\right)e^{-c_2 t}\sin n\pi x\right)\right)\right) + g(x), \tag{3.134}$$

that is, applying the initial condition, we obtain

$$\psi_{11}(x,0) = -a_6\left(f(e-2)\left(\sum_{n=1}^{\infty}\left(\frac{b_n - A_1}{c_2}\right)\sin n\pi x\right) + g(x) = 0\right). \tag{3.135}$$

It implies that;

$$g(x) = -a_6 f(e-2)\sum_{n=1}^{\infty}\left(\frac{b_n - A_1}{c_2}\right)\sin n\pi x, \tag{3.136}$$

$$g(x) = -A_3\sum_{n=1}^{\infty} A_2 \sin n\pi x. \tag{3.137}$$

Where,

$$\left.\begin{aligned} A_2 &= \left(\frac{b_n - A_1}{c_2}\right) \\ A_3 &= a_6 f(e-2) \end{aligned}\right\}. \tag{3.138}$$

Using (3.137) in (3.134) we obtain,

$$\psi_{11}(x,t) = -A_3 \sum_{n=1}^{\infty} A_2 \sin n\pi x - a_6 \left(t + f(e-2) \left(\sigma_1 t + \sum_{n=1}^{\infty} \left(A_1 t - \left(\frac{b_n - A_1}{c_2} \right) e^{-c_2 t} \right) \sin n\pi x \right) \right), \tag{3.139}$$

similarly, using (3.82) and (3.131) in (3.77) we have,

$$\frac{\partial \psi_{21}}{\partial t} = -a_7 \left(1 + \frac{1}{2} \in \left(\sigma_1 + \sum_{n=1}^{\infty} \left(A_1 + (b_n - A_1) e^{-c_2 t} \right) \sin n\pi x \right) \right) \cdot \left(1 + r(e-2) \left(\sigma_1 + \sum_{n=1}^{\infty} \left(A_1 + (b_n - A_1) e^{-c_2 t} \right) \sin n\pi x \right) \right) \tag{3.140}$$

That is,

$$\frac{\partial \psi_{21}}{\partial t} = -a_7 \left(\begin{array}{l} \left(1 + r(e-2) \left(\sigma_1 + \sum_{n=1}^{\infty} \left(A_1 + (b_n - A_1) e^{-c_2 t} \right) \sin n\pi x \right) \right) + \\ \frac{1}{2} \in \left(\sigma_1 + \sum_{n=1}^{\infty} \left(A_1 + (b_n - A_1) e^{-c_2 t} \right) \sin n\pi x \right) + \\ \frac{1}{2} \in (r(e-2)) \left(\begin{array}{l} \sigma^2{}_1 + 2\sigma_1 \sum_{n=1}^{\infty} \left(A_1 + (b_n - A_1) e^{-c_2 t} \right) \sin n\pi x \\ + \sum_{n=1}^{\infty} \sum_{n=1}^{\infty} \left(A_1 + (b_n - A_1) e^{-c_2 t} \right)^2 \sin^2 n\pi x \end{array} \right) \end{array} \right), \tag{3.141}$$

that is,

$$\frac{\partial \psi_{21}}{\partial t} = -a_7 \left(\begin{array}{l} \left(1 + r(e-2) \left(\sigma_1 + \sum_{n=1}^{\infty} \left(A_1 + (b_n - A_1) e^{-c_2 t} \right) \sin n\pi x \right) \right) + \\ \frac{1}{2} \in \left(\sigma_1 + \sum_{n=1}^{\infty} \left(A_1 + (b_n - A_1) e^{-c_2 t} \right) \sin n\pi x \right) + \\ \frac{1}{2} \in r(e-2) \left(\begin{array}{l} \sigma^2{}_1 + 2\sigma_1 \left(\sum_{n=1}^{\infty} \left(A_1 + (b_n - A_1) e^{-c_2 t} \right) \sin n\pi x \right) \\ + \sum_{n=1}^{\infty} \sum_{n=1}^{\infty} \left(A_1{}^2 + 2A_1 (b_n - A_1) e^{-c_2 t} + (b_n - A_1)^2 e^{-2c_2 t} \right) \sin^2 n\pi x \end{array} \right) \end{array} \right). \tag{3.142}$$

Integrating (3.142), it implies that,

$$\psi_{21}(x,t) = -a_7 \left| \begin{array}{l} \left(t + r(e-2) \right| \left(\sigma_1 t + \sum_{n=1}^{\infty} \left| A_1 t - \left(\frac{b_n - A_1}{c_2} \right) e^{-c_2 t} \right| \sin n\pi x \right| + \\ \left| \frac{1}{2} \in \left| \sigma_1 t + \sum_{n=1}^{\infty} \left| A_1 t - \left(\frac{b - A}{c_2} \right) e^{-c_2 t} \right| \sin n\pi x \right| + \right. \\ \left| \frac{1}{2} \in \left(r(e-2) \right) \right| \left(\sigma_1^2 t + 2\sigma_1 \left| \sum_{n=1}^{\infty} \left| A_1 t - \left(\frac{b - A}{c_2} \right) e^{-c_2 t} \right| \sin n\pi x \right| \right) \\ \left| + \sum_{n=1}^{\infty}\sum_{n=1}^{\infty} \left| A_1 t - \frac{2A}{c_2}(b_n - A_1) e^{-c_2 t} - \frac{(b_n - A_1)^2}{2c_2} e^{-2c_2 t} \right| \sin^2 n\pi x \right| \\ \left. + g_1(x) \right| \end{array} \right\}, \tag{3.143}$$

that is, applying the initial condition, we obtain,

$$\psi_{21}(x,0) = -a_7 \left| \begin{array}{l} \left(-r(e-2) \right| \left(\sum_{n=1}^{\infty} \left| \frac{b - A}{c} \right| \sin n\pi x \right| - \frac{1}{2} \in \left| \sum_{n=1}^{\infty} \left| \frac{b - A}{c} \right| \sin n\pi x \right| \right) \\ \left| - \in \left(r(e-2) \right) \sigma_1 \left| \sum_{n=1}^{\infty} \left| \frac{b - A}{c_2} \right| \sin n\pi x + \left(\sum_{n=1}^{\infty}\sum_{n=1}^{\infty} \left| \frac{A_1}{c_2}(b_n - A_1) \right| \sin^2 n\pi x \right| \right. \right. \\ \left. \left. + \frac{(b_n - A_1)^2}{4c_2} \right) \right| + g_1(x) = 0. \end{array} \right. \tag{3.144}$$

This implies that,

$$g_1(x) = -a_7 \left| \begin{array}{l} A_4 \sum_{n=1}^{\infty} A_2 \sin n\pi x + A_5 \sum_{n=1}^{\infty} A_2 \sin n\pi x + A_6 \sum_{n=1}^{\infty} A_2 \sin n\pi x \\ + \sum_{n=1}^{\infty}\sum_{n=1}^{\infty} (A_1 A_2 + A_2 B) \sin^2 n\pi x. \end{array} \right. \tag{3.145}$$

Where,

$$\left.\begin{array}{l} A_4 = r\left(e-2\right) \\ A_5 = \frac{1}{2} \in \\ A_6 = \in \left(r\left(e-2\right)\right)\sigma_1 \\ B = \frac{b_n - A_1}{4}\ . \end{array}\right\} \tag{3.146}$$

So, we have that,

$$g_1(x) = -a_7\left(A_4 + A_5 + A_6 + \sum_{n=1}^{\infty} B_1 \sin n\pi x\right)\left(\sum_{n=1}^{\infty} A_2 \sin n\pi x.\right) \tag{3.147}$$

Where,

$$B_1 = (A_1 + B). \tag{3.148}$$

$$g_1(x) = -a_7\left(A_7 + \sum_{n=1}^{\infty} B_1 \sin n\pi x\right)\left(\sum_{n=1}^{\infty} A_2 \sin n\pi x\right). \tag{3.149}$$

Where,

$$A_7 = (A_4 + A_5 + A_6). \tag{3.150}$$

Therefore, using (3.149) in (3.143) we have,

$$\psi_{21}(x,t) = -a_7 \left| \begin{array}{l} \left| t + r(e-2) \right| \left(\sigma_1 t + \sum_{n=1}^{\infty} \left| A_1 t - \left| \frac{b_n - A_1}{c_2} \right| e^{-c_2 t} \right| \sin n\pi x \right| + \\ \left| \frac{1}{2} \in \left| \sigma_1 t + \sum_{n=1}^{\infty} \left| A_1 t - \left| \frac{b - A}{c_2} \right| e^{-c_2 t} \right| \sin n\pi x \right| + \right. \\ \left. \left| \sigma_1^2 t + 2\sigma_1 \left| \sum_{n=1}^{\infty} \left| A_1 t - \left| \frac{b - A}{c_2} \right| e^{-c_2 t} \right| \sin n\pi x \right| \right| \right. \\ \left| \frac{1}{2} \in \left(r(e-2) \right) \right| \\ \left| + \sum_{n=1}^{\infty} \sum_{n=1}^{\infty} \left(A_1^2 t - \frac{2A}{c_2} (b_n - A_1) e^{-c_2 t} - \frac{(b_n - A_1)^2}{2c_2} e^{-2c_2 t} \right) \sin^2 n\pi x \right| \\ \left(\right) \end{array} \right| \tag{3.151}$$

$$- a_7 \left| A_7 + \sum B_1 \sin n\pi x \right| \sum A_2 \sin n\pi x \, .$$

Using (3.81), (3.83), (3.96) and (3.131) in (3.78) we have,

$$\frac{\partial \psi_{31}}{\partial t} = a_9 \left| 1 + f(e-2) \right| \left(\sigma_1 + \sum_{n=1}^{\infty} \left(A_1 + (b_n - A_1) e^{-c_2 t} \right) \sin n\pi x \right| \tag{3.152}$$

$$- a_8 \left| \sum_{n=1}^{\infty} A e^{-c_1 t} \sin n\pi x + q \right| \left| 1 + (e-2) \right| \left(\sigma_1 + \sum_{n=1}^{\infty} (A_1 + (b_n - A_1) e^{-c_2 t} \right) \sin n\pi x \right| \right|$$

that is,

$$\frac{\partial \psi_{31}}{\partial t} = a_9 \left| 1 + f(e-2) \right| \left(\sigma_1 + \sum_{n=1}^{\infty} \left(A_1 + (b_n - A_1) e^{-c_2 t} \right) \sin n\pi x \right| \tag{3.153}$$

$$\left| (1 + (e-2)\sigma_1) \sum_{n=1}^{\infty} A e^{-c_1 t} \sin n\pi x + (e-2) \sum_{n=1}^{\infty} \sum_{n=1}^{\infty} \left(AA_1 e^{-c_1 t} + A(b_n - A_1) e^{-(c_1 + c_2)t} \right) \sin^2 n\pi x \right|$$

$$- a_8 \left| + \left(1 + (e-2)\sigma_1 \right) q + (e-2) q \sum_{n=1}^{\infty} \left(A_1 + (b_n - A_1) e^{-c_2 t} \right) \sin n\pi x \right|$$

That is, integrating (3.153) we have,

$$\psi_{31}(x,t) = a_9\Big(1+f(e-2)\sigma_1\Big)t + f(e-2)\sum_{n=1}^{\infty}\left(A_1 t - \left(\frac{b_n - A_1}{c_2}\right)e^{-c_2 t}\right)\sin n\pi x$$
$$- a_8\Big(1+(e-2)\sigma_1\Big)\sum_{n=1}^{\infty}\frac{A}{c_1}e^{-c_1 t}\sin n\pi x - (e-2)\sum_{n=1}^{\infty}\sum_{n=1}^{\infty}\frac{A(b_n - A_1)}{(c_1+c_2)}e^{-(c_1+c_2)t}\sin n\pi x \qquad (3.154)$$
$$+\Big(1+(e-2)\sigma_1\Big)qt + (e-2)q\sum_{n=1}^{\infty}\left(A_1 t - \frac{(b_{n1}-A)}{c_2}e^{-c_2 t}\right)\sin n\pi x$$
$$+ g_2(x).$$

It implies that,

$$\psi_{31}(x,t) = a_9\left(A_8 t + A_9\sum\left(A_1 t - A_2 e^{-c_2 t}\right)\sin n\pi x\right)$$
$$+ a_8\left(A_{10}\sum_{n=1}^{\infty}\frac{A}{c_1}e^{-c_1 t}\sin n\pi x + A_{11}\sum_{n=1}^{\infty}\sum_{n=1}^{\infty}\left(B_2 e^{-c_1 t} + B_3 e^{-(c_1+c_2)}\right)\sin^2 n\pi x\right. \qquad (3.155)$$
$$\left. - A_{12}t - A_{13}\sum_{n=1}^{\infty}\left(A_1 t - A_2 e^{-c_2 t}\right)\sin n\pi x\right)$$
$$+ g_2(x).$$

Where,

$$\left.\begin{aligned} A_8 &= \left(1+ f\left(e-2\right)\sigma_1\right) \\ A_9 &= f\left(e-2\right) \\ A_{10} &= \left(1+ \left(e-2\right)\sigma_1\right) \\ A_{11} &= \left(e-2\right) \\ B_2 &= \frac{AA_1}{c_1} \\ B_3 &= \frac{A\left(b_n - A_1\right)}{c_1 + c_2} \\ A_{12} &= \left(1+ \left(e-2\right)\sigma_1\right)q \\ A_{13} &= \left(e-2\right)q \end{aligned}\right\} \tag{3.156}$$

That is, applying the initial condition we obtain,

$$\left.\begin{aligned} \psi_{31}(x,0) = -a_9 \left(A_9 \sum_{n=1}^{\infty} A_2 \sin n\pi x \right) \\ + a_8 \left(A_{10} \sum_{n=1}^{\infty} \frac{}{c_1} \sin n\pi x + A_{11} \sum_{n=1}^{\infty}\sum_{n=1}^{\infty} \left(B_2 + B_3\right) \sin^2 n\pi x + A_{13} \sum_{n=1}^{\infty} A_2 \sin n\pi x \right) \\ + g_2(x) = 0. \end{aligned}\right\} \tag{3.157}$$

It implies that,

$$\left.\begin{aligned} g_2(x) = a_9 A_9 \sum_{n=1}^{\infty} A_2 \sin n\pi x \\ \left(-a_8 \left(A_{10} \sum_{n=1}^{\infty} \frac{A}{c_1} \sin n\pi x + A_{11} \sum_{n=1}^{\infty}\sum_{n=1}^{\infty} \left(B_4\right) \sin^2 n\pi x + A_{13} \sum_{n=1}^{\infty} A_2 \sin n\pi x \right) \right) \end{aligned}\right\} \tag{3.158}$$

Where,

$$B_4 = \left(B_2 + B_3\right). \tag{3.159}$$

We then, substitute (3.158) in (3.155) and obtain,

$$\psi_{31}(x,t) = a_9\left(A_8 t + A_9\sum_{n=1}^{\infty}\left(A_1 t - A_2 e^{-c_2 t}\right)\sin n\pi x\right) + a_8\left(\begin{array}{l} A_{10}\sum_{n=1}^{\infty}\frac{A}{c_1}e^{-c_1 t}\sin n\pi x + A_{11}\sum_{n=1}^{\infty}\sum_{n=1}^{\infty}\left(B_2 e^{-c_1 t} + B_3 e^{(\quad)}\right)\sin^2 n\pi x \\ -A_{12}\,t - A_{13}\sum_{n=1}^{\infty}\left(A_1 t - A_2 e^{-c_2 t}\right)\sin n\pi x \end{array}\right) + a_9 A_9\sum_{n=1}^{\infty}A_2\sin n\pi x - a_8\left(A_{10}\sum_{n=1}^{\infty}\frac{A}{c_1}\sin n\pi x + A_{11}\sum_{n=1}^{\infty}\sum_{n=1}^{\infty}(B_4 \quad)\sin^2 n\pi x + A_{13}\sum_{n=1}^{\infty}A_2\sin n\pi x\right). \tag{3.160}$$

In solving equations (3.79) and (3.80) we use eigenfunction expansion technique and substitute the following equations, that is, (3.81), (3.82), (3.83), (3.96), (3.98) and (3.131) into (3.79) and obtain,

$$\begin{aligned} \frac{\partial\phi_1}{\partial t} &= D_1\frac{\partial^2\phi_1}{\partial x^2} - \beta_1\phi_1 - \sum_{n=1}^{\infty}n\pi A e^{-c_1 t}\cos n\pi x \\ &\quad - a_1\left(\sum_{n=1}^{\infty}Ae^{-c_1 t}\sin n\pi x + q\right)\left(1 + f(e-2)\left(\sigma_1 + \sum_{n=1}^{\infty}\left(A_1 + (b_n - A_1)e^{-c_2 t}\right)\sin n\pi x\right)\right) \\ &\quad - a_2\left(1 + \frac{1}{2}\left(\sigma_1 + \sum_{n=1}^{\infty}(A_1 + (b_n - A_1 \quad)e^{-c_2 t}\right)\sin n\pi x\right)\left(\sum_{n=1}^{\infty}Ae^{-c_1 t}\sin n\pi x + q\right)\right) \\ &\quad \left(1 + r(e-2)\left(\sigma_1 + \sum_{n=1}^{\infty}\left(A_1 + (b_n - A_1)e^{-c_2}\right)\sin n\pi x\right)\right) \\ &\quad - a_3\left(\sum_{n=1}^{\infty}Ae^{-c_1 t}\sin n\pi x + p\right)\left(\sum_{n=1}^{\infty}Ae^{-c_1 t}\sin n\pi x + q\right). \\ &\quad \left(1 + (e-2)\left(\sigma_1 + \sum_{n=1}^{\infty}\left(A_1 + (b_n - A_1)e^{-c_2 t}\right)\sin n\pi x\right)\right) \end{aligned} \tag{3.161}$$

$$\phi_1(x,0) = 0, \quad \phi_1(0,t) = 0, \quad \phi_1(1,t) = 0$$

That is, expanding the brackets we have,

$$\frac{\partial \phi_1}{\partial t}^2 = D_1 \frac{\partial \phi_1}{\partial x}^2 - \beta_1 \phi_1 - \sum_{n=1}^{\infty} n\pi A e^{-c_1 t} \cos n\pi x$$

$$- a_1 \left(\left(1 + f(e-2)\sigma_1\right) \sum_{n=1}^{\infty} A e^{-c_1 t} \sin n\pi x + \right.$$

$$+ A\left(b_n - A_1\right) e^{-(c_1 + c_2)t} \sin n\pi x$$

$$+ \left(1 + f(e-2)\sigma_1\right) q$$

$$\left. + f(e-2) q \sum_{n=1}^{\infty} \left[A_1 + \left(b_n - A_1\right) e^{-c_2 t} \right] \sin n\pi x \right)$$

$$- a_2 \left(\sum_{n=1}^{\infty} A e^{-c_1 t} \sin n\pi x + q \right.$$

$$+ \frac{1}{2} \in \sum_{n=1}^{\infty} \sum_{n=1}^{\infty} A\left(b_n - A_1\right) e^{-(c_1 + c_2)t} \sin^2 n\pi x$$

$$\left. + q \sum_{n=1}^{\infty} \left[A_1 + \left(b_n - A_1\right) e^{-c_2 t} \right] \sin n\pi x \right)$$

$$- a_3 \left(\left(1 + r(e-2)\sigma_1\right) + r(e-2) \sum_{n=1}^{\infty} \left[A_1 + \left(b_n - A_1\right) e^{-c_2 t} \right] \sin n\pi x \right.$$

$$\left. \sum_{n=1}^{\infty} \sum_{n=1}^{\infty} A^2 e^{-2c_1 t} \sin^2 n\pi x + (p+q) \sum_{n=1}^{\infty} A e^{-c_1 t} \sin n\pi x + pq \right)$$

$$\left(1 + (e-2)\sigma_1 + (e-2) \sum_{n=1}^{\infty} \left[A_1 + \left(b_n - A_1\right) e^{-c_2 t} \right] \sin n\pi x \right) \tag{3.162}$$

$$\phi_1(x, 0) = 0, \quad \phi_1(0, t) = 0, \quad \phi_1(1, t) = 0.$$

That is, expanding further we obtain,

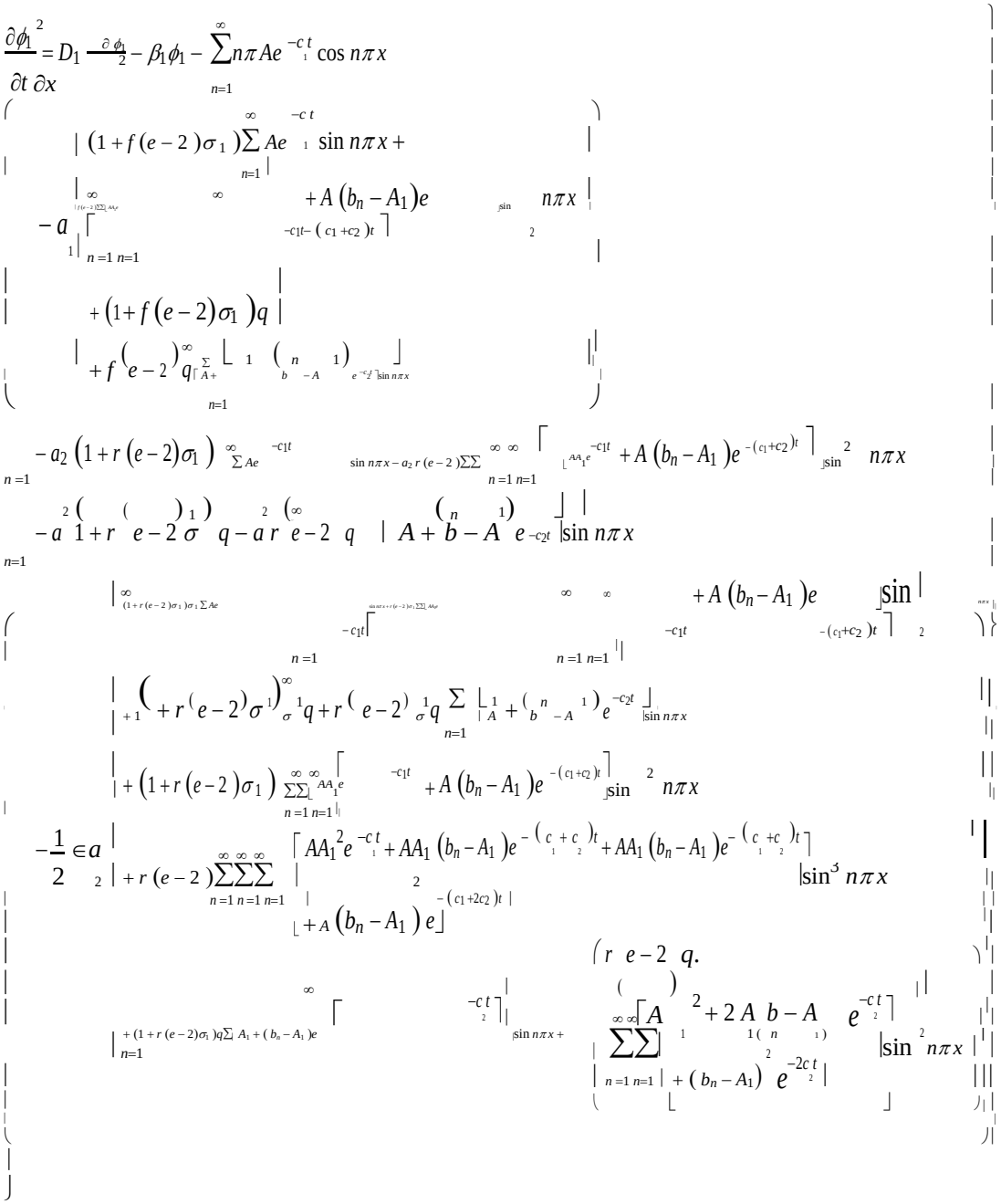

$$
\begin{aligned}
&\Big(1+(e-2)\sigma_1\Big)\sum_{n=1}^{\infty}\sum_{n=1}^{\infty} A^2 e^{-2c_1 t}\sin^2 n\pi x + \\
&(e-2)\sum_{n=1}^{\infty}\sum_{n=1}^{\infty}\sum_{n=1}^{\infty}\Big[A^2 A_1 e^{-2c_1 t} + A^2\left(b_n - A_1\right)e^{-(2c_1+c_2)t}\Big]\sin^3 n\pi x \\
-a_3\Big[&+(p+q)\Big(1+(e-2)\sigma_1\Big)\sum_{n=1}^{\infty} A e^{-c_1 t}\sin n\pi x + \\
&\sum_{n=1}^{\infty}\sum_{n=1}^{\infty}\Big[+A\left(b_n - A_1\right)e^{-c_1 t} + A\left(b_n - A_1\right)e^{-(c_1+c_2)t}\Big]\sin^2 n\pi x \\
&+(pq)\Big(1+(e-2)\sigma^1\Big)+(pq)(e-2)\sum_{n=1}^{\infty}\Big[A + \left(b_n - A_1\right)e^{-c_2 t}\Big]\sin n\pi x
\end{aligned}
\qquad (3.163)
$$

$$\phi_1(x,0)=0, \qquad \phi_1(0,t)=0, \qquad \phi_1(1,t)=0.$$

That is,

$$\frac{\partial \phi_1}{\partial t} = D_1 \frac{\partial^2 \phi_1}{\partial x^2} - \beta_1 \phi_1 - \sum_{n=1}^{\infty} n\pi A e^{-c_1 t} \cos n\pi x$$

$$\left(\begin{array}{l} \left(A_8 \sum_{n=1}^{\infty} A e^{-c_1 t} \sin n\pi x + \right. \\ \left. - a_1 \left(A_9 \sum_{n=1}^{\infty} \sum_{n=1}^{\infty} \left[A A_1 e^{-c_1 t} + A (b_n - A_1) e^{-(c_1 + c_2)t} \right] \sin^2 n\pi x \right. \right. \\ \left. \left. + A_{14} + A_{15} \sum_{n=1}^{\infty} \left[A_1 + (b_n - A_1) e^{-c_2 t} \right] \sin n\pi x \right) \end{array} \right)$$

$$- a_2 A_{16} \sum_{n=1}^{\infty} A e^{-c_1 t} \sin n\pi x - a_2 A_{17} \sum_{n=1}^{\infty} \sum_{n=1}^{\infty} \left[A A_1 e^{-c_1 t} - A (b_n - A_1) e^{-(c_1 + c_2)t} \right] \sin^2 n\pi x$$

$$- a_{18}^2 A - a_{19} A \sum_{n=1}^{\infty} \left[A_1 + (b_n - A_1) e^{-c_2 t} \right] \sin n\pi x$$

$$\left(\begin{array}{l} \left(A_{20} \sum_{n=1}^{\infty} A e^{-c_1 t} \sin n\pi x + A_{21} \sum_{n=1}^{\infty} \sum_{n=1}^{\infty} \left[A A_1 e^{-c_1 t} + A (b_n - A_1) e^{-(c_1 + c_2)t} \right] \sin^2 n\pi x \right. \\ \left. + A_{22} + A_{23} \sum_{n=1}^{\infty} \left[A_1 + (b_n - A_1) e^{-c_2 t} \right] \sin n\pi x \right. \\ \left. + A_{24} \sum_{n=1}^{\infty} \sum_{n=1}^{\infty} \left[A A_1 e^{-c_1 t} + A (b_n - A_1) e^{-(c_1 + c_2)t} \right] \sin^2 n\pi x \right. \\ \left. - a_2 \left(A_{25} \sum_{n=1}^{\infty} \sum_{n=1}^{\infty} \sum_{n=1}^{\infty} \left[A A_1^2 e^{-c_1 t} + A A_1 (b_n - A_1) e^{-(c_1 + c_2)t} + A A_1 (b_n - A_1) e^{-(c_1 + c_2)t} \right. \right. \right. \\ \left. \left. \left. + A (b_n - A_1)^2 e^{-(c_1 + 2c_2)t} \right] \sin^3 n\pi x \right. \right. \\ \left. \left. + A_{26} \sum_{n=1}^{\infty} \left[A_1 + (b_n - A_1) e^{-c_2 t} \right] \sin n\pi x + \left(A_{27} \sum_{n=1}^{\infty} \sum_{n=1}^{\infty} \left[A_1^2 + 2 A_1 (b_n - A_1) e^{-c_2 t} \right. \right. \right. \right. \\ \left. \left. \left. \left. + (b_n - A_1)^2 e^{-2c_2 t} \right] \sin^2 n\pi x \right) \right) \end{array} \right)$$

$$\left(\begin{array}{l} \left(A_{10} \sum_{n=1}^{\infty} \sum_{n=1}^{\infty} A^2 e^{-2c_1 t} \sin^2 n\pi x + \right. \\ \left. - a_3 \left(A_{11} \sum_{n=1}^{\infty} \sum_{n=1}^{\infty} \sum_{n=1}^{\infty} \left[A^2 A_1 e^{-2c_1 t} + A^2 (b_n - A_1) e^{-(2c_1 + c_2)t} \right] \sin^3 n\pi x \right. \right. \\ \left. \left. + A_{28} \sum_{n=1}^{\infty} A e^{-c_1 t} \sin n\pi x + \right. \right. \\ \left. \left. A_{29} \sum_{n=1}^{\infty} \sum_{n=1}^{\infty} \left[A A_1 e^{-c_1 t} + A (b_n - A_1) e^{-(c_1 + c_2)t} \right] \sin^2 n\pi x \right. \right. \\ \left. \left. + A_{30} + A_{31} \sum_{n=1}^{\infty} \left[A_1 + (b_n - A_1) e^{-c_2 t} \right] \sin n\pi x \right) \end{array} \right)$$

$$\phi_1(x, 0) = 0, \qquad \phi_1(0, t) = 0, \qquad \phi_1(1, t) = 0$$

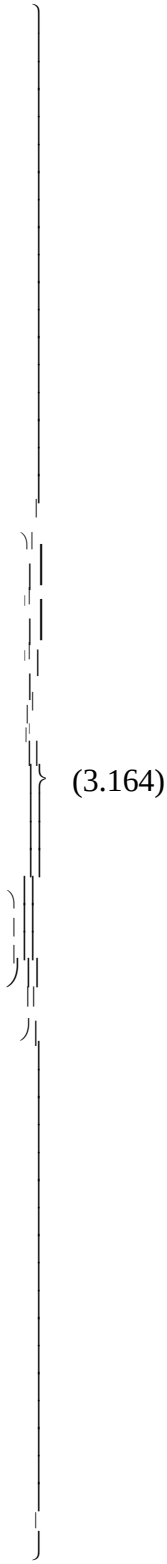

(3.164)

Where,

$$\left.\begin{aligned}
A_{14} &= \left(1+f\,(e-2)\sigma_1\right)q \\
A_{15} &= f\,(e-2)q \\
A_{16} &= \left(1+r\,(e-2)\sigma_1\right) \\
A_{17} &= r\,(e-2) \\
A_{18} &= \left(1+r\,(e-2)\sigma_1\right)q \\
A_{19} &= r\,(e-2)q \\
A_{20} &= \tfrac{1}{2}\in\left(\left(1+r\,(e-2)\sigma_1\right)\sigma_1\right) \\
A_{21} &= \tfrac{1}{2}\in r\,(e-2)\sigma_1 \\
A_{22} &= \tfrac{1}{2}\in\left(\left(1+r\,(e-2)\sigma_1\right)\sigma_1 q\right) \\
A_{23} &= \tfrac{1}{2}\in r\,(e-2)\sigma_1 q \\
A_{24} &= \tfrac{1}{2}\in\left(1+r\,(e-2)\sigma_1\right) \\
A_{25} &= \tfrac{1}{2}\in r\,(e-2) \\
A_{26} &= \tfrac{1}{2}\in\left(1+r\,(e-2)\sigma_1\right)q \\
A_{27} &= \tfrac{1}{2}\in r\,(e-2)q \\
A_{28} &= (p+q)\left(1+(e-2)\sigma_1\right) \\
A_{29} &= (p+q)(e-2) \\
A_{30} &= (pq)\left(1+(e-2)\sigma_1\right) \\
A_{31} &= (pq)(e-2).
\end{aligned}\right\} \qquad (3.165)$$

That is,

$$\left.\begin{aligned}
\frac{\partial\phi}{\partial t} &= D\,\frac{\partial^2\phi}{\partial x^2} - \beta\,\phi - b \\
\phi_1(x,0) &= 0, \quad \phi_1(0,t) = 0,\ \phi_1(1,t) = 0
\end{aligned}\right\}, \qquad (3.166)$$

where

$$
b_3 = \left(
\begin{aligned}
&\sum_{n=1}^{\infty} n\pi A e^{-c_1 t} \cos n\pi x \\
&+ a_1 \left(\begin{aligned} & A_8 \sum_{n=1}^{\infty} A e^{-c_1 t} \sin n\pi x + A_9 \sum_{n=1}^{\infty}\sum_{n=1}^{\infty} \left[A A_1 e^{-c_1 t} + A\left(b_n - A_1\right) e^{-\left(c_1+c_2\right)t} \right] \sin^2 n\pi x \\ & + A_{14} + A_{15} \sum_{n=1}^{\infty} \left[A_1 + \left(b_n - A_1\right) e^{-c_2 t} \right] \sin n\pi x \end{aligned} \right) \\
&+ a_2 A_{16} \sum_{n=1}^{\infty} A e^{-c_1 t} \sin n\pi x + a_2 A_{17} \sum_{n=1}^{\infty}\sum_{n=1}^{\infty} \left[A A_1 e^{-c_1 t} + A\left(b_n - A_1\right) e^{-\left(c_1+c_2\right)t} \right] \sin^2 n\pi x \\
&+ a_2 A_{18} + a_2 A_{19} \sum_{n=1}^{\infty} \left[A_1 + \left(b_n - A_1\right) e^{-c_2 t} \right] \sin n\pi x \\
&+ a_2 \left(\begin{aligned} & A_{20} \sum_{n=1}^{\infty} A e^{-c_1 t} \sin n\pi x + A_{21} \sum_{n=1}^{\infty}\sum_{n=1}^{\infty} \left[A A_1 e^{-c_1 t} + A\left(b_n - A_1\right) e^{-\left(c_1+c_2\right)t} \right] \sin^2 n\pi x \\ & + A_{22} + A_{23} \sum_{n=1}^{\infty} \left[A_1 + \left(b_n - A_1\right) e^{-c_2 t} \right] \sin n\pi x \\ & + A_{24} \sum_{n=1}^{\infty}\sum_{n=1}^{\infty} \left[A A_1 e^{-c_1 t} + A\left(b_n - A_1\right) e^{-\left(c_1+c_2\right)t} \right] \sin^2 n\pi x \\ & + A_{25} \sum_{n=1}^{\infty}\sum_{n=1}^{\infty}\sum_{n=1}^{\infty} \left[\begin{aligned} & A A_1^2 e^{-c_1 t} + A A_1 \left(b_n - A_1\right) e^{-\left(c_1+c_2\right)t} + A A_1 \left(b_n - A_1\right) e^{-\left(c_1+c_2\right)t} \\ & + A\left(b_n - A_1\right)^2 e^{-\left(c_1+2c_2\right)t} \end{aligned} \right] \sin^3 n\pi x \\ & + A_{26} \sum_{n=1}^{\infty} \left[A_1 + \left(b_n - A_1\right) e^{-c_2 t} \right] \sin n\pi x + A_{27} \sum_{n=1}^{\infty}\sum_{n=1}^{\infty} \left[\begin{aligned} & A_1^2 + 2A_1\left(b_n - A_1\right) e^{-c_2 t} \\ & + \left(b_n - A_1\right)^2 e^{-2c_2 t} \end{aligned} \right] \sin^2 n\pi x \end{aligned} \right) \\
&+ a_3 \left(\begin{aligned} & A_{10} \sum_{n=1}^{\infty}\sum_{n=1}^{\infty} A^2 e^{-2c_1 t} \sin^2 n\pi x + \\ & A_{11} \sum_{n=1}^{\infty}\sum_{n=1}^{\infty}\sum_{n=1}^{\infty} \left[A^2 A_1 e^{-2c_1 t} + A^2 \left(b_n - A_1\right) e^{-\left(2c_1+c_2\right)t} \right] \sin^3 n\pi x \\ & + A_{28} \sum_{n=1}^{\infty} A e^{-c_1 t} \sin n\pi x + \\ & A_{29} \sum_{n=1}^{\infty}\sum_{n=1}^{\infty} \left[A A_1 e^{-c_1 t} + A\left(b_n - A_1\right) e^{-\left(c_1+c_2\right)t} \right] \sin^2 n\pi x \\ & + A_{30} + A_{31} \sum_{n=1}^{\infty} \left[A_1 + \left(b_n - A_1\right) e^{-c_2 t} \right] \sin n\pi x \end{aligned} \right)
\end{aligned}
\right). \qquad (3.167)
$$

Now we compare (3.166) with (3.84)—(3.88) we have the following,

$$\left.\begin{array}{l} u=\phi_1,\ k=D_1, \qquad \alpha=-\beta_1, F(x,t)=-b_3 \\ f(x)=0, \quad L=1. \end{array}\right\} \tag{3.168}$$

Then, it implies that,

$$b_n = 0. \tag{3.169}$$

Similarly,

$$F_n(t) = -2\int_0^1 b_3 \sin n\pi x dx\ . \tag{3.170}$$

That is, substituting equation (3.167) into equation (3.170) we have,

$$
F_n(t) = -2\int_0^1 \Bigg(\sum_{n=1}^{\infty} n\pi A e^{-c_1 t} \cos n\pi x \sin n\pi x + a_1 A_{14} \sin n\pi x
$$

$$
+ \Bigg(a_1 A_8 \sum_{n=1}^{\infty} A e^{-c_1 t} + a_1 A_{15} \sum_{n=1}^{\infty} \Big[A_1 + (b_n - A_1) e^{-c_2 t} \Big] \Bigg) \sin^2 n\pi x +
$$

$$
+ \Bigg(a_2 A_{16} \sum_{n=1}^{\infty} A e^{-c_1 t} + a_2 A_{19} \sum_{n=1}^{\infty} \Big[A + (b_n - A_1) e^{-c_2 t} \Big] + a_2 A_{20} \sum_{n=1}^{\infty} A e^{-c_1 t} \Bigg) \sin^2 n\pi x
$$

$$
+ \Bigg(a_2 A_{23} \sum_{n=1}^{\infty} \Big[A_1 + (b_n - A_1) e^{-c_2 t} \Big] + a_2 A_{26} \sum_{n=1}^{\infty} \Big[A_1 + (b_n - A_1) e^{-c_2 t} \Big] \Bigg)
$$

$$
\Bigg(a_2 A_{17} \sum_{n=1}^{\infty} \sum_{n=1}^{\infty} \Big[AA_1 e^{-c_1 t} - A (b_n - A_1) e^{-(c_1 + c_2) t} \Big] +
$$

$$
+ \Bigg(a_2 A_{21} \sum_{n=1}^{\infty} \sum_{n=1}^{\infty} \Big[AA_1 e^{-c_1 t} + A (b_n - A_1) e^{-(c_1 + c_2) t} \Big] +
$$

$$
+ \Bigg(a_2 A_{24} \sum_{n=1}^{\infty} \sum_{n=1}^{\infty} \Big[AA_1 e^{-c_1 t} + A (b_n - A_1) e^{-(c_1 + c_2) t} \Big] +
$$

$$
\Bigg(a_2 A_{27} \sum_{n=1}^{\infty} \sum_{n=1}^{\infty} \Big[A_1^2 + 2A_1 (b_n - A_1) e^{-c_2 t} + (b_n - A_1)^2 e^{-2c_2 t} \Big] \Bigg) \Bigg) \Bigg) \sin^3 n\pi x \Bigg) dx \qquad (3.171)
$$

$$
+ a_2 A_{25} \sum_{n=1}^{\infty} \sum_{n=1}^{\infty} \sum_{n=1}^{\infty} \Bigg(\Big[AA_1^2 e^{-c_1 t} + AA_1 (b_n - A_1) e^{-(c_1 + c_2) t} \Big] + AA_1 (b_n - A_1) e^{-(c_1 + c_2) t} + Ab \Big(n - A_1 \Big)^2 e^{-(c_1 + 2c_2) t} \Bigg) \sin^4 n\pi x
$$

$$
\Bigg(a_3 A_{10} \sum_{n=1}^{\infty} \sum_{n=1}^{\infty} A^2 e^{-2c_1 t} + \Bigg) \sin^3 n\pi x
$$

$$
+ (a_2 A_{18} + a_2 A_{22}) \sin n\pi x + \Bigg(a_3 A_{29} \sum_{n=1}^{\infty} \sum_{n=1}^{\infty} \Big[AA_1 e^{-c_1 t} + A (b_n - A_1) e^{-(c_1 + c_2) t} \Big] \Bigg) \sin n\pi x
$$

$$
+ a_3 A_{32} \sum_{n=1}^{\infty} \sum_{n=1}^{\infty} \sum_{n=1}^{\infty} \Big[A_1 e^{-2c_1 t} + A (b_n - A_1) e^{-(2c_1 + c_2) t} \Big] \sin^4 n\pi x
$$

$$
+ \Bigg(a_3 A_{28} \sum_{n=1}^{\infty} A e^{-c_1 t} + a_3 A_{31} \sum_{n=1}^{\infty} \Big[A_1 + (b_n - A_1) e^{-c_2 t} \Big] \Bigg) \sin^2 n\pi x + a_3 A_{30} \sin n\pi x. \Bigg)
$$

That is,

$$
\begin{aligned}
F_n(t) = -2 &\left(\sum_{n=1}^{\infty} n\pi A e^{-c_1 t} \left[-\frac{\cos 2n\pi x}{4n\pi} \right]_0^1 + \left(a_1 A_{14} + a_2 A_{18} + a_2 A_{22} + a_3 A_{30} \right) \left[-\frac{\cos n\pi x}{n\pi} \right]_0^1 \right. \\
&+ \left(a_3 A_{28} \sum_{n=1}^{\infty} A e^{-c_1 t} + a_3 A_{31} \sum_{n=1}^{\infty} A_1 + \left(b_n - A_1 \right) e^{-c_2 t} \right] \left[x - \sin \frac{2n\pi x}{2n\pi} \right]_0^1 \\
&+ a_2 A_{27} \sum_{n=1}^{\infty} \sum_{n=1}^{\infty} \left[A_1^2 + 2A_1 \left(b_n - A_1 \right) e^{-c_2 t} + \left(b_n - A_1 \right)^2 e^{-2c_2 t} \right] \\
&+ a_2 A_{25} \sum_{n=1}^{\infty} \sum_{n=1}^{\infty} \sum_{n=1}^{\infty} \left[AA_1^2 e^{-c_1 t} + AA_1 \left(b_n - A_1 \right) e^{-(c_1 + c_2) t} \right. \\
&\left. + A \left(b_n - A_1 \right)^2 e^{-(c_1 + 2c_2) t} \right] \left[\frac{\sin 4n\pi x}{4n\pi} - \frac{2\sin 2n\pi x}{n\pi} + 3x \right]_0^1 \\
&+ a_3 A_{10} \sum_{n=1}^{\infty} \sum_{n=1}^{\infty} A^2 e^{-2c_1 t} + \sum_{n=1}^{\infty} \left[AA_1 e^{-c_1 t} + A \left(b_n - A_1 \right) e^{-(c_1 + c_2) t} \right] \left[\frac{\cos 3n\pi x}{3n\pi} - \frac{3\cos n\pi x}{n\pi} \right]_0^1 \\
&+ a_3 A_{29} \sum_{n=1}^{\infty} \sum_{n=1}^{\infty} \left[A_1^2 e^{-2c_1 t} + A_1 \left(b_n - A_1 \right) e^{-(c_1 + c_2) t} \right] \\
&+ a_3 A_{11} \sum_{n=1}^{\infty} \sum_{n=1}^{\infty} \sum_{n=1}^{\infty} \left[A^2 A_1 e^{-2c_1 t} + A^2 \left(b_n - A_1 \right) e^{-(2c_1 + c_2) t} \right] \left[\frac{\sin 4n\pi x}{4n\pi} - \frac{2\sin 2n\pi x}{n\pi} + 3x \right]_0^1 \\
&\left. + a_3 A_{28} \sum_{n=1}^{\infty} A e^{-c_1 t} + a_3 A_{31} \sum_{n=1}^{\infty} \left[A_1 + \left(b_n - A_1 \right) e^{-c_2 t} \right] \left[x - \sin \frac{2n\pi x}{2n\pi} \right]_0^1 \right).
\end{aligned}
\tag{3.172}
$$

That is,

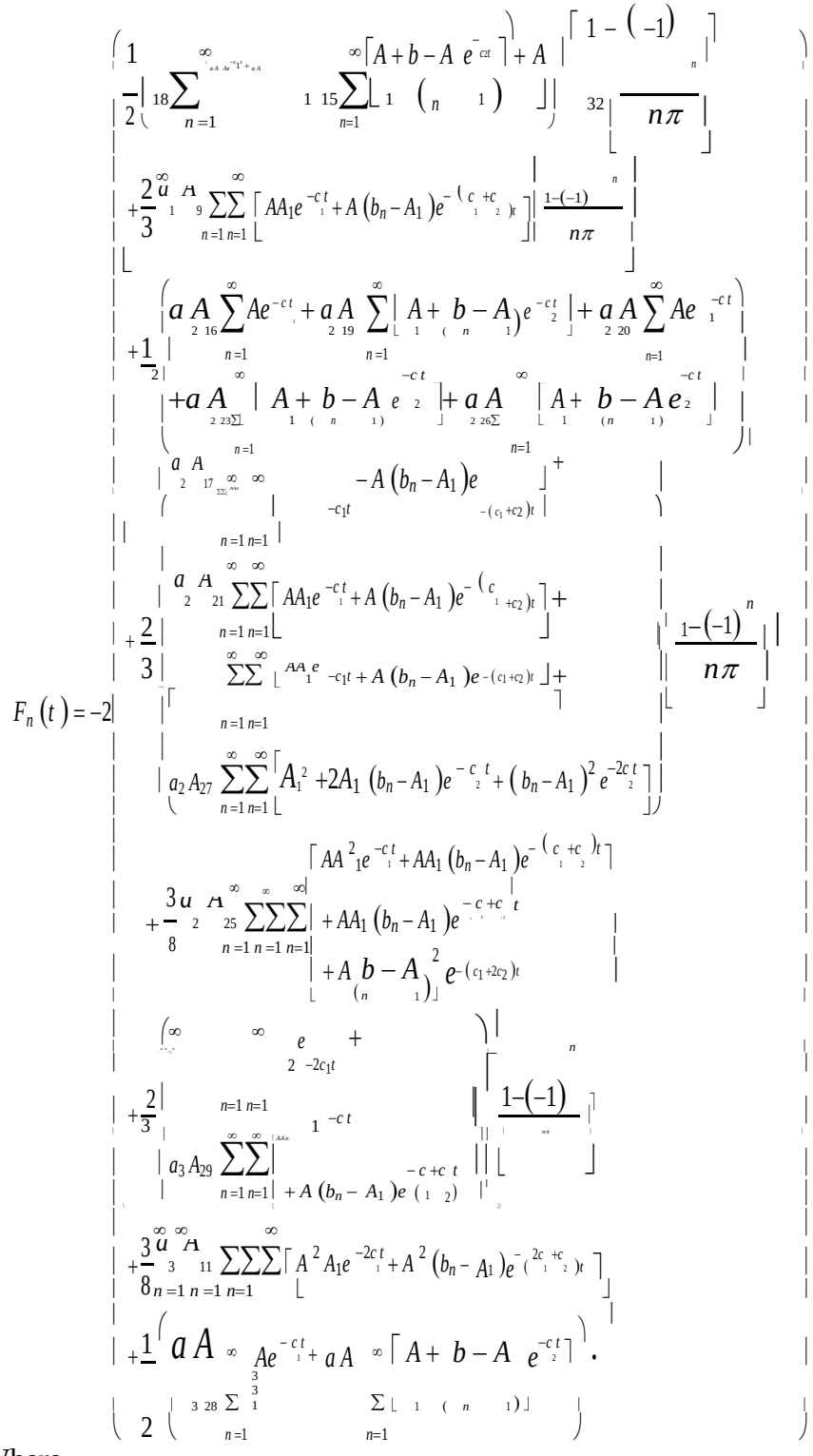

Where,

$$A_{32} = \left(a_1 A_{14} + a_2 A_{18} + a_2 A_{22} + a_3 A_{30} \right).$$

(3.173)

(3.174)

It implies that,

$$
\begin{aligned}
&\left(\frac{1}{2}\left(18\sum_{n=1}^{\infty}\left(15\sum_{n=1}^{\infty}\left(1\left(n\ 1\right)\right)\right)\right)+A\left(32\left(\frac{1-(-1)^{n}}{n\pi}\right)\right)\right)\\
&+\frac{2}{3}a_1A_9\sum_{n=1}^{\infty}\sum_{n=1}^{\infty}\left[AA_1e^{-c_1t}+A\left(b_n-A_1\right)e^{-(c_1+c_2)t}\right]\left(\frac{1-(-1)}{n\pi}\right)\\
&+\frac{1}{2}\left(A_{33}\sum_{n=1}^{\infty}Ae^{-c_1t}+A_{34}\sum_{n=1}^{\infty}\left[A+\left(b_n-A_1\right)e^{-c_2t}\right]\right)\\
&+\frac{2}{3}\left(A_{35}\sum_{n=1}^{\infty}\sum_{n=1}^{\infty}\left[AA_1e^{-c_1t}+A(b_n-A_1)e^{-(c_1+c_2)t}\right]+\left(\frac{1-(-1)^{n}}{n\pi}\right)\right)\\
&+\frac{3}{8}\left(a_2A_{25}\sum_{n=1}^{\infty}\sum_{n=1}^{\infty}\sum_{n=1}^{\infty}\left(AA_1^{2}e^{-c_1t}+AA_1\left(b_n-A_1\right)e^{-(c_1+c_2)t}+A\left(b_n-A_1\right)^{2}e^{-(c_1+2c_2)t}\right)\right)\\
&+\frac{2}{3}\left(a_3A_{10}\sum_{n=1}^{\infty}\sum_{n=1}^{\infty}\left(e^{-2c_1t}+\left(\frac{1-(-1)^{n}}{n\pi}\right)\right)\right)\\
&+\frac{2}{3}\left(a_3A_{29}\sum_{n=1}^{\infty}\sum_{n=1}^{\infty}\left(+A\left(b-A_1\right)\right)e^{-(c_1+c_2)t}\right)\\
&+\frac{3}{8}\left(a_3A_{11}\sum_{n=1}^{\infty}\sum_{n=1}^{\infty}\sum_{n=1}^{\infty}\left[A^{2}A_1e^{-2c_1t}+A^{2}\left(b_n-A_1\right)e^{-(2c_1+c_2)t}\right]\right)\\
&+\frac{1}{2}\left(a_3A_{28}\sum_{n=1}^{\infty}Ae^{-c_1t}+a_3A_{31}\sum_{n=1}^{\infty}\left(A+\left(b_n-A_1\right)e^{-c_2t}\right)\right).
\end{aligned}
\qquad (3.175)
$$

Where,

$$
\left.
\begin{aligned}
A_{33} &= \left(a_1A_{16}+a_2A_{20}\right)\\
A_{34} &= \left(a_2A_{19}+a_2A_{23}+a_2A_{26}\right)\\
A_{35} &= \left(a_2A_{17}+a_2A_{21}+a_2A_{22}+a_2A_{24}\right)
\end{aligned}
\right\} \qquad (3.176)
$$

Using (3.169) and (3.175) in (3.86) we have,

$$
\begin{aligned}
&\Bigg(A_{36}\sum_{n=1}^{\infty} Ae^{-c_1\tau} + A_{37}\sum_{n=1}^{\infty}\left[A + (b_n - A_1)e^{-c_2\tau}\right] + A_{32}\left[\frac{1-(-1)^n}{n\pi}\right] \\
&\quad \sum_{n=1}^{\infty}\sum_{n=1}^{\infty} \left[\quad\right)e^{(\quad)\tau}\left[\frac{1-(-1)^n}{n\pi}\right] \\
&\quad + A_{39}\sum_{n=1}^{\infty} Ae^{-c_1\tau} + A_{40}\sum_{n=1}^{\infty}\left[A + (b_n - A_1)e^{-c_2\tau}\right] \\
&\quad + A_{41}\sum_{n=1}^{\infty}\sum_{n=1}^{\infty}\left[AA_1e^{-c_1\tau} + A(b_n - A_1)e^{-(c_1+c_2)\tau}\right]\left[\frac{1-(-1)^n}{n\pi}\right] + \\
&\int_0^t \Bigg[\sum_{n=1}^{\infty}\sum_{n=1}^{\infty}\left[\quad\right]\left[\frac{1-(-1)^n}{n\pi}\right] \\
&\quad + A_{43}\sum_{n=1}^{\infty}\sum_{n=1}^{\infty}\sum_{n=1}^{\infty}\left[\begin{array}{l} AA_1^2e^{-c_1\tau} + AA_1(b_n - A_1)e^{-(c_1+c_2)\tau} \\ + AA_1(b_n - A_1)e^{-(c_1+c_2)\tau} \\ + A(b_n - A_1)e^{-(c_1+2c_2)\tau}\end{array}\right] \\
&\quad + \Bigg(A_{44}\sum_{n=1}^{\infty}\sum_{n=1}^{\infty} A^2e^{-2c_1\tau} + A_{45}\sum_{n=1}^{\infty}\sum_{n=1}^{\infty}\left[\begin{array}{l} AA_1e^{-c_1\tau} \\ + A(b_n - A_1)e^{-(c_1+c_2)\tau}\end{array}\right]\left[\frac{1-(-1)^n}{n\pi}\right] \Bigg)\left(\quad\right) \\
&\quad + A_{47}\sum_{n=1}^{\infty} Ae^{-c_1\tau} + A_{48}\sum_{n=1}^{\infty}\left[A + (b_n - A_1)e^{-c_2\tau}\right] \Bigg] d\tau \\
&\quad + \sum_{n=1}^{\infty}\sum_{n=1}^{\infty}\sum_{n=1}^{\infty}\left[A^2e^{-2c_1\tau} + A(b_n - A_1)e^{-(2c_1+c_2)\tau}\right] \Bigg) \qquad (3.177)
\end{aligned}
$$

Where,

$$\left.\begin{aligned}
A_{36} &= \frac{1}{2} a_{18} A_{18} \\
A_{37} &= \frac{1}{2} a_{1\,15} A_{15} \\
A_{38} &= \frac{2}{3} a_{1\,9} A_{9} \\
A_{39} &= \frac{1}{2} A_{33} \\
A_{40} &= \frac{1}{2} A_{34} \\
A_{41} &= \frac{2}{3} A_{35} \\
A_{42} &= \frac{2}{3} a_{2\,27} A_{27} \\
A_{43} &= \frac{3}{8} a_{2\,25} A_{25} \\
A_{44} &= \frac{2}{3} a_{3\,10} A_{10} \\
A_{45} &= \frac{2}{3} a_{3\,29} A_{29} \\
A_{46} &= \frac{3}{8} a_{3\,11} A_{11} \\
A_{47} &= \frac{1}{2} a_{3\,38} A_{38} \\
A_{48} &= \frac{1}{2} a_{3\,31} A_{31}
\end{aligned}\right\} \qquad (3.178)$$

That is, (3.177) becomes

$$\phi_n(t) = -2e^{-c_1 t}\Bigg[A_{42}\sum_{n=1}^{\infty} A_1 e^{c_1 t} + 2A_1(b_n - A_1)e^{t}\Bigg[\sum_{n=1}^{\infty}\sum_{n=1}^{\infty}\Bigg[\frac{1-(-1)^n}{n\pi}\Bigg] \Bigg[\frac{e^{(c_1+c_2)t}-1}{c_1+c_2} \Bigg] + \sum_{n=1}^{\infty}\Bigg[\frac{1-(-1)^n}{n\pi}\Bigg] \Bigg[\frac{e^{(c_1-c_2)t}-1}{c_1-c_2} \Bigg] \Bigg] \Bigg]$$

$$+ A_{43}\sum_{n=1}^{\infty}\sum_{n=1}^{\infty}\sum_{n=1}^{\infty}\Bigg[\frac{1-(-1)^n}{n\pi}\Bigg] \Bigg[\frac{AA_1^2\left(e^{-c_1 t}-1\right)}{-c_1} + \frac{AA_1(b_n - A_1)\left(e^{-c_2 t}-1\right)}{-c_2} + \frac{A(b_n - A_1)^2\left(e^{-2c_2 t}-1\right)}{-2c_2} \Bigg]$$

$$+ \Bigg(A_{44}\sum_{n=1}^{\infty}\sum_{n=1}^{\infty} A^2 e^{-c_1 t} + A_{45}\sum_{n=1}^{\infty}\sum_{n=1}^{\infty}\Bigg[\frac{AA_1}{-c_1}\left(e^{-c_1 t}-1\right) + \frac{A(b_n - A_1)}{-c_2}\left(e^{-c_2 t}-1\right) \Bigg] \Bigg[\frac{1-(-1)^n}{n\pi}\Bigg] \Bigg]$$

$$+ A_{46}\sum_{n=1}^{\infty}\sum_{n=1}^{\infty}\sum_{n=1}^{\infty} A_1 e^{-c_1 t} + A_2(b_n - A_1)e^{-(c_1+c_2)t} \Bigg]$$

$$+ A_{47}\sum_{n=1}^{\infty} A + A_{48}\sum_{n=1}^{\infty}\Big[A_1 e^{c_1 t} + (b_n - A_1)e^{(c_1+c_2)t} \Big]. \qquad (3.179)$$

That is,

$$\phi_{1n}(t) = -2e^{-c_1 t}\int_0^t \left(\begin{array}{l} A_{49}\sum_{n=1}^{\infty} A + A_{50}\sum_{n=1}^{\infty}\left[A_1 e^{c_1\tau} + (b_n - A_1)e^{(c_1 - c_2)\tau}\right] + A_{32}\left[\frac{1-(-1)^n}{n\pi}\right]e^{c_1\tau} \\ + A_{51}\sum_{n=1}^{\infty}\sum_{n=1}^{\infty}\left[AA_1 + A(b_n - A_1)e^{-c_2\tau}\right]\left[\frac{1-(-1)^n}{n\pi}\right] \\ \sum_{n=1}^{\infty}\sum_{n=1}^{\infty}\left[(c_1 - c_2)\tau + (b_n - A_1)_2 e^{(c_1 - 2c_2)\tau}\right]\left[\frac{1-(-1)^n}{n\pi}\right] \\ + A_{43}\sum_{n=1}^{\infty}\sum_{n=1}^{\infty}\sum_{n=1}^{\infty}\left[AA_1^2 + AA_1(b_n - A_1)e^{-c_2\tau}\right] \\ + AA_1(b_n - A_1)e^{-c_2\tau} \\ + A(b_n - A_1)^2 e^{-2c_2\tau} \\ + \left(A_{44}\sum_{n=1}^{\infty}\sum_{n=1}^{\infty}A^2 e^{-c_1\tau} + A_{45}\sum_{n=1}^{\infty}\sum_{n=1}^{\infty}\left[\frac{AA_1}{+A(b_n - A_1)}\right]e^{-c_2\tau}\right)\left[\frac{1-(-1)^n}{n\pi}\right] \\ \sum_{n=1}^{\infty}\sum_{n=1}^{\infty}\sum_{n=1}^{\infty}A_1 e^{-c_1\tau} + A_2(b_n - A_1)e^{(c_1 - c_2)\tau}. \end{array}\right)d\tau \qquad (3.180)$$

Where,

$$\left.\begin{array}{l} A_{49} = (A_{36} + A_{39} + A_{47}) \\ A_{50} = (A_{37} + A_{40} + A_{48}) \\ A_{51} = (A_{38} + A_{41}) \end{array}\right\}, \qquad (3.181)$$

Integrating (3.180) with respect to τ, we have

$$\phi_{1n}(t) = -2e^{-c_1 t}\left(\begin{array}{l} A_{49}\sum_{n=1}^{\infty} A\tau\Big|_0^t + A_{50}\sum_{n=1}^{\infty}\left[\frac{A}{c_1}e^{c_1\tau} + \left(\frac{b-A}{c_1-c_2}\right)e^{(c_1-c_2)\tau}\right]_0^t + \frac{A\,A}{c_1}e^{c_1\tau}\Big|_0^t \\ +A_{51}\sum_{n=1}^{\infty}\sum_{n=1}^{\infty} A_{52}\left[AA_1\tau - \frac{A(b_n-A_1)}{c_2}e^{-c_2\tau}\right]_0^t \\ A_{42}\sum_{n=1}^{\infty}\sum_{n=1}^{\infty} A_{52}\left[\frac{A^2}{c_1}e^{c_1\tau} + \frac{2A(b-A)}{c_1-c_2}e^{(c_1-c_2)\tau} + \frac{(b-A)^2}{(c_1-2c_2)}e^{(c_1-2c_2)\tau}\right]_0^t \\ \left[AA_1^2\tau - \frac{AA_1(b_n-A_1)}{c_2}e^{-c_2\tau}\right]_0^t \\ +A_{43}\sum_{n=1}^{\infty}\sum_{n=1}^{\infty}\sum_{n=1}^{\infty}\left[-\frac{AA_1(b_n-A_1)}{c_2}e^{-c_2\tau} - \frac{A(b_n-A_1)^2}{2c_2}e^{-2c_2\tau}\right]_0^t \\ -A_{44}\sum_{n=1}^{\infty}\sum_{n=1}^{\infty}\frac{A_{52}A^2}{c_1}e^{-c_1\tau}\Big|_0^t + A_{45}\sum_{n=1}^{\infty}\sum_{n=1}^{\infty}A_{52}\left[\frac{AA_1\tau}{c_2} - \frac{A(b_n-A_1)}{c_2}e^{-c_2\tau}\right]_0^t \\ -A_{46}\sum_{n=1}^{\infty}\sum_{n=1}^{\infty}\sum_{n=1}^{\infty}\left[\frac{A^2A}{c_1}e^{-c_1\tau} + \frac{A^2(b-A)}{(c_1+c_2)}e^{(c_1+c_2)\tau}\right]_0^t. \end{array}\right) \quad (3.182)$$

Where,

$$A_{52} = \left[\frac{1-(-1)^n}{n\pi}\right]. \quad (3.183)$$

That is we have,

$$\phi_{1n}(t)=\left(\begin{array}{l}
2A_{49}\sum_{n=1}^{\infty}Ate^{-c_1t}+2A_{50}\sum_{n=1}^{\infty}\left[\frac{A}{c_1}+\left(\frac{b-A}{c_1-c_2}\right)\right]e^{-c_2t}-\left[\frac{A_1(c_1-c_2)+c_1(b_n-A_1)}{c_1(c_1-c_2)}\right]e^{-c_1t} \\
+2\frac{A_{32}A_{52}}{c_1}\left[1-e^{-c_1t}\right]+2A_{51}\sum_{n=1}^{\infty}\sum_{n=1}^{\infty}A_{52}\left[\begin{array}{l}AAte^{-c_1t}-\frac{(b-A)}{c_2}e^{-(c_1+c_2)t} \\ +\frac{A(b_n-A_1)}{c_2}e^{-c_1t}\end{array}\right] \\
+2A_{42}\sum_{n=1}^{\infty}\sum_{n=1}^{\infty}A_{52}\left[\begin{array}{l}\frac{A_1^2}{c_1}+\frac{2A_1(b_n-A_1)}{c_1-c_2}e^{-c_2t}+\frac{(b_n-A_1)^2}{(c_1-2c_2)}e^{-2c_2t}-\frac{A_1^2}{c_1}e^{-c_1t} \\ -\frac{2A_1(b_n-A_1)}{c_1-c_2}e^{-c_1t}-\frac{(b_n-A_1)^2}{(c_1-2c_2)}e^{-c_2t}\end{array}\right] \\
+2A_{43}\sum_{n=1}^{\infty}\sum_{n=1}^{\infty}\sum_{n=1}^{\infty}\left[\begin{array}{l}AA_1^2te^{-c_1t}-\frac{AA_1(b_n-A_1)}{c_2}e^{-(c_1+c_2)t} \\ -\frac{AA_1(b_n-A_1)}{c_2}e^{-(c_1+c_2)t}-\frac{A(b_n-A_1)^2}{2c_2}e^{-(c_1+2c_2)t} \\ +\frac{AA_1(b_n-A_1)}{c_2}e^{-c_2t}+\frac{AA_1(b_n-A_1)}{c_2}e^{-c_1t}+\frac{A(b_n-A_1)^2}{2c_2}e^{-c_1t}\end{array}\right] \\
-2A_{44}\sum_{n=1}^{3}\sum_{n=1}^{3}\frac{A_{52}A^2}{c_1}\left[1-e^{-c_1t}\right]+2A_{45}\sum_{n=1}^{\infty}\sum_{52}^{\infty}A\left[\begin{array}{l}AA_1te^{-c_1t} \\ -\frac{A(b_n-A_1)}{c_2}e^{-(c_1+c_2)t} \\ +\frac{A(b_n-A_1)}{c_2}e^{-c_1t}\end{array}\right] \\
-2A_{46}\sum_{n=1}^{\infty}\sum_{n=1}^{\infty}\sum_{n=1}^{\infty}\left[\frac{A^2A}{c_1}e^{-2c_1t}+\frac{A^2(b-A)}{(c_1+c_2)}e^{-(2c_1+c_2)t}-\frac{A^2A}{c_1}e^{-c_1t}-\frac{A^2(b-A)}{(c_1+c_2)}e^{-c_1t}\right]
\end{array}\right) \tag{3.184}$$

That is,

$$\phi_{1n}(t) = \begin{pmatrix} 2A_{49}\sum_{n=1}^{\infty} Ate^{-c_1 t} + 2A_{50}\sum_{n=1}^{\infty}\left[\frac{A_1}{c_1} + A_{53}e^{-c_2 t} - A_{54}e^{-c_1 t}\right] \\ +A_{56}\left[1-e^{-c_1 t}\right]+2A_{51}\sum_{n=1}^{\infty}\sum_{n=1}^{\infty}\left[\frac{AA_1 te^{-c_1 t}}{A_{55}} - \frac{A_1}{A_{55}}e^{-(c_1+c_2)t}\right] \\ +2A_{42}\sum_{n=1}^{\infty}\sum_{n=1}^{\infty}A_{52}\left[\frac{A_1^2}{c_1} + A_{57}e^{-c_2 t} + A_{58}e^{-2c_2 t} - \frac{A_1^2}{c_1}e^{-c_1 t}\right. \\ \left. - A_{57}e^{-c_1 t} - A_{58}e^{-c_1 t}\right] \\ +4A_{43}\sum_{n=1}^{\infty}\sum_{n=1}^{\infty}\sum_{n=1}^{\infty}\left[-A_{59}e^{-2c_1 t} - A_{59}e^{-(c_1+c_2)t} - A_{60}e^{-(c_1+2c_2)t}\right. \\ \left. + A_{59}e^{-c_1 t} + A_{59}e^{-c_1 t} + A_{60}e^{-c_1 t}\right] \\ -2A_{44}\sum_{n=1}^{3}\sum_{n=1}^{3}A_{61}\left[1-e^{-c_1 t}\right]+2A_{45}\sum_{n=1}^{\infty}\sum_{n=1}^{\infty}A_{52}\left[\frac{AA_1 te^{-c_1 t}}{A_{55}} - A_{55}e^{-(c_1+c_2)t}\right. \\ \left. + A_{55}e^{-c_1 t}\right] \\ -2A_{46}\sum_{n=1}^{\infty}\sum_{n=1}^{\infty}\sum_{n=1}^{\infty}\left[A_{62}e^{-2c_1 t} + A_{63}e^{-(2c_1+c_2)t} - A_{62}e^{-c_1 t} - A_{63}e^{-c_1 t}\right] \end{pmatrix} \quad (3.185)$$

Where,

$$A_{53} = \frac{b_n - A_1}{c_1 - c_2} \qquad A_{59} = \frac{AA_1(b_n - A_1)}{c_2}$$

$$A_{54} = \frac{A_1(c_1 - c_2) + c_1(b_n - A_1)}{c_1(c_1 - c_2)} \qquad A_{60} = \frac{A(b_n - A_1)^2}{2c_2}$$

$$A_{55} = \frac{A(b_n - A_1)}{c_2} \qquad A_{61} = \frac{AA^2}{c_1}$$

$$A_{56} = 2\frac{A_{32}A_{52}}{c_1} \qquad A_{62} = \frac{A^2 A_1}{c_1}$$

$$A_{57} = \frac{2A_1(b_n - A_1)}{c_1 - c_2} \qquad A_{63} = \frac{A^2(b_n - A_1)}{(c_1 + c_2)}$$

$$A_{58} = \frac{(b_n - A_1)^2}{(c_1 - 2c_2)} \quad (3.186)$$

Now, we substitute (3.185) in (3.85) and obtain,

$$\phi_1(x,t)=\sum_{n=1}^{\infty}\Bigg(-2A_{49}\sum_{n=1}^{\infty}Ate^{-c_1t}-2A_{50}\sum_{n=1}^{\infty}\left[\frac{A_1}{c_1}+A_{53}e^{-c_2t}-A_{54}e^{-c_1t}\right]$$
$$-A_{56}\left[\frac{1-e^{-c_1t}}{2A_{51}}\right]\sum_{n=1}^{\infty}\sum_{n=1}^{\infty}A_{52}\left[AA_1te^{-c_1t}-\frac{A_1}{A_{55}}e^{-(c_1+c_2)t}+A_{55}e^{-c_1t}\right]$$
$$-2A_{42}\sum_{n=1}^{\infty}\sum_{n=1}^{\infty}A_{52}\left[\frac{A_1^2}{c_1}+A_{57}e^{-c_1t}+A_{58}e^{-2c_2t}-\frac{A_1^2}{c_1}e^{-c_1t}-A_{57}e^{-c_1t}-A_{58}e^{-c_1t}\right]$$
$$\Bigg)\sin n\pi x$$
$$\Bigg(-2A_{49}\sum_{n=1}^{\infty}\sum_{n=1}^{\infty}\sum_{n=1}^{\infty}\left[AA_1^2te^{-c_1t}-A_{59}e^{-(c_1+c_2)t}+A_{59}e^{-c_1t}+A_{59}e^{-c_1t}+A_{60}e^{-c_1t}\right]$$
$$+2A_{44}\sum_{n=1}^{3}\sum_{n=1}^{3}A_{61}\left[\frac{1-e^{-c_1t}}{2A_{45}}\right]\sum_{n=1}^{\infty}\sum_{n=1}^{\infty}A_{52}\left[\frac{AA_1te^{-c_1t}}{A_{55}}-A_{55}e^{-(c_1+c_2)t}+A_{55}e^{-c_1t}\right]$$
$$-2A_{42}\sum_{n=1}^{\infty}\sum_{n=1}^{\infty}\sum_{n=1}^{\infty}\left[A_{62}e^{-2c_1t}+A_{63}e^{-(2c_1+c_2)t}-A_{62}e^{-c_1t}-A_{63}e^{-c_1t}\right]\Bigg)\sin n\pi x \quad (3.187)$$

Finally, to obtain θ_1, we substitute (3.82), (3.83), (3.96), (3.131) and (3.132) in (3.80) and obtain,

$$\frac{\partial\theta_1}{\partial t}=\lambda_1\frac{\partial^2\theta_1}{\partial x^2}-(4R_a\in+\alpha_1)\theta_1-\sum_{n=1}^{\infty}n\pi\left(A_1+(b_n-A_1)e^{-c_2t}\right)\cos n\pi x$$
$$-a_4\left(\left(1+\frac{1}{2}\right)\left(\sigma_1+\sum_{n=1}^{\infty}\left(A_1+(b_n-A_1)e^{-c_2t}\right)\sin n\pi x\right)\right)$$
$$+r(e-2)\left(\sigma_1+\sum_{n=1}^{\infty}\left(A_1+(b_n-A_1)e^{-c_2t}\right)\sin n\pi x\right)\Bigg)+\cdots \quad (3.188)$$
$$+a_5\left(\sum_{n=1}^{\infty}Ae^{-c_1t}\sin n\pi x+q\left(1+(e-2)\left(\sigma_1+\sum_{n=1}^{\infty}\left(A_1+(b_n-A_1)e^{-c_2t}\right)\sin n\pi x\right)\right)\right)$$

$$\theta_1(x,0)=0,\quad \theta_1(0,t)=0,\quad \theta_1(1,t)=0$$

That is, we expand (3.188) and obtain,

$$\frac{\partial \theta_1}{\partial t} = \lambda_1 \frac{\partial^2 \theta_1}{\partial x^2} - \left(4R_a \in +\alpha_1\right)\theta_1 - \sum_{n=1}^{\infty} n\pi \left(A_1 + \left(b_n - A_1\right)e^{-c_2 t}\right)\cos n\pi x$$

$$-a_4 \left\{ \begin{array}{l} \left(1+r\left(e-2\right)\sigma_1\right)+r\left(e-2\right)\left(\sum_{n=1}^{\infty}\left(A_1+\left(b_n-A_1\right)e^{-c_2 t}\right)\sin n\pi x\right) \\ +\frac{1}{2}\in\left(1+r\left(e-2\right)\sigma_1\right)\sigma_1+\frac{1}{2}\in\left(r\left(e-2\right)\right)\sigma_1\sum_{n=1}^{\infty}\left(A_1+\left(b_n-A_1\right)e^{-c_2 t}\right)\sin n\pi x+ \\ \frac{1}{2}\in\left(1+r\left(e-2\right)\sigma_1\right)\sum_{n=1}^{\infty}\left(A_1+\left(b_n-A_1\right)e^{-c_2 t}\right)\sin n\pi x+\frac{1}{2}\in\left(r\left(e-2\right)\right). \\ \left(\sum_{n=1}^{\infty}\sum_{n=1}^{\infty} 2+2A_1\left(b_n-A_1\right)e^{-c_2 t}+\left(b_n-A_1\right)2e^{-2c_2 t}\right)\sin 2 \end{array} \right\}.$$

$$+a_5 \left\{ \begin{array}{l} \left(1+\left(e-2\right)\sigma_1\right)\sum_{n=1}^{\infty} Ae^{-c_1 t}\sin n\pi x+\left(e-2\right)\sum_{n=1}^{\infty}\sum_{n=1}^{\infty}\left(AA_1e^{-c_1 t}+A\left(b_n-A_1\right)e^{-\left(c_1+c_2\right)t}\right)\sin 2 n\pi x \\ +\left(1+\left(e-2\right)\sigma_1\right)q+\left(e-2\right)q\sum_{n=1}^{\infty}\left(A_1+\left(b_n-A_1\right)e^{-c_2 t}\right)\sin n\pi x \end{array} \right\} \quad (3.189)$$

$$\theta_1\left(x,0\right)=0, \quad \theta_1\left(0,t\right)=0, \quad \theta_1\left(1,t\right)=0$$

It implies that,

$$\frac{\partial \theta_1}{\partial t} = \lambda_1 \frac{\partial^2 \theta_1}{\partial x^2} - b_1\theta_1 - b_4$$

$$\theta_1\left(x,0\right)=0, \quad \theta_1\left(0,t\right)=0, \quad \theta_1\left(1,t\right)=0. \quad (3.190)$$

Where,

$$
\begin{aligned}
v_4 = \Bigg(& \sum_{n=1}^{\infty} n\pi \left(A_1 + \left(b_n - A_1 \right) e^{-c_2 t} \right) \cos n\pi x \\
& + a_4 \Bigg(A_{16} + A_{17} \left(\sum_{n=1}^{\infty} \left(A_1 + \left(b_n - A_1 \right) e^{-c_2 t} \right) \sin n\pi x \right) \\
& + A_{20} + A_{21} \sum_{n=1}^{\infty} \left(A_1 + \left(b_n - A_1 \right) e^{-c_2 t} \right) \sin n\pi x + \\
& A_{24} \sum_{n=1}^{\infty} \left(A_1 + \left(b_n - A_1 \right) e^{-c_2 t} \right) \sin n\pi x + \\
& A_{25} \left(\sum_{n=1}^{\infty} \sum_{n=1}^{\infty} \left(A_1^2 + 2 A_1 \left(b_n - A_1 \right) e^{-c_2 t} \right) + A_2^2 e^{-2c_2 t} \right) \sin^2 n\pi x \Bigg) \\
& - a_5 \Bigg(A_{10} \sum_{n=1}^{\infty} A e^{-c_1 t} \sin n\pi x + A \sum_{n=1}^{\infty} \sum_{n=1}^{\infty} \left(A A_1 e^{-c_1 t} + A \left(b_n - A_1 \right) e \right) \sin^2 n\pi x \Bigg) \\
& + A_{12} + A_{13} \sum_{n=1}^{\infty} \left(A_1 + \left(b_n - A_1 \right) e^{-c_2 t} \right) \sin n\pi x \Bigg) .
\end{aligned}
\tag{3.191}
$$

We then compare (3.190) with (3.84)—(3.88) and obtain,

$$
\left.
\begin{aligned}
& u = \theta_1, \quad k = \lambda_1, \quad \alpha = -b_1, \; F(x,t) = -b_4 \\
& f(x) = 0, \quad L = 1.
\end{aligned}
\right\}
\tag{3.192}
$$

So, it implies that,

$$
b_n = 0. \tag{3.193}
$$

Similarly,

$$
F_n(\mathrm{t}) = -2 \int_0^1 b_4 \sin n\pi x dx \, . \tag{3.194}
$$

That is, we substitute (3.191) into (3.194) and obtain,

$$F_n(t) = -2\int_0^1 \Bigg(\sum_{n=1}^{\infty} n\pi \left(A_1 + \left(b_n - A_1 \right) e^{-c_2 t} \right) \sin n\pi x \cos n\pi x + a_4 A_{16} \sin n\pi x + a_4 A_{17} \left(\sum_{n=1}^{\infty} \left(A_1 + \left(b_n - A_1 \right) e^{-c_2 t} \right) \sin^2 n\pi x \right) + a_4 A_{20} \sin n\pi x + a_4 A_{21} \sum_{n=1}^{\infty} \left(A_1 + \left(b_n - A_1 \right) e^{-c_2 t} \right) \sin^2 n\pi x + a_4 A_{24} \sum_{n=1}^{\infty} \left(A_1 + \left(b_n - A_1 \right) e^{-c_2 t} \right) \sin^2 n\pi x + a_4 A_{25} \left(\sum_{n=1}^{\infty} \sum_{n=1}^{\infty} \left(A_1^2 + 2 A_1 \left(b_n - A_1 \right) e^{-c_2 t} + \left(b_n - A_1 \right)^2 e^{-2c_2 t} \right) \sin^3 n\pi x \right) - a_5 A_{10} \sum_{n=1}^{\infty} A e^{-c_1 t} \sin^2 n\pi x - a_5 A_{11} \sum_{n=1}^{\infty} \sum_{n=1}^{\infty} \left(AA e^{-c_1 t} + A \left(b_n - A_1 \right) e^{-(c_1 + c_2)t} \right) \sin^2 n\pi x - a_5 A_{12} \sin n\pi x - a_5 A_{13} \sum_{n=1}^{\infty} \left(A_1 + \left(b_n - A_1 \right) e^{-c_2 t} \right) \sin^2 n\pi x. \Bigg) dx \qquad (3.195)$$

Integrating (3.195) we have,

$$
\begin{aligned}
F_n(t) = -2\Bigg| & \sum_{n=1}^{\infty} n\pi \left(A_1 + \left(b_n - A_1\right)e^{-c_2 t}\right)\left[-\frac{\cos 2n\pi x}{4n\pi}\right]_0^1 \\
& + a_4 A_{16}\left[-\frac{\cos n\pi x}{n\pi}\right]_0^1 + \frac{aA}{2}\sum_{n=1}^{\infty}\left(A_1 + \left(b_n - A_1\right)e^{-c_2 t}\right)\left[x - \sin\frac{2n\pi x}{2n\pi}\right]_0^1 \\
& + a_4 A_{20}\left[-\frac{\cos n\pi x}{n\pi}\right]_0^1 + \frac{aA}{2}\sum_{n=1}^{\infty}\left(A_1 + \left(b_n - A_1\right)e^{-c_2 t}\right)\left[x - \sin\frac{2n\pi x}{2n\pi}\right]_0^1 \\
& + \frac{aA}{2}\sum_{n=1}^{\infty}\left(A_1 + \left(b_n - A_1\right)e^{-c_2 t}\right)\left[x - \sin\frac{2n\pi x}{2n\pi}\right]_0^1 + \\
& \frac{aA}{4}\sum_{n=1}^{\infty}\sum_{n=1}^{\infty}\left(A_1^2 + 2A_1\left(b_n - A_1\right)e^{-c_2 t}\right)\left[\frac{\cos 3n\pi x}{3n\pi} - \frac{3\cos n\pi x}{n\pi}\right]_0^1 \\
& - \frac{aA}{2}\sum_{n=1}^{\infty} Ae^{-c_1 t}\left[x - \sin\frac{2n\pi x}{2n\pi}\right]_0^1 - \frac{aA}{4}\sum_{n=1}^{\infty}\sum_{n=1}^{\infty}\left(AA_1 e^{-c_1 t} + A\left(b_n - A_1\right)e^{-(c_1+c_2)t}\right)\left[\frac{\cos 3n\pi x}{3n\pi} - \frac{3\cos n\pi x}{n\pi}\right]_0^1 \\
& - a_5 A_{12}\left[\frac{\cos 2n\pi x}{4n\pi}\right]_0^1 - \frac{aA}{2}\sum_{n=1}^{\infty}\left(A_1 + \left(b_n - A_1\right)e^{-c_2 t}\right)\left[x - \sin\frac{2n\pi x}{2n\pi}\right]_0^1
\end{aligned}
\qquad (3.196)
$$

That is (3.196) becomes

$$
\begin{aligned}
F_n(t) = -2\Bigg| & A_{64}A_{52} + A_{65}\sum_{n=1}^{\infty}\left(A_1 + \left(b_n - A_1\right)e^{-c_2 t}\right) + A_{66}\sum_{n=1}^{\infty}\left(A_1 + \left(b_n - A_1\right)e^{-c_2 t}\right) \\
& + A_{67}\sum_{n=1}^{\infty}\left(A_1 + \left(b_n - A_1\right)e^{-c_2 t}\right) + A_{68}\sum_{n=1}^{\infty}\sum_{n=1}^{\infty}A_{52}\left(A_1^2 + 2A_1\left(b_n - A_1\right)e^{-c_2 t} + \left(b_n - A_1\right)^2 e^{-2c_2 t}\right) \\
& - A_{69}\sum_{n=1}^{\infty}Ae^{-c_1 t} - A_{70}\sum_{n=1}^{\infty}\sum_{n=1}^{\infty}A_{52}\left(AA_1 e^{-c_1 t} + A\left(b_n - A_1\right)e^{-(c_1+c_2)t}\right) - A_{71}\sum_{n=1}^{\infty}\left(A_1 + \left(b_n - A_1\right)e^{-c_2 t}\right)
\end{aligned}
\qquad (3.197)
$$

Where,

$$\left.\begin{aligned}
A_{64} &= \left(a_4 A_{16} + a_4 A_{20} - a_5 A_{12}\right) \\
A_{65} &= \frac{a_4 A_{17}}{2} \\
A_{66} &= \frac{a_4 A_{21}}{2} \\
A_{67} &= \frac{a_4^2 A_{24}}{2} \\
A_{68} &= \frac{2a_4 A_{25}}{3} \\
A_{69} &= \frac{a_5 A_{10}}{2} \\
A_{70} &= \frac{2a_5 A_{11}}{3} \\
A_{71} &= \frac{a_5 A_{13}}{2}
\end{aligned}\right\} \qquad (3.198)$$

This implies that,

$$F_n(t) = -2\left[\begin{array}{l}
A_{72} + A_{73}\sum_{n=1}^{\infty}\left(A_1 + \left(b_n - A_1\right)e^{-c_2 t}\right) \\
+A_{68}\sum_{n=1}^{\infty}\sum_{n=1}^{\infty}A_{52}\left(A_1^2 + 2A_1\left(b_n - A_1\right)e^{-c_2 t} + \left(b_n - A_1\right)^2 e^{-2c_2 t}\right) \\
-A_{69}\sum_{n=1}^{\infty}Ae^{-c_1 t} - A_{70}\sum_{n=1}^{\infty}\sum_{n=1}^{\infty}A_{52}\left(AA_1 e^{-c_1 t} + A\left(b_n - A_1\right)e^{-(c_1+c_2)t}\right)
\end{array}\right]. \qquad (3.199)$$

Where,

$$\left.\begin{aligned}
A_{72} &= \left(A_{64} A_{\infty}\right) \\
A_{73} &= \left(A_{65} + A_{66} + A_{67} - A_{71}\right)
\end{aligned}\right] \qquad (3.200)$$

Using (3.193) and (3.199) in (3.86) to have,

$$\theta_{1n}(t) = -2e^{-c_2 t}\int_0^t e^{c_2\tau}\left[\begin{array}{l} A_{72} + A_{73}\sum_{n=1}^{\infty}(A_1 + (b_n - A_1)e^{-c_2\tau}) \\ + A_{68}\sum_{n=1}^{\infty}\sum_{n=1}^{\infty} A_{52}\left(A_1^2 + 2A_1(b_n - A_1)e^{-c_2\tau} + (b_n - A_1)^2 e^{-2c_2\tau}\right) \\ - A_{69}\sum_{n=1}^{\infty} Ae^{-c_1\tau} - A_{70}\sum_{n=1}^{\infty}\sum_{n=1}^{\infty} A_{52}\left[\begin{array}{l} AA_1 e^{-c_1\tau} + \\ A(b_n - A_1)e^{-(c_1+c_2)\tau} \end{array}\right] \end{array}\right] d\tau. \quad (3.201)$$

That is,

$$\theta_{1n}(t) = -2e^{-c_2 t}\int_0^t \left[\begin{array}{l} A_{72}\int e^{c_2\tau} d\tau + A_{73}\sum_{n=1}^{\infty}\left(A_1 e^{c_2\tau} + (b_n - A_1)\right)d\tau \\ + A_{68}\sum_{n=1}^{\infty}\sum_{n=1}^{\infty} A_{52}\left(A_1^2 e^{c_2\tau} + 2A_1(b_n - A_1) + (b_n - A_1)^2 e^{-c_2\tau}\right)d\tau \\ -A_{69}\sum Ae^{(\quad)}\quad d\tau - A_{70}\sum_{n=1}^{\infty}\sum_{n=1}^{\infty} A_{52}\left[\begin{array}{l} (AAe^{(\quad} \\ A(b_n - A_1)e^{\quad} \end{array}\right] d\tau \end{array}\right]. \quad (3.202)$$

It implies that,

$$\theta_{1n}(t) = -2e^{-c_2 t}\left[\begin{array}{l} \left[\frac{A_{72}}{c_2}e^{c_2\tau}\right]_0^t + A_{73}\sum_{n=1}^{\infty}\left[\frac{A_1}{c_2}e^{c_2\tau} + (b_n - A_1)\tau\right]_0^t \\ + A_{68}\sum_{n=1}^{\infty}\sum_{n=1}^{\infty} A_{52}\left[\frac{A^2}{c_2}e^{c_2\tau} + 2A_1(b_n - A_1)\tau - \frac{(b_n - A_1)^2}{c_2}e^{-c_2\tau}\right]_0^t \\ - A_{69}\sum_{n=1}^{\infty}\frac{A}{(c_2 - c_1)}e^{(c_2 - c_1)\tau}\Big|_0^t - A_{70}\sum_{n=1}^{\infty}\sum_{n=1}^{\infty} A_{52}\left[\frac{AA_1}{(c_2 - c_1)}e^{(c_2 - c_1)\tau} - \frac{A(b - A)}{c_1}e^{-c_1\tau}\right] \end{array}\right] \quad (3.203)$$

That is,

$$\theta_{1n}(t) = -2e^{-c_2 t}\left(\begin{array}{l} \dfrac{A_{72}}{c_2}\left[e^{c_2 t}-1\right] + A_{73}\sum_{n=1}^{\infty}\left[\dfrac{A_1}{c_2}e^{c_2 t} + (b_n - A_1)t - \dfrac{A_1}{c_2}\right] \\ +A_{68}\sum_{n=1}^{\infty}\sum_{n=1}^{\infty}\left[\dfrac{A_2}{c_2}e^{c_2 t} + 2A_1(b_n - A_1)t - \dfrac{(b_n - A_1)^2}{c_2}e^{-c_2 t} - \dfrac{A_2}{c_2} - \dfrac{(b_n - A_1)^2}{c_2}\right] \\ -A_{69}\sum_{n=1}^{\infty}\dfrac{A_{52}}{(c_2 - c_1)}\left[e^{(c_2 - c_1)t} - 1\right] - A_{70}\sum_{n=1}^{\infty}\sum_{n=1}^{\infty}A_{52}\left[\dfrac{AA_1}{(c_2 - c_1)}e^{(c_2 - c_1)t} - \dfrac{A_1(b_n - A_1)}{c_1}e^{-c_1 t}\right] \\ \left[-\dfrac{AA_1}{c_2 - c_1} - \dfrac{A_1(b_n - A_1)}{c_1}\right] \end{array}\right). \qquad (3.204)$$

That is,

$$\theta_{1n}(t) = -2\left(\begin{array}{l} \dfrac{A_{72}}{c_2}\left[1 - e^{-c_2 t}\right] + A_{73}\sum_{n=1}^{\infty}\left[\dfrac{A_1}{c_2} + (b_n - A_1)te^{-c_2 t} - \dfrac{A_1}{c_2}e^{-c_2 t}\right] \\ +A_{68}\sum_{n=1}^{\infty}\sum_{n=1}^{\infty}\left[\dfrac{A_1^2}{2}\left|1 - e^{-c_2 t}\right| + 2A_1(b_n - A_1)te^{-c_2 t} + \left|e^{-c_2 t} - 1\right|\dfrac{(b_n - A_1)^2}{2}\right] \\ -A_{69}\sum_{n=1}^{\infty}\dfrac{A_{52}}{(c_2 - c_1)}\left|e^{-c_1 t} - e^{-c_2 t}\right| - A_{70}\sum_{n=1}^{\infty}\sum_{n=1}^{\infty}A_{52}\left[\dfrac{AA_1}{(c_2 - c_1)}e^{-c_1 t} - \dfrac{A_1(b_n - A_1)}{c_1}e^{-(c_2 + c_1)t}\right] \\ \left[-\dfrac{AA_1}{(c_2 - c_1)_1}e^{-c_2 t} + \dfrac{A_1(b_n - A_1)}{c}e^{-c_2 t}\right] \end{array}\right). \qquad (3.205)$$

Using (3.205) in (3.85) we have,

$$\theta_1(x,t)=\sum_{n=1}^{\infty}\left[\begin{array}{l}\left(-2\frac{A}{c_2}\left[1-e^{-c_2t}\right]-2A_7\sum_{n=1}^{\infty}\left[\frac{A}{c_2}+\left(b_n-A_1\right)te^{-c_2t}-\frac{A}{c_2}e^{-c_2t}\right]\right.\\ \left.-2A\sum_{n=1}^{\infty}\sum_{n=1}^{\infty}A\left[\left[1-e^{-c_2t}\right]\frac{A_1^2}{2}+2A\left(b-A\right)te^{-c_2t}+e^{-c_2t}-1\right]\frac{\left(b_n-A_1\right)^2}{2}\right]\\ +2A_{69}\sum_{n=1}^{\infty}\frac{A}{\left(c_2-c_1\right)}\left[e^{-c_1t}-e^{-c_2t}\right]+2A_{70}\sum_{n=1}^{\infty}\sum_{n=1}^{\infty}A_{52}\left[\frac{AA}{\left(c_2-c_1\right)}-\frac{A\left(b-A\right)}{c_1}e^{-c_1+c_1t}\right]\\ \left[-\frac{AA}{\left(c_2-c_1\right)}e^{-c_2t}+\frac{A\left(b_n-A_1\right)}{c_1}e^{-c_2t}\right]\end{array}\right]\sin n\pi x. \quad (3.206)$$

Then the solution for dimensionless equations (3.56) – (3.60) are;

$$\psi_1(x,t)=1+v\left[-A_3\sum_{n=1}^{\infty}A_2\sin n\pi x-a_6\left[t+\left[\left(f\left(e-2\right)\cdot\left(\sigma_1t+\sum_{n=1}^{\infty}\left[A_1t-\left(\frac{b_n-A_1}{c_2}\right)e^{-c_2t}\right]\right)\right)\sin\left(\frac{n\pi}{2}\right)x\right]\right], \quad (3.207)$$

$$\psi_2(x,t)=1+v\left[\begin{array}{l}-a_7\left[\begin{array}{l}t+r\left(e-2\right)\left[\sigma_1t+\sum_{n=1}^{\infty}\left[A_1t-\left(\frac{b_n-A_1}{c_2}\right)e^{-c_2t}\right]\sin n\pi x\right]+\\ \frac{1}{2}\in\left[\sigma_1t+\sum_{n=1}^{\infty}\left[A_1t-\left(\frac{b-A}{c_2}\right)e^{-c_2t}\right]\sin n\pi x\right]+\\ \left[\sigma_1^2t+2\sigma_1\sum_{n=1}^{\infty}\left[A_1t-\left(\frac{b-A}{c_2}\right)e^{-c_2t}\right]\sin n\pi x\right]\end{array}\right]\\ \frac{1}{2}\in\left(r\left(e-2\right)\right)\left[\begin{array}{l}A_1^2t-\frac{2A_1}{c_2}\left(b_n-A_1\right)e^{-c_2t}\\ +\sum_{n=1}^{\infty}\sum_{n=1}^{\infty}\left[\frac{\left(b_n-A_1\right)^2}{2c_2}e^{-2c_2t}\right]\end{array}\right]\sin^2 n\pi x\\ -a_7\left[A_7+\sum_{n=1}^{\infty}B_1\sin n\pi x\right]\left[\sum_{n=1}^{\infty}A_2\sin n\pi x\right]\end{array}\right], \quad (3.208)$$

$$\psi_3(x,t) = 1+\nu\left|\begin{array}{l} a_9\left|\begin{array}{l} A_8 t + A_9\sum_{n=1}^{\infty}\left(A_1 t - A_2 e^{-c_2 t}\right)\sin n\pi x \end{array}\right| \\ +a_8\left|\begin{array}{l} A_{10}\sum_{n=1}^{\infty}\dfrac{A}{c_1}e^{-c_1 t}\sin n\pi x + A_{11}\sum_{n=1}^{\infty}\sum_{n=1}^{\infty}\left(B_2 e^{-c_1 t} + B_3 e^{-(c_1+c_2)t}\right)\sin^2 n\pi x \\ -A_{12}\,t - A_{13}\sum_{n=1}^{\infty}\left(A_1 t - A_2 e^{-c_2 t}\right)\sin n\pi x \end{array}\right| \\ +a_9 A_9\sum_{n=1}^{\infty}A_2\sin n\pi x - a_8\left|\begin{array}{l} A_{10}\sum_{n=1}^{\infty}\dfrac{A}{c_1}\sin n\pi x + A_{11}\sum_{n=1}^{\infty}\sum_{n=1}^{\infty}\left(B_4\right)\sin^2 n\pi x \\ +A_{13}\sum_{n=1}^{\infty}A_2\sin n\pi x \end{array}\right| \end{array}\right|, \tag{3.209}$$

$$\phi(x,t) = \sum_{n=1}^{\infty}Ae^{-c_1 t}\sin n\pi x + \nu\left|\begin{array}{l} \sum_{n=1}^{\infty}\left|\begin{array}{l} -2A_{49}\sum_{n=1}^{\infty}Ate^{-c_1 t} - 2A_{50}\sum_{n=1}^{\infty}\left[\dfrac{A}{c_1} + A_{53}e^{-c_2 t} - A_{54}e^{-c_1 t}\right] \\ -A_{56}\left[1-e^{-c_1 t}\right] - 2A_{51}\sum_{n=1}^{\infty}\sum_{n=1}^{\infty}A_{52}\left|\begin{array}{l} \left[AA_1 te^{-c_1 t} - A_{55}e^{-(c_1+c_2)t}\right] \\ +A_{55}e^{-c_1 t} \end{array}\right| \\ -2A_{42}\sum_{n=1}^{\infty}\sum_{n=1}^{\infty}A_{52}\left|\begin{array}{l} \left[\dfrac{A_2}{c_1} + A_{57}e^{-c_2 t} + A_{58}e^{-2c_2 t} - \dfrac{A_2}{c_1}e^{-c_1 t}\right] \\ -Ae^{-c_1 t} - Ae^{-c_1 t} \end{array}\right| \\ -2A_{43}\sum_{n=1}^{\infty}\sum_{n=1}^{\infty}\sum_{n=1}^{\infty}\left|\begin{array}{l} \left[AA_1^2 te^{-c_1 t} - A_{59}e^{-(c_1+c_2)t}\right] \\ -A_{59}e^{-(c_1+c_2)t} - A_{60}e^{-(c_1+2c_2)t} \\ +A_{59}e^{-c_1 t} + A_{59}e^{-c_1 t} + A_{60}e^{-c_1 t} \end{array}\right| \\ +2A_{44}\sum_{n=1}^{3}\sum_{n=1}^{3}A_{61}\left[1-e^{-c_1 t}\right] - 2A_{45}\sum_{n=1}^{\infty}\sum_{n=1}^{\infty}A_{52}\left|\begin{array}{l} \left[AA_1 te^{-c_1 t}\right] \\ -Ae^{-(c_1+c_2)t} \\ +A_{55}e^{-c_1 t} \end{array}\right| \\ +2A_{46}\sum_{n=1}^{\infty}\sum_{n=1}^{\infty}\sum_{n=1}^{\infty}\left[A_{62}e^{-2c_1 t} + A_{63}e^{-(2c_1+c_2)t} - A_{62}e^{-c_1 t} - A_{63}e^{-c_1 t}\right] \end{array}\right|\sin n\pi x, \end{array}\right| \tag{3.210}$$

$$\theta(x,t)=\bigcup_{n=1}^{\infty}\left\{\left|\sigma_1+\sum^{\infty}\left(A_1+(b_n-A_1)e^{-c_2 t}\right)\sin n\pi x\right|+\right.$$

$$\left.\left|\left(-2\frac{A}{c_2}\left[1-e^{-c_2 t}\right]\sum_{n=1}^{\infty}\left[\frac{A_1}{c_2}+(b_n-A_1)te^{-c_2 t}-\frac{A_1}{c_2}e^{-c_2 t}\right]\right.\right.\right.$$

$$\left.\left.\left.\left[\frac{A_2}{c_2}\left[1-e^{-c_2 t}\right]+2A_1(b_n-A_1)te^{-c_2 t}\right]\right.\right.\right.$$

$$\left.\left.\left.-2A_{68}\sum_{n=1}^{\infty}\sum_{n=1}^{\infty}A_{52}\left[+\left[e^{-c_2 t}-1\right]\frac{(b_n-A_1)^2}{c_2}\right]\right.\right.\right.$$

$$\left.\left.\left.\sum_{n=1}^{\infty}\left[\frac{AA}{(c_2-c_1)}e^{-c_1 t}-\frac{A(b-A_1)}{c_1}e^{-c_2 t}\right]\right.\right.\right.$$

$$\left.\left.\left.+2A_{69}\sum_{n=1}^{\infty}\frac{A}{\left(c_2-c_1\right)}\left[e^{-c_1 t}-e^{-c_2 t}\right]+2A_{70}\sum_{n=1}^{\infty}\sum_{n=1}^{\infty}A_{52}\left[-\frac{AA}{c_2-c_1}e^{-c_2 t}+\frac{A(b_n-A_1)}{c_1}e^{-c_2 t}\right]\right.\right.\right.$$

$$\left.\left.\left.\sin n\pi x\right.\right.\right\}. \quad (3.211)$$

The computations were done using Maple 17 and the graphs generated were shown and discuss in Chapter four.

CHAPTER FOUR

4.0 RESULTS AND DISCUSSION

4.1 Results

To conclude this analysis we examine the effects of the Frank-Kamenetskii numbers (δ, δ_1), Radiation number (R_a), Peclet energy number (P_e), Peclet mass number (P_{em}), Activation energy number $(\in)$and the Equilibrium wind velocity (v) on the transient state temperature $\theta(x, t)$, the oxygen concentration $\phi(x, t)$, the volume fraction of dry organic substance $\psi_1(x, t)$, the volume fraction of moisture $\psi_2(x, t)$ and the volume fraction of coke $\psi_3(x, t)$. Analytical solutions given by equation (3.207), (3.208), (3.209), (3.210) and (3.211) were computed using computer symbolic algebraic package MAPLE 17. The numerical results obtained from the solutions are shown in Figure 4.1 to 4.46. The effect of Frank-Kamenetskii number (δ) on temperature $\theta(x, t)$ against distance is depicted in figure 4.1. The effect of Frank-Kamenetskii number (δ) on temperature $\theta(x, t)$ against time is depicted in figure 4.2. The effect of Frank-Kamenetskii number (δ) on temperature $\theta(x, t)$ against distance and time is depicted in figure 4.3. The effect of Radiation number (R_a)on temperature $\theta(x, t)$ against distance is depicted in figure 4.4. The effect of Radiation number (R_a)on temperature $\theta(x, t)$ against time is depicted in figure 4.5. The effect of Radiation number (R_a)on temperature $\theta(x, t)$ against distance and time is depicted in figure 4.6. The effect of Radiation number (R_a)on oxygen concentration

$\phi(x, t)$ against distance is depicted in figure 4.7. The effect of Radiation number (R_a) on oxygen concentration $\phi(x, t)$ against distance and time is depicted in figure 4.8. The effect of Radiation number (R_a) on volume fraction of dry organic substance $\psi_1(x, t)$ against distance is depicted in figure 4.9. The effect of Radiation number (R_a) on volume fraction of dry organic substance $\psi_1(x, t)$ against time is depicted in figure 4.10. The effect of Radiation number (R_a) on volume fraction of dry organic substance $\psi_1(x, t)$ against distance and time is depicted in figure 4.11. The effect of Radiation number (R_a) on volume fraction of moisture $\psi_2(x, t)$ against distance is depicted in figure 4.12. The effect of Radiation number (R_a) on volume fraction of moisture $\psi_2(x, t)$ against time is depicted in figure 4.13. The effect of Radiation number (R_a) on volume fraction of moisture $\psi_2(x, t)$ against distance and time is depicted in figure 4.14. The effect of Radiation number (R_a) on volume fraction of coke $\psi_3(x, t)$ against distance is depicted in figure 4.15. The effect of Radiation number (R_a) on volume fraction of coke $\psi_3(x, t)$ against time is depicted in figure 4.16. The effect of Radiation number (R_a) on volume fraction of coke $\psi_3(x, t)$ against distance and time is depicted in figure 4.17. The effect of Peclet energy number (P_e) on temperature $\theta(x, t)$ against distance is depicted in figure 4.18. The effect of Peclet energy number (P_e) on temperature $\theta(x, t)$ against time is depicted in figure 4.19. The effect of Peclet energy number (P_e) on temperature $\theta(x, t)$

against distance and time is depicted in figure 4.20. The effect of Peclet energy number (P_e) on oxygen concentration $\phi(x, t)$ against distance is depicted in figure 4.21. The effect of Peclet energy number (P_e) on volume fraction of dry organic substance $\psi_1(x, t)$ against distance is depicted in figure 4.22. The effect of Peclet energy number (P_e)on volume fraction of dry organic substance $\psi_1(x, t)$ against time is depicted in figure 4.23. The effect of Peclet energy number (P_e) on volume fraction of dry organic substance $\psi_1(x, t)$ against distance and time is depicted in figure 4.24. The effect of Peclet energy number (P_e) on volume fraction of moisture $\psi_2(x, t)$ against distance is depicted in figure 4.25. The effect of Peclet energy number (P_e) on volume fraction of moisture $\psi_2(x, t)$ against time is depicted in figure 4.26. The effect of Peclet energy number (P_e) on volume fraction of moisture against distance and time is depicted in figure 4.27. The effect of Peclet energy number (P_e) on volume fraction of coke $\psi_3(x, t)$ against distance is depicted in figure 4.28. The effect of Peclet energy number (P_e) on volume fraction of coke $\psi_3(x, t)$ against time is depicted in figure 4.29. The effect of Peclet energy number (P_e) on volume fraction of coke $\psi_3(x, t)$ against distance and time is depicted in figure 4.30. The effect of Peclet mass number (P_{em}) on oxygen concentration $\phi(x, t)$ against distance is depicted in figure 4.31. The effect of Peclet mass number (P_{em}) on oxygen concentration $\phi(x, t)$ against time is depicted in figure 4.32. The effect of Peclet mass number (P_{em}) on oxygen concentration $\phi(x, t)$ against distance and time is depicted in figure 4.33. The effect of dimensionless

Activation energy number $(\in)$ on temperature $\theta(x, t)$ against distance is depicted in figure 4.34. The effect of dimensionless Activation energy number $(\in)$ on temperature $\theta(x, t)$ against time depicted in figure 4.35. The effect of dimensionless Activation energy number $(\in)$ on temperature $\theta(x, t)$ against distance and time depicted is depicted in figure 4.36. The effect of dimensionless Activation energy number $(\in)$ on volume fraction of dry organic substance $\psi_1(x, t)$ against distance is depicted in figure 4.37. The effect of dimensionless Activation energy number $(\in)$ on volume fraction of dry organic substance $\psi_1(x, t)$ against time is depicted in figure 4.38. The effect of dimensionless Activation energy number $(\in)$ on volume fraction of dry organic substance $\psi_1(x, t)$ against distance and time is depicted in figure 4.39. The effect of dimensionless Activation energy number $(\in)$ on volume fraction of moisture $\psi_2(x, t)$ against distance is depicted in figure 4.40. The effect of dimensionless Activation energy number $(\in)$ on volume fraction of moisture $\psi_2(x, t)$ against time is depicted in figure 4.41. The effect of dimensionless Activation energy number $(\in)$ on volume fraction of moisture $\psi_2(x, t)$ against distance and time is depicted in figure 4.42. The effect of dimensionless Activation energy number $(\in)$ on volume fraction of coke $\psi_3(x, t)$ against distance is depicted in figure 4.43. The effect of dimensionless Activation energy number $(\in)$on volume fraction of coke $\psi_3(x, t)$ against

time is depicted in figure 4.44. The effect of dimensionless Activation energy number $(\in)$ on volume fraction of coke $\psi_3\,(x\,,\,t\,)$ against distance and time is depicted in figure 4.45.

The effect of Equilibrium wind velocity $(v\,)$ on oxygen concentration $\phi\,(x\,,\,t\,)$ against distance depicted in figure 4.46.

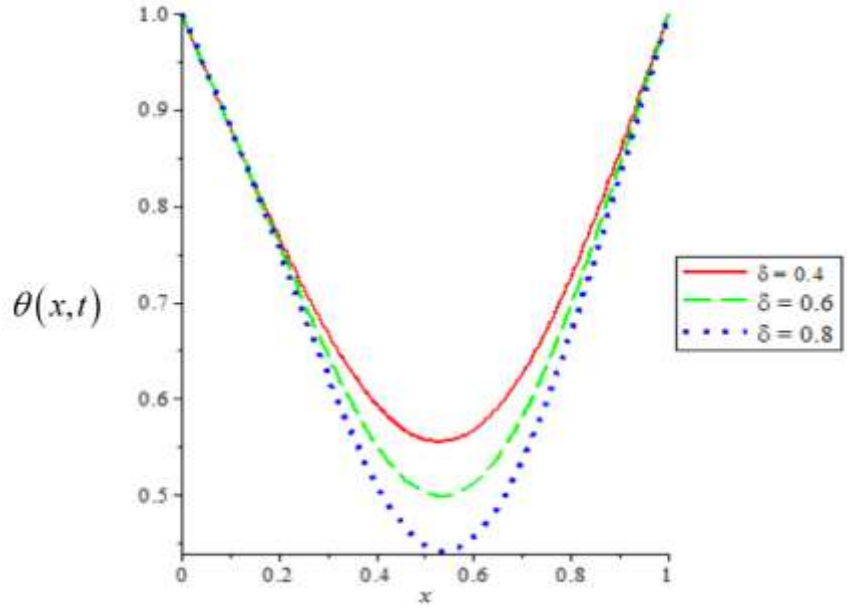

Figure 4.1: Graph of temperature $\theta(x, t)$ against distance *x* for different values of Frank-Kamenetskii number (δ). $(\delta) = 0.4$ (Red), $(\delta) = 0.6$ (Green) and $(\delta) = 0.8$ (Blue).

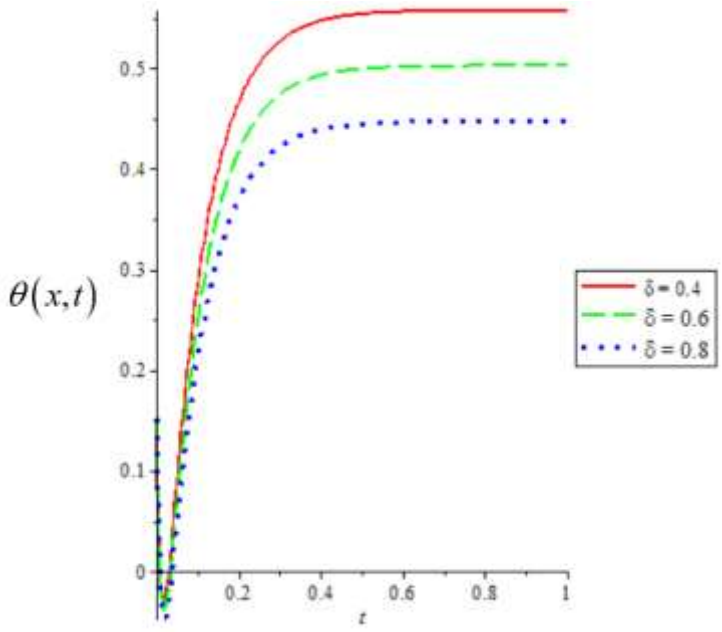

Figure 4.2: Graph of temperature $\theta(x, t)$ against time t for different values of Frank-Kamenetskii number (δ). $(\delta) = 0.4$ (Red), $(\delta) = 0.6$ (Green) and $(\delta) = 0.8$ (Blue).

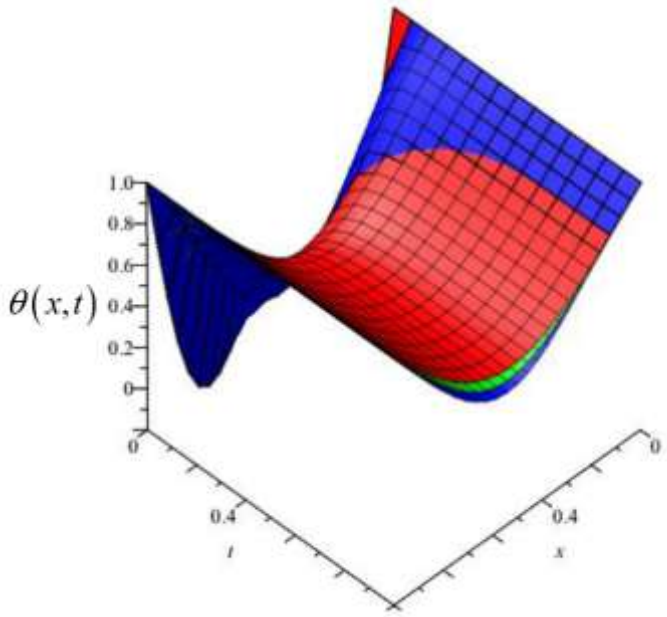

Figure 4.3: Graph of temperature $\theta(x,t)$ against distance x and time t for different values of Frank-Kamenetskii number (δ). $(\delta) = 0.4$ (Red), $(\delta) = 0.6$ (Green) and $(\delta) = 0.8$ (Blue).

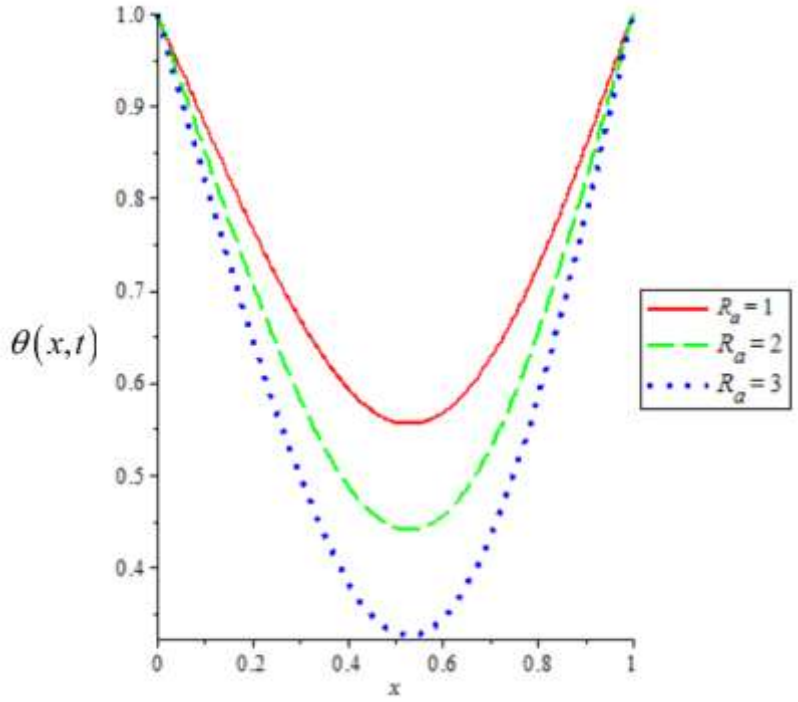

Figure 4.4: Graph of temperature $\theta(x, t)$ against distance x for different values of Radiation number (R_a). (R_a) =1 (Red), $(R_a) = 2$ (Green) and $(R_a) = 3$ (Blue).

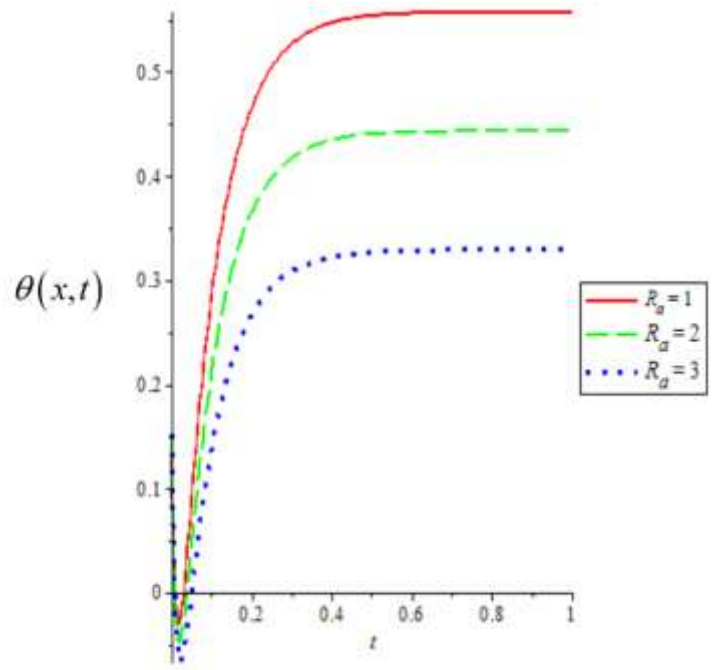

Figure 4.5: Graph of temperature $\theta\left(x\,,\,t\,\right)$ against time t for different values of $\left(R_a\,\right)$ =1 (Red),

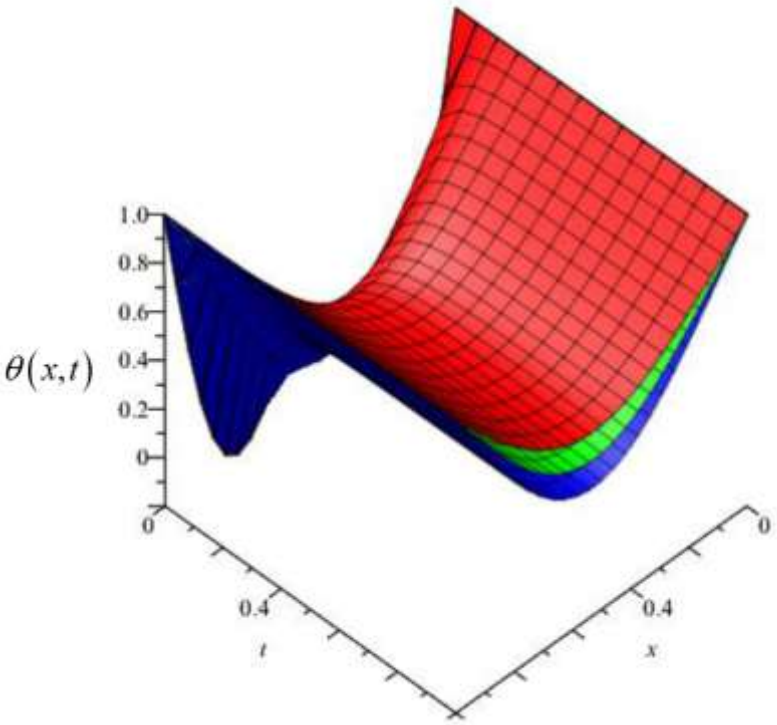

Figure 4.6: Graph of temperature $\theta\left(x\,,\,t\,\right)$ against distance x and time t for different values of Radiation number $\left(R_a\,\right)$. $\left(R_a\,\right)$ =1 (Red), $\left(R_a\,\right)=2$ (Green) and $\left(R_a\,\right)=3$ (Blue).

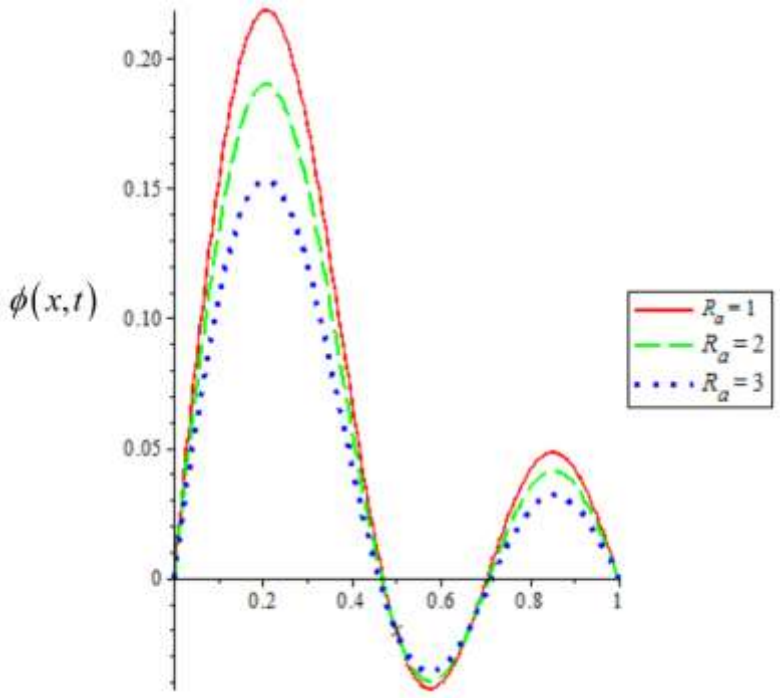

Figure 4.7: Graph of oxygen concentration $\phi\left(x\,,\,t\right)$ against distance x for different values of Radiation number $\left(R_a\right)$. $\left(R_a\right)$ =1 (Red), $\left(R_a\right)$ = 2 (Green) and $\left(R_a\right)$ = 3 (Blue).

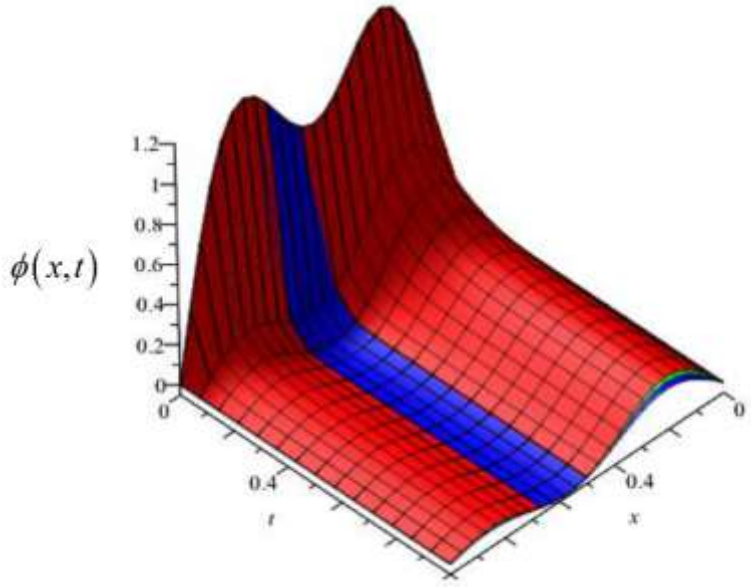

Figure 4.8: Graph of oxygen concentration $\phi\left(x\,,\,t\right)$ against distance x and time t for different values of Radiation number $\left(R_a\right)$. $\left(R_a\right)$ =1 (Red), $\left(R_a\right)$ = 2 (Green) and $\left(R_a\right)$ = 3 (Blue).

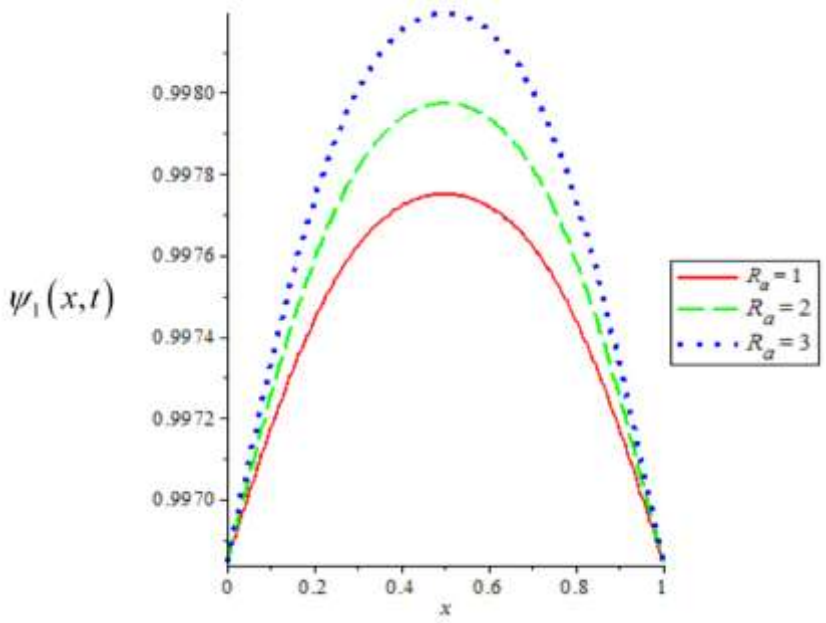

Figure 4.9: Graph of volume fraction of dry organic substance $\psi_1(x, t)$ against distance x for different values of Radiation number (R_a). $(R_a) = 2$ (Green) and $(R_a) = 1$ (Red), $(R_a) = 3$ (Blue).

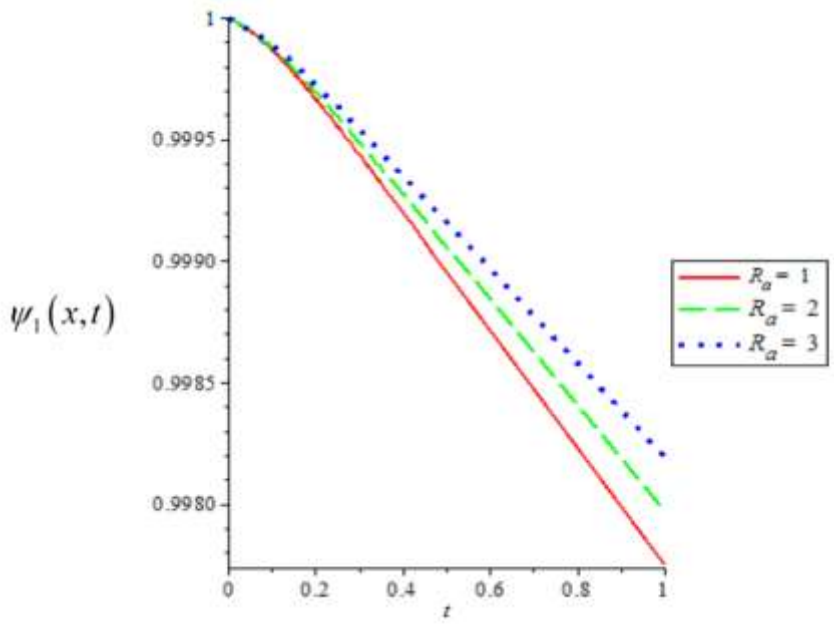

Figure 4.10: Graph of volume fraction of dry organic substance $\psi_1(x, t)$ against time t for different values of Radiation number (R_a). $(R_a) = 1$ (Red), $(R_a) = 2$ (Green) and $(R_a) = 3$ (Blue).

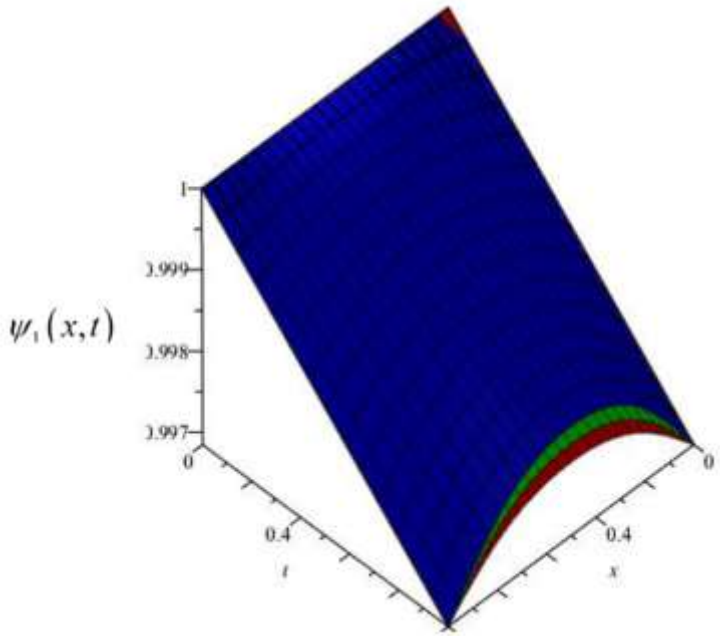

Figure 4.11: Graph of volume fraction of dry organic substance $\psi_1\ (x\ ,\ t\ )$ against distance x and time t for different values of Radiation number $(R_a\ )$. $(R_a\ ) = 1$ (Red), $(R_a\ ) = 2$ (Green) and $(R_a\ ) = 3$ (Blue).

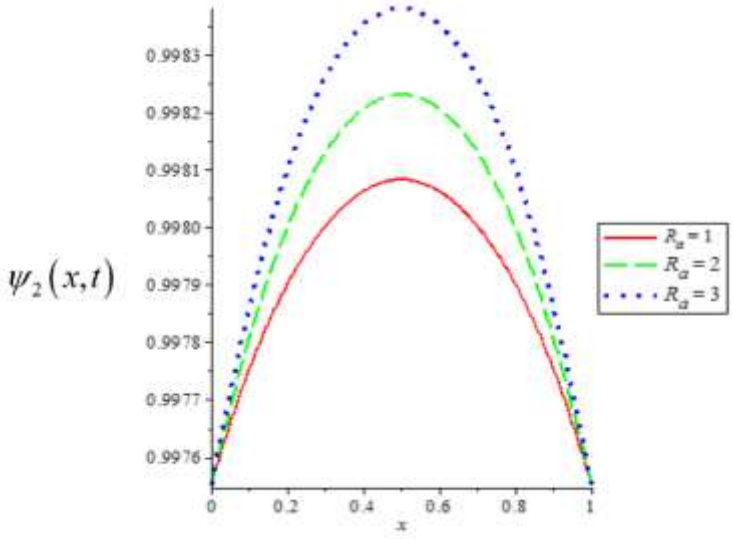

Figure 4.12: Graph of volume fraction of moisture $\psi_2\ (x\ ,\ t\ )$ against distance x for different values of Radiation number $(R_a\ )$. $(R_a\ ) = 1$ (Red), $(R_a\ ) = 2$ (Green) and $(R_a\ ) = 3$ (Blue).

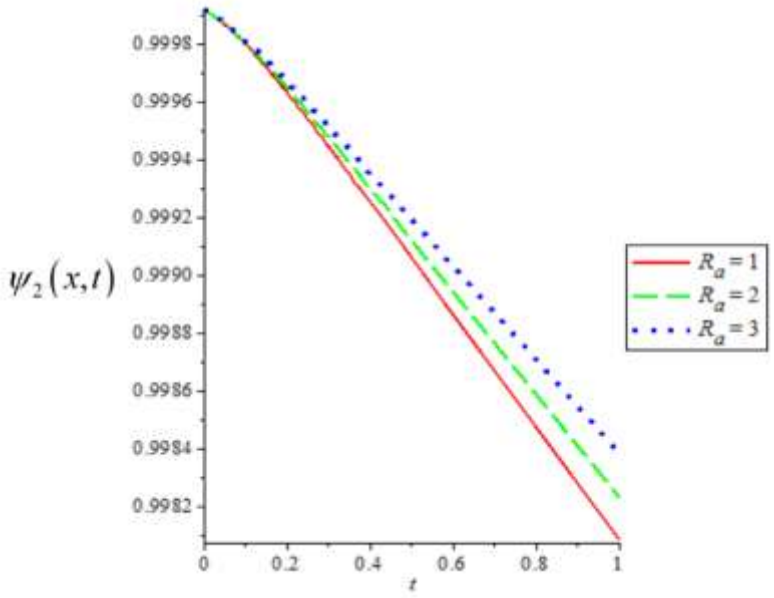

Figure 4.13: Graph of volume fraction of moisture $\psi_2(x, t)$ against time t for different values of Radiation number (R_a). $(R_a) = 1$ (Red), $(R_a) = 2$ (Green) and $(R_a) = 3$ (Blue).

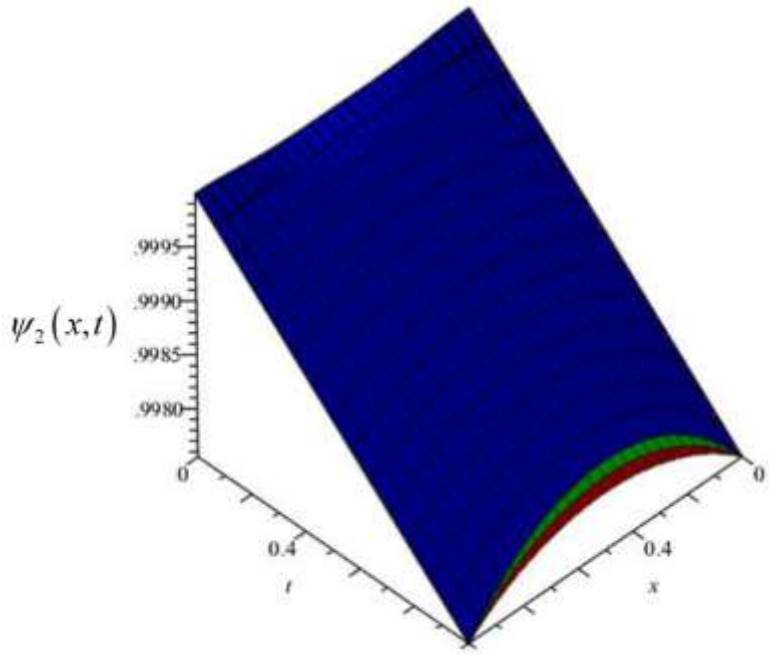

Figure 4.14: Graph of volume fraction of moisture $\psi_2(x, t)$ against distance x and time t for different values of Radiation number (R_a). $(R_a) = 1$ (Red), $(R_a) = 2$ (Green) and $(R_a) = 3$ (Blue).

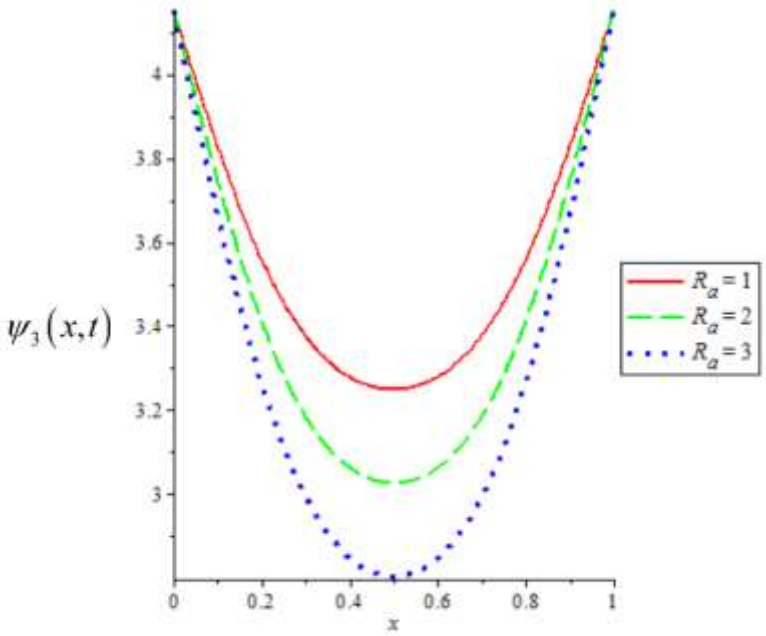

Figure 4.15: Graph of volume fraction of coke $\psi_3\ (x\ ,\ t\ )$ against distance x for different values of Radiation number $(R_a\ )$. $(R_a\ ) = 1$ (Red), $(R_a\ ) = 2$ (Green) and $(R_a\ ) = 3$ (Blue).

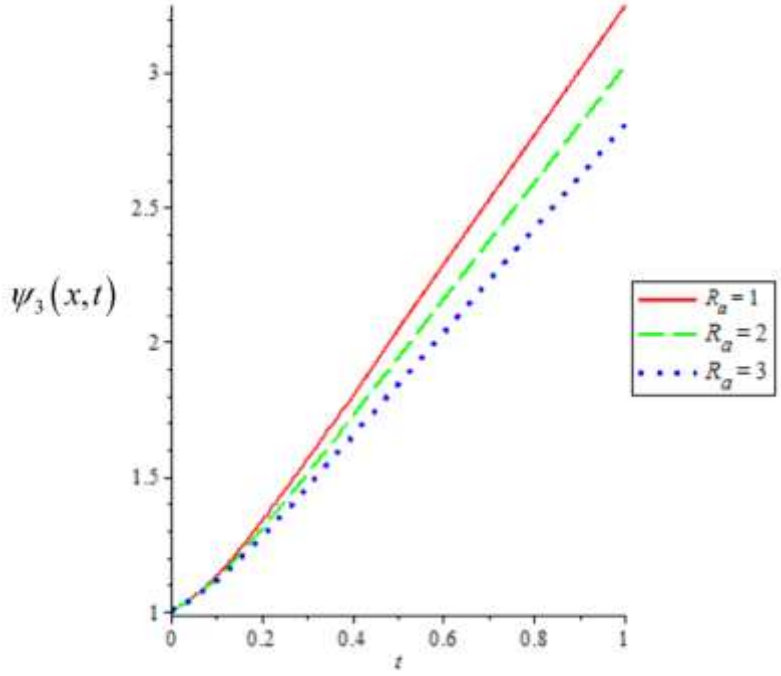

Figure 4.16: Graph of volume fraction of coke $\psi_3\ (x\ ,\ t\ )$ against time t for different values of Radiation number $(R_a\ )$. $(R_a\ ) = 1$ (Red), $(R_a\ ) = 2$ (Green) and $(R_a\ ) = 3$ (Blue).

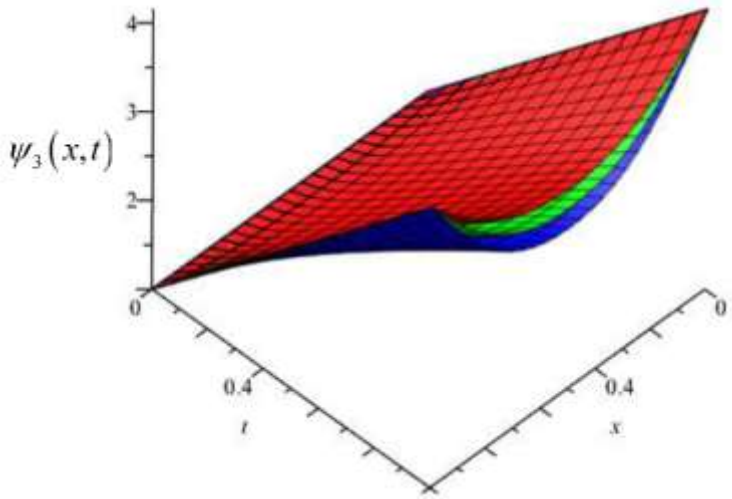

Figure 4.17: Graph of volume fraction of coke $\psi_3\ (x\ ,\ t\ )$ against distance x and time t for different values of Radiation number $(R_a\ )$. $(R_a\ ) = 1$ (Red), $(R_a\ ) = 2$ (Green) and $(R_a\ ) = 3$ (Blue).

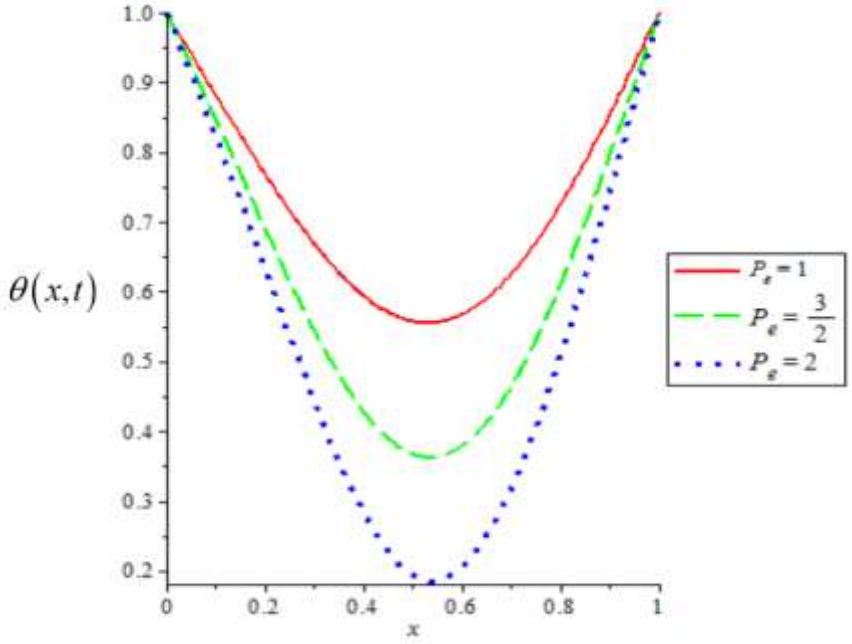

Figure 4.18: Graph of temperature $\theta\ (\ x\ ,\ t\ )$ against distance x for different values of Peclet energy number $(P_e\ )$. $(P_e\ ) = 1$ (Red), $(P_e) = \frac{2}{3}$ (Green) and $(P_e\ ) = 2$ (Blue).

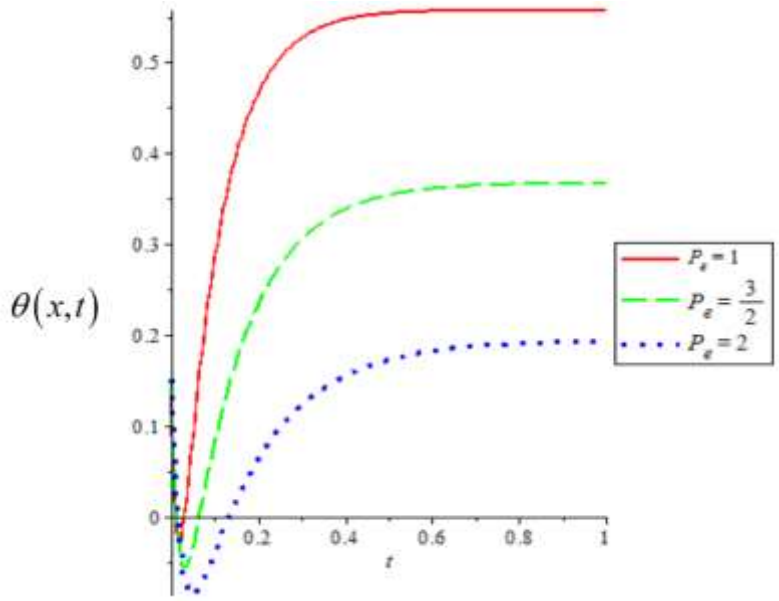

Figure 4.19: Graph of temperature $\theta(x, t)$ against time t for different values of Peclet energy number (P_e). $(P_e) = 1$ (Red), $P_e = \frac{3}{2}$ (Green) and $(P_e) = 2$ (Blue).

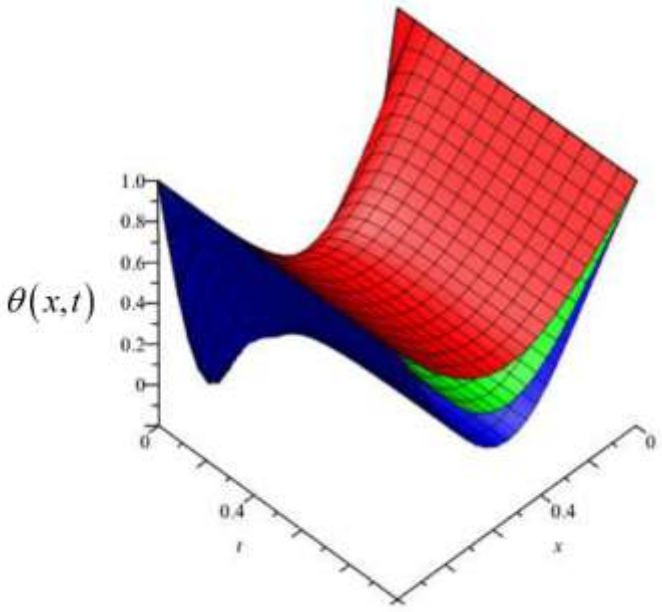

Figure 4.20: Graph of temperature $\theta(x, t)$ against distance x and time t for different values of Peclet energy number (P_e). $(P_e) = 1$ (Red), $P_e = \frac{3}{2}$ (Green) and $(P_e) = 2$ (Blue).

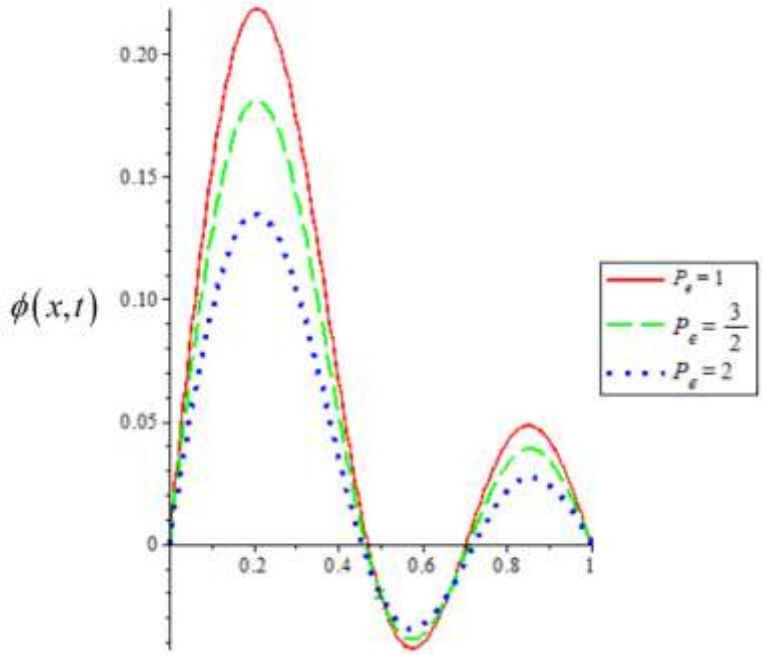

Figure 4.21: Graph of oxygen concentration $\phi(x, t)$ against distance x for different values of Peclet energy number (P_e). $(P_e) = 1$ (Read), $P_e = \frac{3}{2}$ (Green) and $(P_e) = 2$ (Blue).

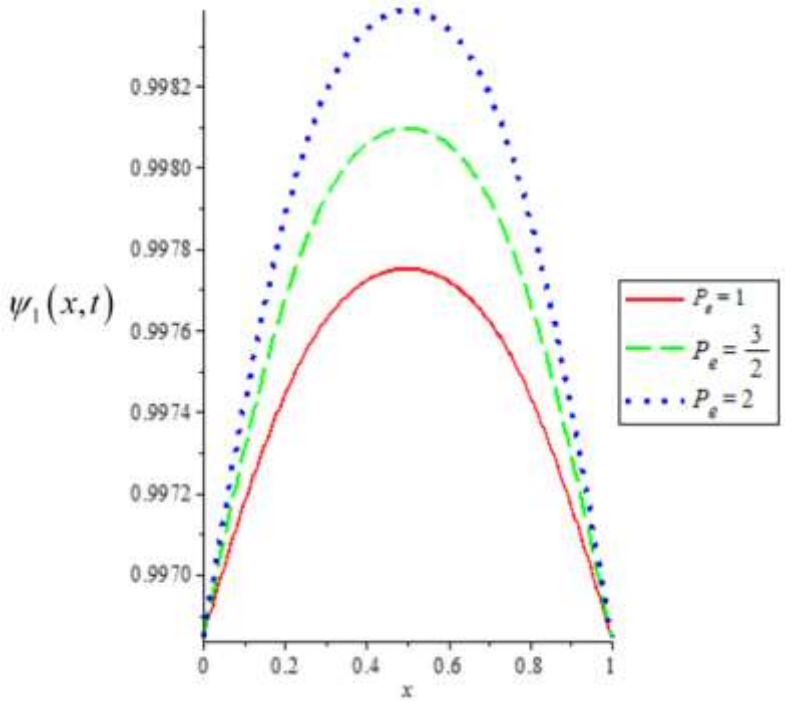

Figure 4.22: Graph of volume fraction of dry organic substance $\psi_1(x, t)$ against distance x for differentvalues of Peclet energy number (P_e). $(P_e) = 1$ (Red), $P_e = \frac{3}{2}$ (Green) and $(P_e) = 2$ (Blue).

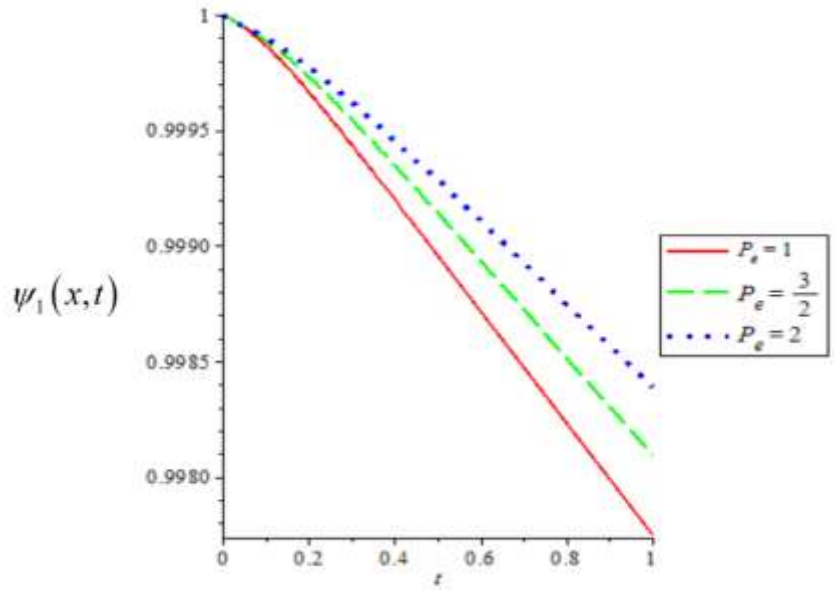

Figure 4.23: Graph of volume fraction of dry organic substance $\psi_1(x,t)$ against time t for different values of Peclet energy number (P_e). (P_e) =1 (Red), $P_e = \frac{2}{3}$ (Green) and $(P_e) = 2$ (Blue).

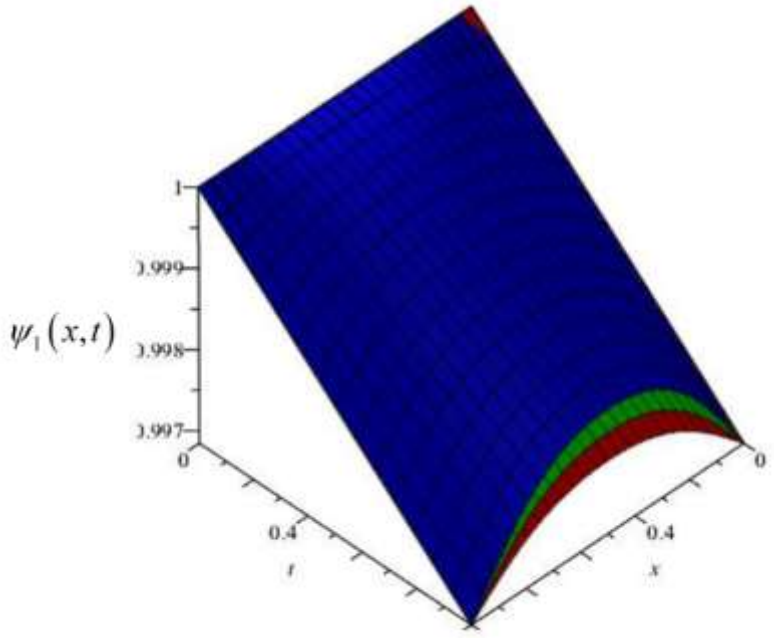

Figure 4.24: Graph of volume fraction of dry organic substance $\psi_1(x,t)$ against distance x and time t for different values of Peclet energy number (P_e). (P_e) =1 (Red), $P_e = \frac{2}{3}$ (Green) and $(P_e) = 2$ (Blue).

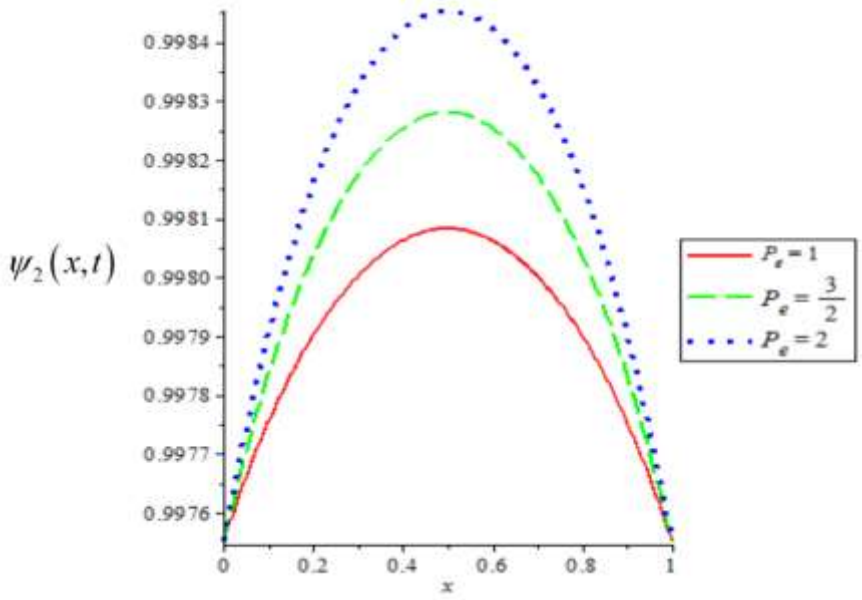

Figure 4.25: Graph of volume fraction of moisture $\psi_2(x,t)$ against distance x for different values of Peclet energy number (P_e). (P_e) =1 (Red), $(P_e) = \frac{3}{2}$ (Green) and $(P_e) = 2$ (Blue).

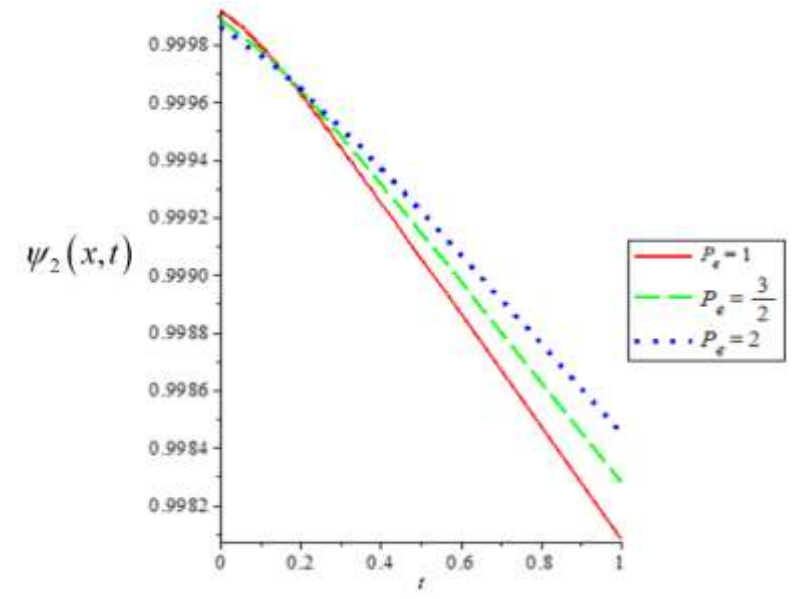

Figure 4.26: Graph of volume fraction of moisture $\psi_2(x,t)$ against time t for different values of Peclet energy number (P_e). (P_e) =1 (Red), $(P_e) = \frac{3}{2}$ (Green) and $(P_e) = 2$ (Blue).

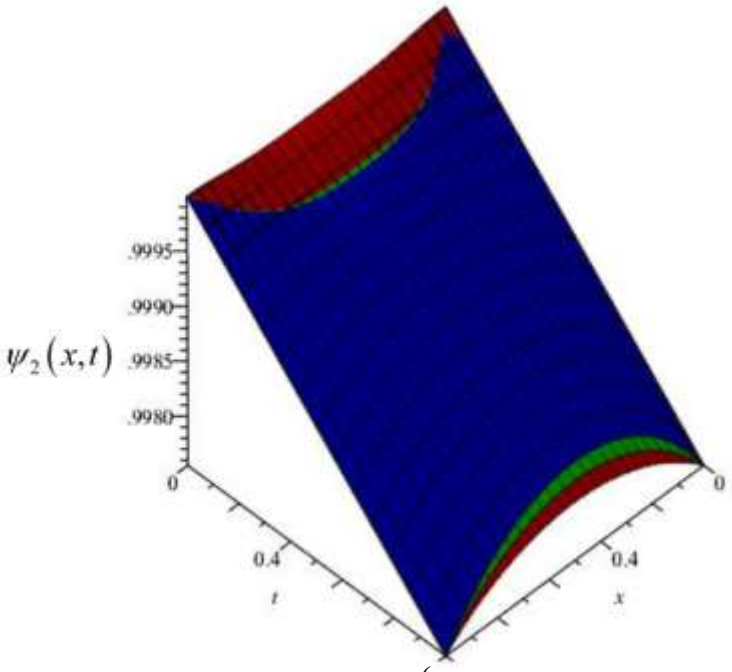

Figure 4.27: Graph of volume fraction of moisture ψ_2 (x , t) against distance x and time t for different values of Peclet energy number (P_e). (P_e) =1 (Red), $P_e = \frac{3}{2}$ (Green) and $(P_e) = 2$ (Blue).

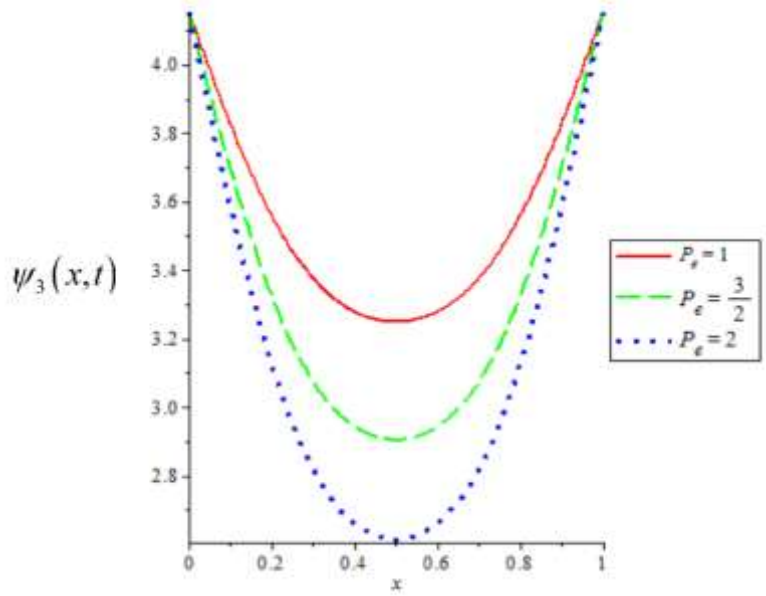

Figure 4.28: Graph of volume fraction of coke ψ_3 (x , t) against distance x for different values of Peclet energy number (P_e). (P_e) =1 (Red), $P_e = \frac{3}{2}$ (Green) and $(P_e) = 2$ (Blue).

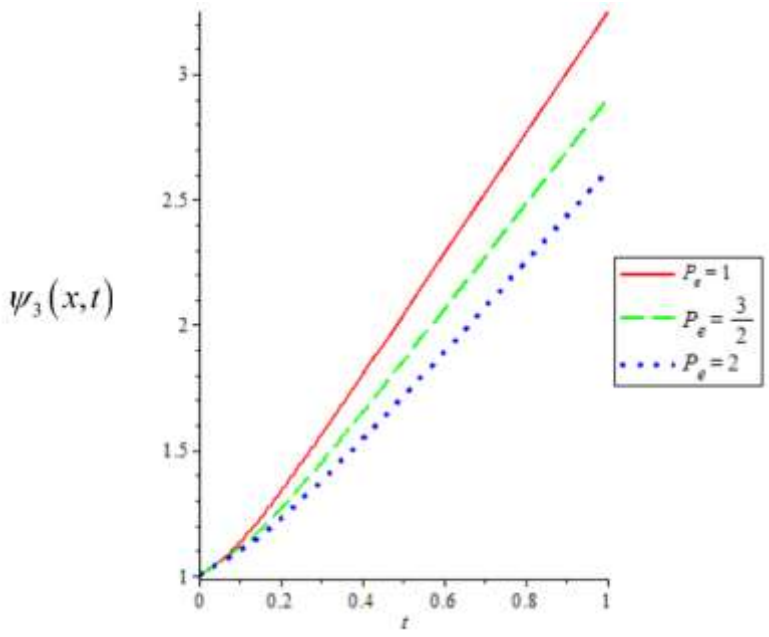

Figure 4.29: Graph of volume fraction of coke $\psi_3(x, t)$ of Peclet energy number (P_e). $(Pe) = 1$ (Red), $(P_e) = \frac{3}{2}$ (Green) and $(P_e) = 2$ (Blue).

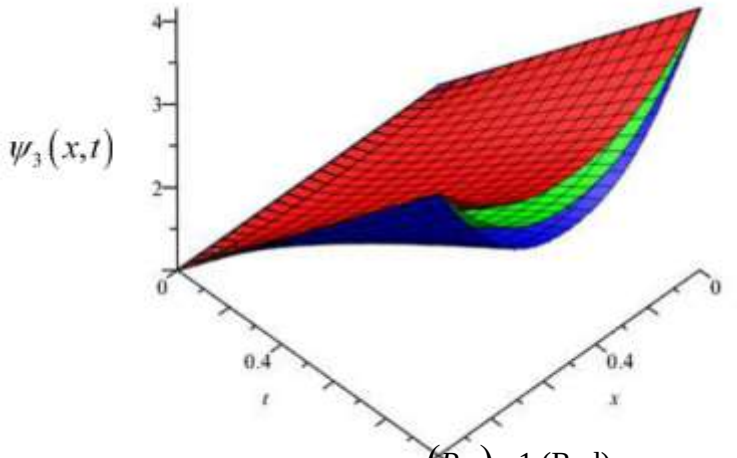

Figure 4.30: Graph of volume fraction of coke $\psi_3(x, t)$ different values of Peclet energy number (P_e). $(P_e) = 1$ (Red), $(P_e) = 2$ (Blue).

against time t for different values

$(P_e) = 2$ (Blue).

against distance x and time t for

$(\underline{P}_e) = 3$ (Green) and

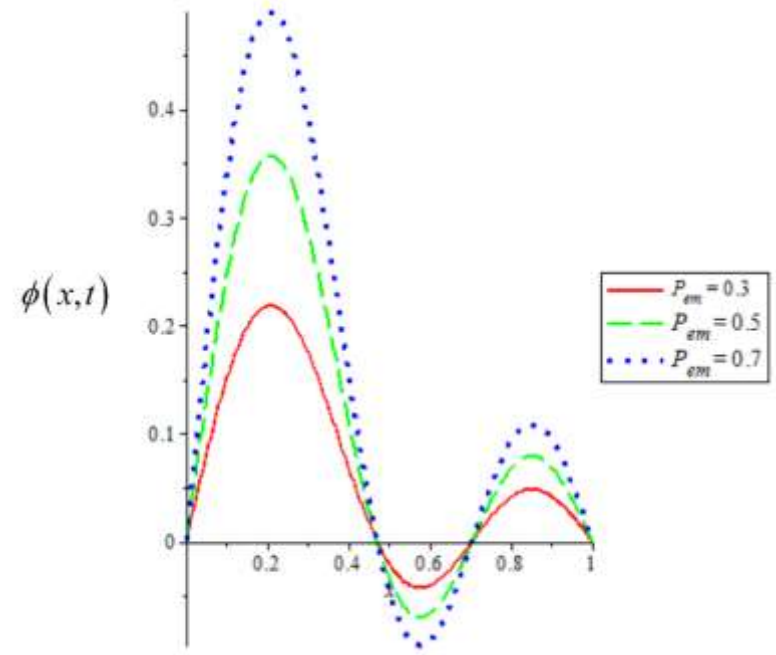

Figure 4.31: Graph of oxygen concentration $\phi\left(x\,,\,t\right)$ against distance x for different values of Peclet mass number $\left(P_{em}\right)$. $\left(P_{em}\right)$ = 0.3 (Red), $\left(P_{em}\right)$ = 0.5 (Green) and $\left(P_{em}\right)$ = 0.7 (Blue).

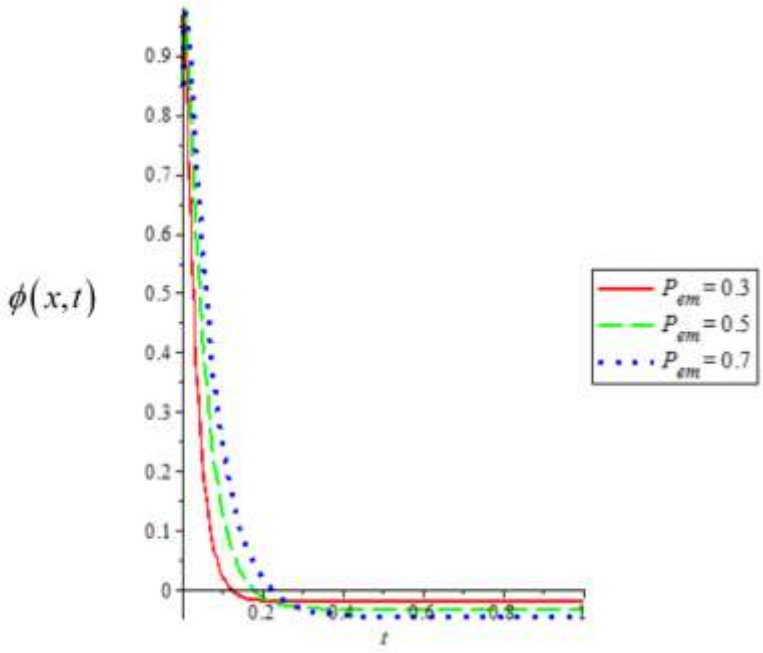

Figure 4.32: Graph of oxygen concentration $\phi\left(x\,,\,t\right)$ against time t for different values of Peclet mass number $\left(P_{em}\right)$. $\left(P_{em}\right)$ = 0.3 (Red), $\left(P_{em}\right)$ = 0.5 (Green) and $\left(P_{em}\right)$ = 0.7 (Blue).

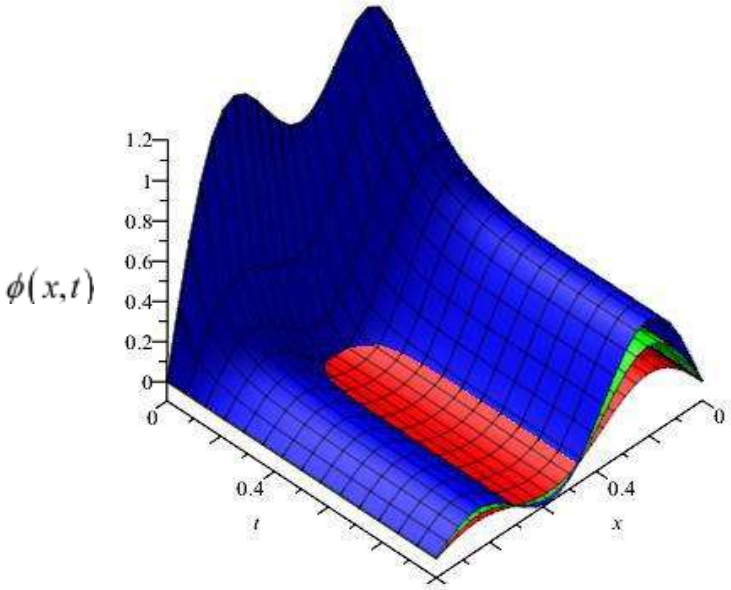

Figure 4.33: Graph of oxygen concentration $\phi(x,t)$ against distance x and time t for different values of Peclet mass number (P_{em}). $(P_{em}) = 0.3$ (Red), $(P_{em}) = 0.5$ (Green) and $(P_{em}) = 0.7$ (Blue).

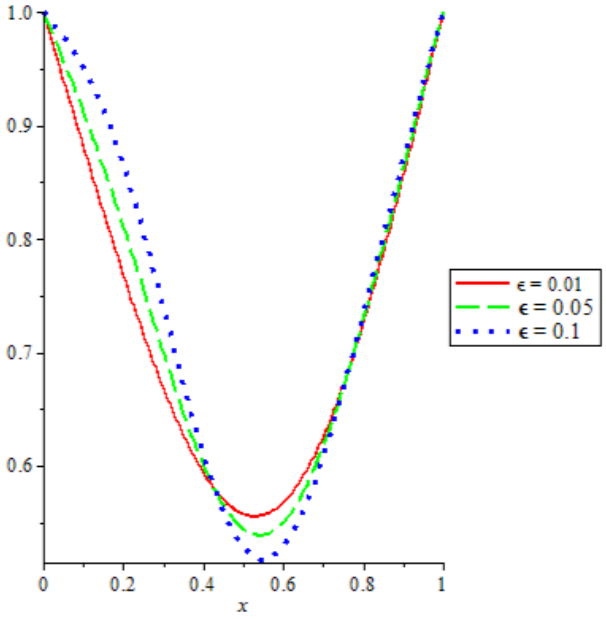

Figure 4.34: Graph of temperature $\theta(x, t)$ against distance x for different values of dimensionless activation energy number $(\in)$. $(\in) = 0.01$ (Red), $(\in) = 0.05$ (Green) and $(\in) = 0.1$ (Blue).

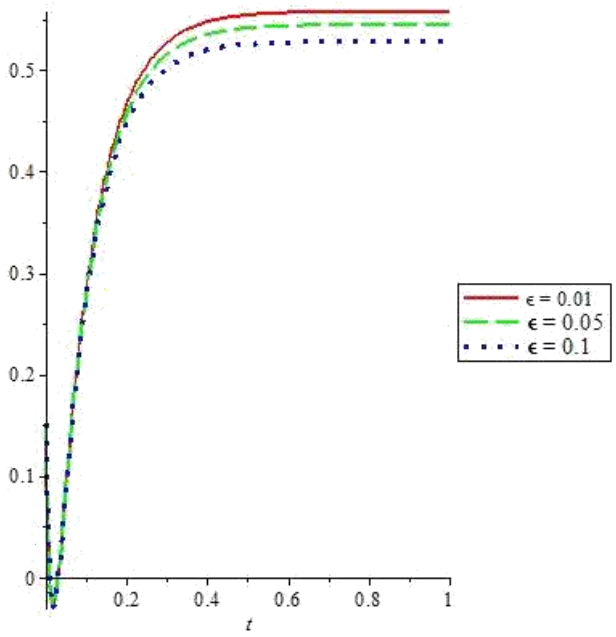

Figure 4.35: Graph of temperature $\theta(x, t)$ against time t for different values of dimensionless activation energy number $(\in)$. $(\in) = 0.01$ (Red), $(\in) = 0.05$ (Green) and $(\in) = 0.1$ (Blue).

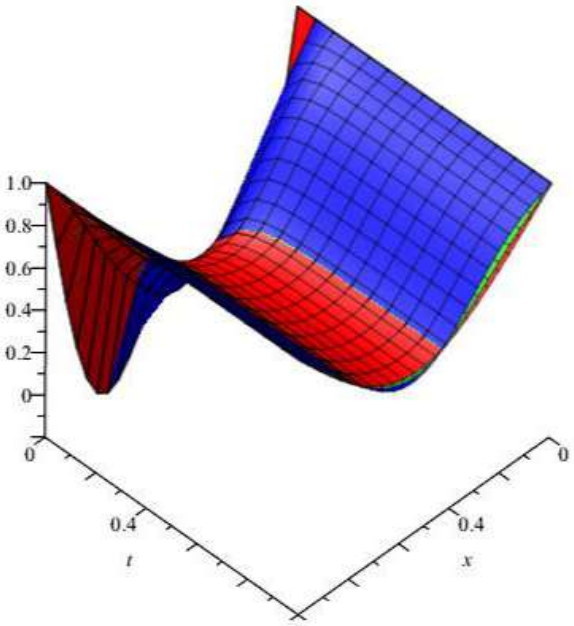

Figure 4.36: Graph of temperature $\theta(x, t)$ against distance x and time t for different values of dimensionless activation energy number ($\in$). $\in = 0.01$ (Red), $\in = 0.05$ (Green) and $\in = 0.1$ (Blue).

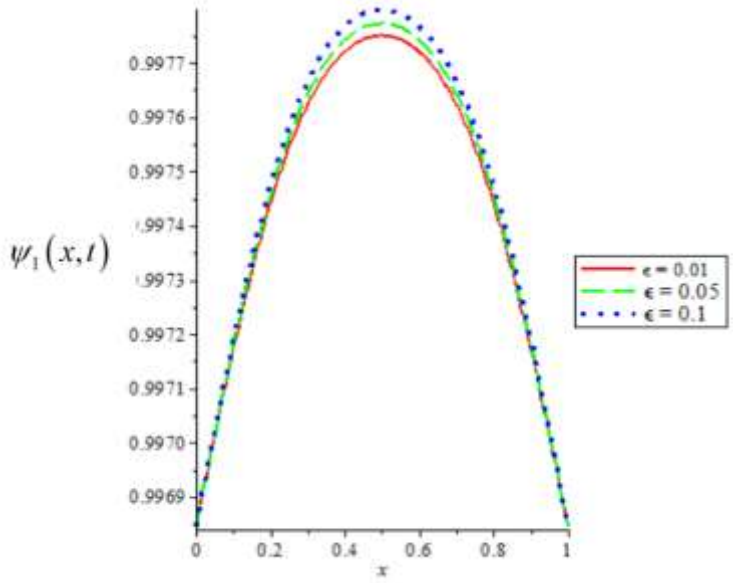

Figure 4.37: Graph of volume fraction of dry organic substance $\psi_1(x, t)$ against distance x for different values of dimensionless activation energy number $(\in)$. $(\in) = 0.01$ (Red), $(\in) = 0.05$ (Green) and $(\in) = 0.1$ (Blue).

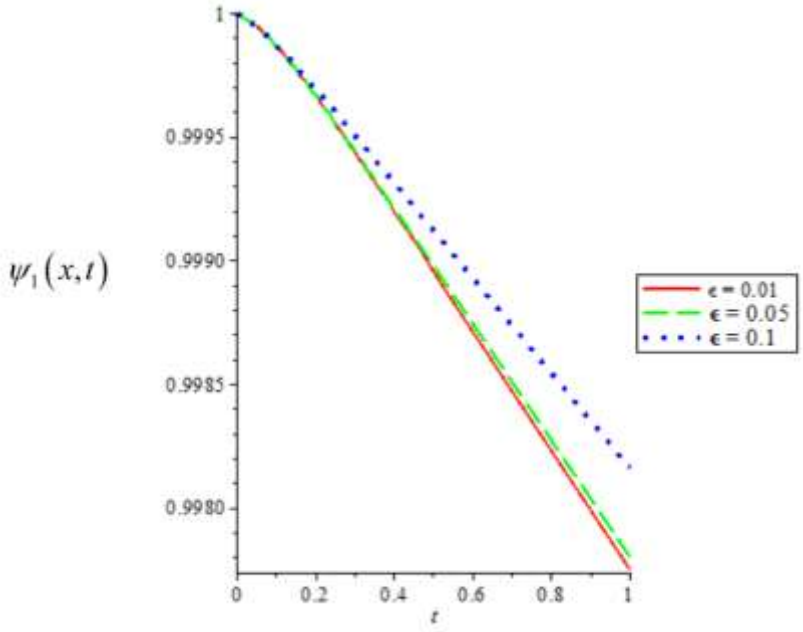

Figure 4.38: Graph of volume fraction of dry organic substance $\psi_1(x,$ against time t for $t)$ different values of dimensionless activation energy number $(\in)$. $(\in) = 0.01$ (Red), $(\in) = 0.05$ (Green) and $(\in) = 0.1$ (Blue).

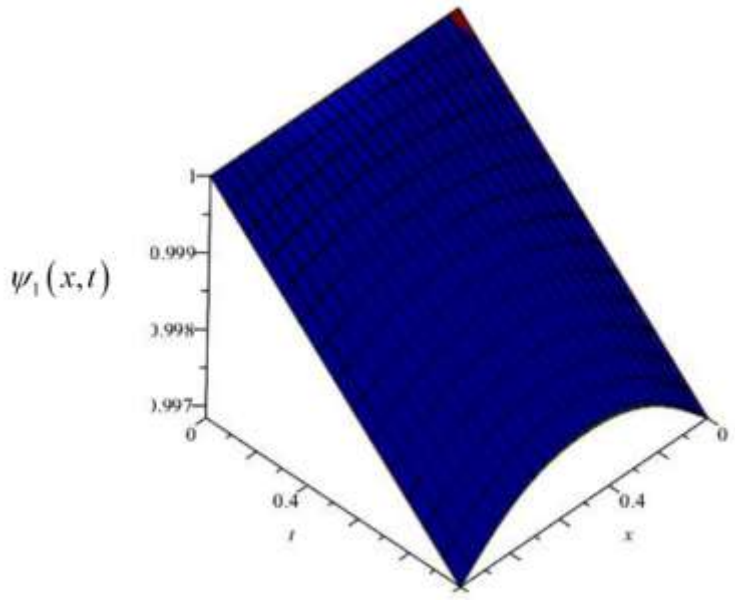

Figure 4.39: Graph of volume fraction of dry organic substance $\psi_1(x, t)$ against distance x and time t for different values of dimensionless activation energy number $(\in)$.
$(\in) = 0.01$ (Red), $(\in) = 0.05$ (Green) and $(\in) = 0.1$ (Blue).

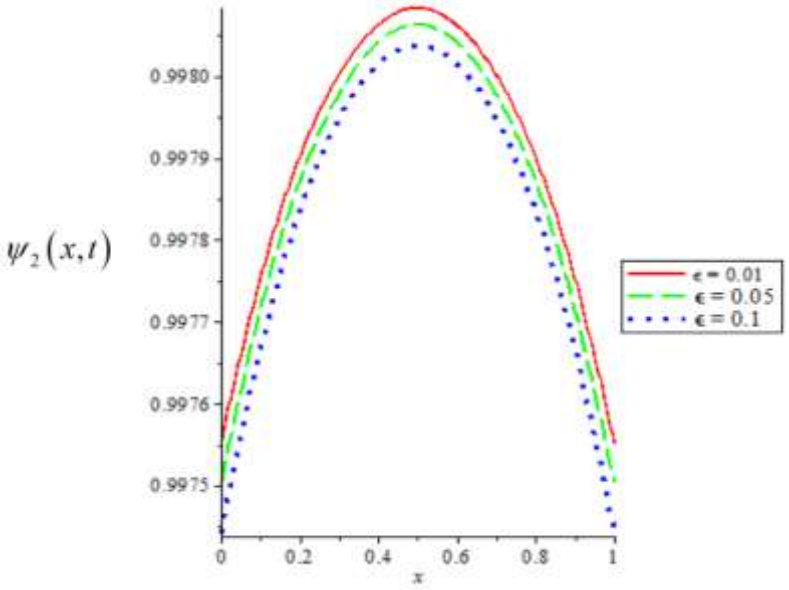

Figure 4.40: Graph of volume fraction of moisture $\psi_2(x, t)$ against distance x for different values of dimensionless activation energy number ($\in$). ( ) $\in = 0.01$ (Red), $(\in) = 0.05$ (Green) and $(\in) = 0.1$ (Blue).

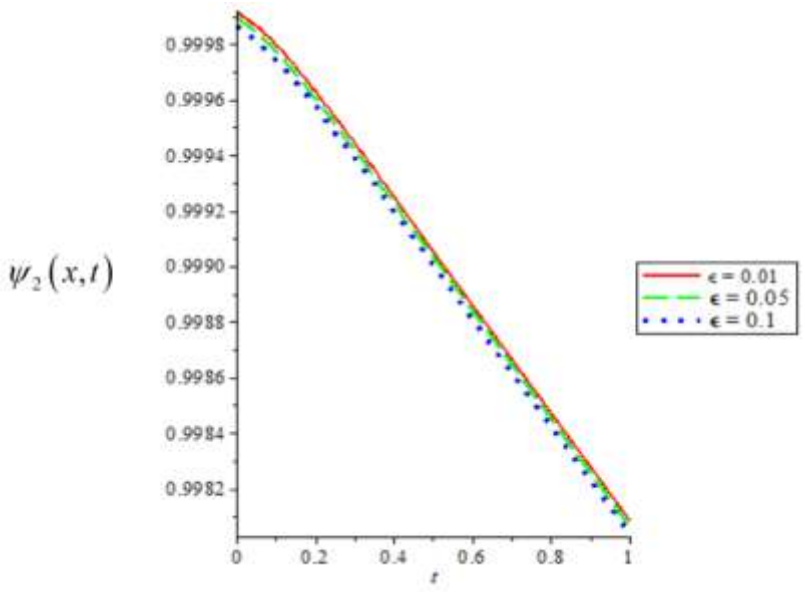

Figure 4.41: Graph of volume fraction of moisture $\psi_2(x, t)$ against time t for different values of dimensionless activation energy number ($\in$). $(\in) = 0.01$ (Red), $\in = 0.05$ (Green) and $\in = 0.1$ (Blue).

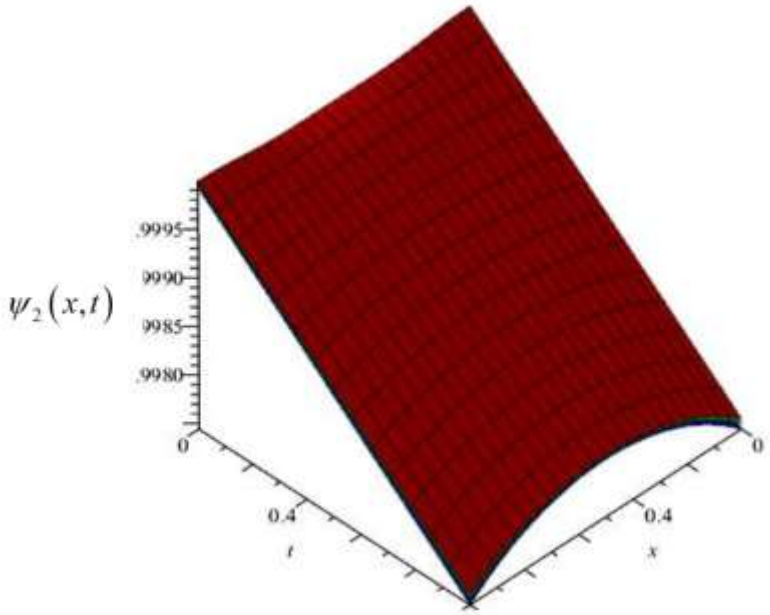

Figure 4.42: Graph of volume fraction of moisture $\psi_2(x, t)$ against distance x and time t for different values of dimensionless activation energy number $(\in)$. $(\in) = 0.01$ (Red), $(\in) = 0.05$ (Green) and $(\in) = 0.1$ (Blue).

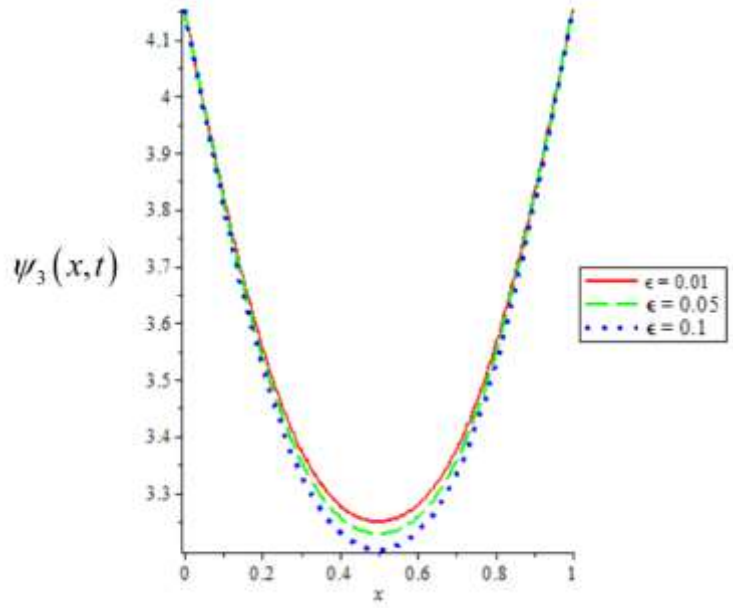

Figure 4.43: Graph of volume fraction of coke $\psi_3(x, t)$ against distance x for different values of dimensionless activation energy number ($\in$). $(\in) = 0.01$ (Red), $\in = 0.05$ (Green) and $\in = 0.1$ (Blue).

( ) ( )

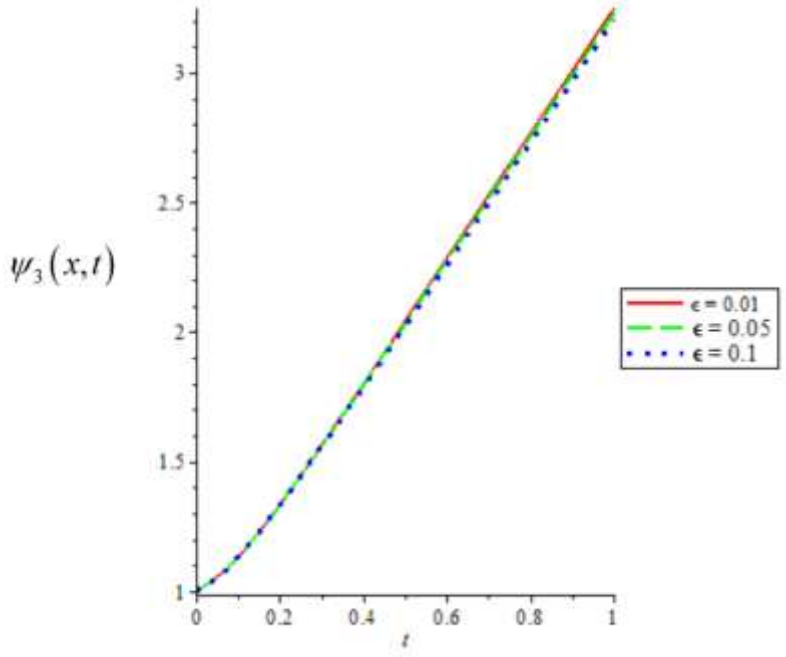

Figure 4.44: Graph of volume fraction of coke $\psi_3(x, t)$ against time t for different values of dimensionless activation energy number ( ). $\in$ ( ) $\in = 0.01$ (Red), $(\in) = 0.05$ (Green) and $(\in) = 0.1$ (Blue).

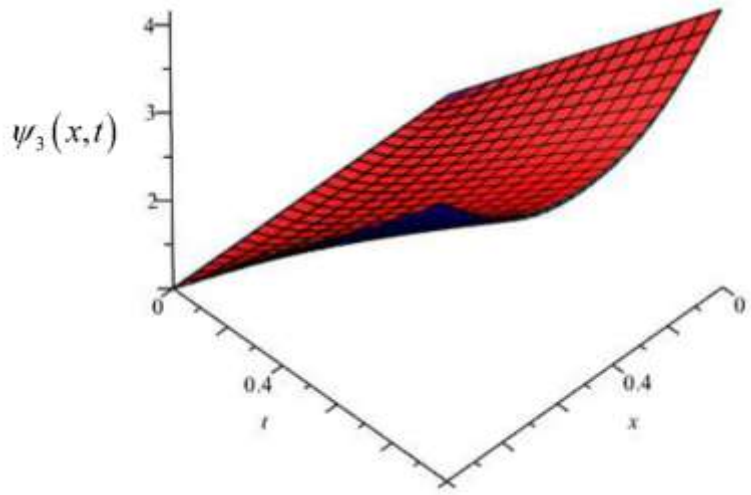

Figure 4.45: Graph of volume fraction of coke $\psi_3\,(x\,,\,t\,)$ against distance x time t for $\in$ $\in$ = 0.01 (Red), different values of dimensionless activation energy number ( ). $\in$ = 0.05 (Green) and $\in$ = 0.1 (Blue).

( ) ( )

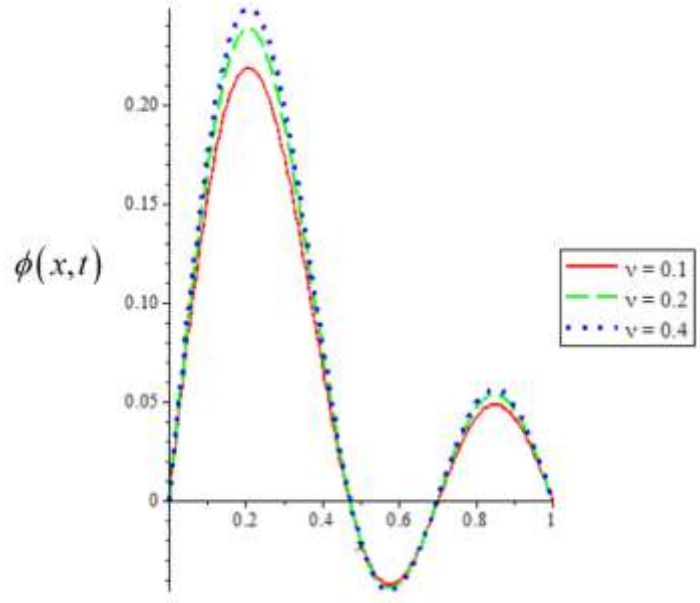

Figure 4.46: Graph of oxygen concentration $\phi\,(x\,,\,t\,)$ against distance x for different values of equilibrium wind velocity $(v\,)$. (v) = 0.1 (Red), (v) = 0.2 (Green) and (v) = 0.4 (Blue).

4.2 Discussion of the Results

Figure 4.1 depicts the graph of temperature $\theta(x, t)$ against distance x for different values of Frank-Kamenetskii number (δ). It is observed that the temperature decreases but later increases along the distance and the minimum temperature decreases as Frank-Kamenetskii number increases.

Figure 4.2 shows the graph of temperature $\theta(x, t)$ against time t for different values of Frank-Kamenetskii number (δ). It is observed that the temperature decreases and later increases and becomes steady with time but decreases as the Frank-Kamenetskii number increases.

Figure 4.3 displays the graph of temperature $\theta(x, t)$ against distance x and time t for different values of Frank-Kamenetskii number (δ). It is observed that the temperature decreases but later increases along the distance. It decreases and later increases and becomes steady with time while it decreases as the Frank-Kamenetskii number increases.

Figure 4.4 depicts the graph of temperature $\theta(x, t)$ against distance x for different values of Radiation number (R_a). It is observed that the temperature decreases but later increases along the distance and the minimum temperature decreases as Radiation number increases.

Figure 4.5 shows the graph of temperature $\theta(x, t)$ against time t for different values of Radiation number (R_a). It is observed that the temperature decreases and later increases and becomes steady with time but decreases as the Radiation number increases.

Figure 4.6 displays the graph of temperature $\theta(x, t)$ against distance x and time t for different values of Radiation number (R_a). It is observed that the temperature decreases but later increases along the distance. It decreases and later increases and becomes steady with time while it decreases as the Radiation number increases.

Figure 4.7 depicts the graph of oxygen concentration $\phi(x, t)$ against distance x for different values of Radiation number (R_a). It is observed that the oxygen concentration oscillates along the distance and maximum concentration decreases as the Radiation number increases.

Figure 4.8 displays the graph of oxygen concentration $\phi(x, t)$ against distance x and time

t for different values of Radiation number (R_a). It is observed that the oxygen concentration oscillates along the distance and does not change with time but the maximum concentration decreases as the Radiation number increases.

Figure 4.9 depicts the graph of volume fraction of dry organic substance $\psi_1(x, t)$ against distance x for different values of Radiation number (R_a). It is observed that the volume fraction of dry organic substance increases but later decreases along the distance and maximum volume fraction of dry organic substance increases as the Radiation number increases.

Figure 4.10 displays the graph of volume fraction of dry organic substance $\psi_1(x, t)$ against time t for different values of Radiation number (R_a). It is observed that the volume

fraction of dry organic substance decreases with time and increases as the Radiation number increases.

Figure 4.11 depicts the graph of volume fraction of dry organic substance $\psi_1(x, t)$ against distance x and time t for different values of Radiation number (R_a). It is observed that the volume fraction of dry organic substance increases but later decreases along the distance. It decreases with time and increases as the Radiation number increases.

Figure 4.12 displays the graph of volume fraction of moisture $\psi_2(x, t)$ against distance x for different values of Radiation number (R_a). It is observed that the volume fraction of moisture increases but later decreases along the distance and maximum volume fraction of moisture increases as the Radiation number increases.

Figure 4.13 depicts the graph of volume fraction of moisture $\psi_2(x, t)$ against time t for different values of Radiation number (R_a). It is observed that the volume fraction of moisture decreases with time and increases as the Radiation number increases.

Figure 4.14 displays the graph of volume fraction of moisture $\psi_2(x, t)$ against distance x and time t for different values of Radiation number (R_a). It is observed that the volume fraction of moisture increases but later decreases along the distance. It decreases with time and increases as the Radiation number increases.

Figure 4.15 depicts the graph of volume fraction of coke $\psi_3(x, t)$ against distance x for different values of Radiation number (R_a). It is observed that the volume fraction of coke

decreases but later increases along the distance and decreases as Radiation number increases.

Figure 4.16 displays the graph of volume fraction of coke $\psi_3(x, t)$ against time t for different values of Radiation number (R_a). It is observed that the of volume fraction of coke increases with time and decreases as the Radiation number increases.

Figure 4.17 depicts the graph of volume fraction of coke $\psi_3(x, t)$ against distance x and time t for different values of Radiation number (R_a). It is observed that the volume fraction of coke decreases but later increases along the distance. It increases with time and decreases as the Radiation number increases.

Figure 4.18 depicts the graph of temperature $\theta(x, t)$ against distance x for different values of Peclet energy number (P_e). It is observed that the temperature decreases but later increases along the distance and the minimum temperature decreases as Peclet energy number increases.

Figure 4.19 shows the graph of temperature $\theta(x, t)$ against time t for different values of Peclet energy number (P_e). It is observed that the temperature decreases and later increases and becomes steady with time but decreases as the Peclet energy number increases.

Figure 4.20 displays the graph of temperature $\theta(x, t)$ against distance x and time t for different values of Peclet energy number (P_e). It is observed that the temperature

decreases but later increases along the distance. It decreases and later increases and becomes steady with time while it decreases as the Peclet energy number increases.

Figure 4.21 depicts the graph of oxygen concentration $\phi(x,t)$ against distance x for different values of Peclet energy number (P_e). It is observed that the oxygen concentration oscillates along the distance and maximum concentration decreases as the Peclet energy number increases.

Figure 4.22 displays the graph of volume fraction of dry organic substance $\psi_1(x,t)$ against distance x for different values of Peclet energy number (P_e). It is observed that the volume fraction of dry organic substance increases but later decreases along the distance and maximum volume fraction of dry organic substance increases as the Peclet energy number increases.

Figure 4.23 depicts the graph of volume fraction of dry organic substance $\psi_1(x,t)$ against time t for different values of Peclet energy number (P_e). It is observed that the volume fraction of dry organic substance decreases with time and increases as Peclet energy number increases.

Figure 4.24 displays the graph of volume fraction of dry organic substance $\psi_1(x,t)$ against distance x and time t for different values of Peclet energy number (P_e). It is observed that the volume fraction of dry organic substance increases but later decreases along the distance. It decreases with time and increases as the Peclet energy number increases.

Figure 4.25 depicts the graph of volume fraction of moisture $\psi_2(x, t)$ against distance x for different values of Peclet energy number (P_e). It is observed that the volume fraction of moisture increases but later decreases along the distance and maximum volume fraction of moisture increases as the of Peclet energy number increases.

Figure 4.26 depicts the graph of volume fraction of moisture $\psi_2(x, t)$ against time t for different values of Peclet energy number (P_e). It is observed that the of volume fraction of moisture decreases with time and increases as the Peclet energy number increases.

Figure 4.27 displays the graph of volume fraction of moisture $\psi_2(x, t)$ against distance x and time t for different values of Peclet energy number (P_e). It is observed that the of volume fraction of moisture increases but later decreases along the distance. It decreases with time and increases as the Peclet energy number increases.

Figure 4.28 depicts the graph of volume fraction of coke $\psi_3(x, t)$ against distance x for different values of Peclet energy number (P_e). It is observed that the volume fraction of coke decreases but later increases along the distance and decreases as Peclet energy number increases.

Figure 4.29 displays the graph of volume fraction of coke $\psi_3(x, t)$ against time t for different values of Peclet energy number (P_e). It is observed that the of volume fraction of coke increases with time and decreases as the Peclet energy number increases.

Figure 4.30 depicts the graph of volume fraction of coke $\psi_3(x, t)$ against distance x and time t for different values of Peclet energy number (P_e). It is observed that the volume fraction of coke decreases but later increases along the distance. It increases with time and decreases as the Peclet energy number increases.

Figure 4.31 depicts the graph of oxygen concentration $\phi(x, t)$ against distance x for different values of Peclet mass number (P_{em}). It is observed that the oxygen concentration oscillates along the distance and maximum concentration increases as the Peclet mass number increases.

Figure 4.32 shows the graph of oxygen concentration $\phi(x, t)$ against time t for different values of Peclet mass number (P_{em}). It is observed that the oxygen concentration decreases but later becomes steady with time and decreases as the Peclet mass number increases. Figure 4.33 displays the graph of oxygen concentration $\phi(x, t)$ against distance x and time t for different values of Peclet mass number (P_{em}). It is observed that the oxygen concentration oscillates along the distance and decreases but later becomes steady with time and increases as the Peclet mass number increases.

Figure 4.34 depicts the graph of temperature $\theta(x, t)$ against distance x for different values of dimensionless activation energy number $(\in)$. It is observed that the temperature decreases but later increases along the distance and the minimum temperature decreases as dimensionless activation energy number increases.

Figure 4.35 displays the graph of temperature $\theta(x, t)$ against time t for different values of dimensionless activation energy number $(\in)$. It is observed that the temperature decreases and later increases and becomes steady with time but decreases as the dimensionless activation energy number increases.

Figure 4.36 displays the graph of temperature $\theta(x, t)$ against distance x and time t for different values of dimensionless activation energy number $(\in)$. It is observed that the temperature decreases but later increases along the distance. It decreases and later increases and becomes steady with time while it decreases as the dimensionless activation energy number increases.

Figure 4.37 depicts the graph of volume fraction of dry organic substance $\psi_1(x, t)$ against distance x for different values of dimensionless activation energy number $(\in)$. It is observed that the volume fraction of dry organic substance increases but later decreases along the distance and maximum volume fraction of dry organic substance increases as the dimensionless activation energy number increases.

Figure 4.38 depicts the graph of volume fraction of dry organic substance $\psi_1(x, t)$ against time t for different values of dimensionless activation energy number $(\in)$. It is observed that the volume fraction of dry organic substance decreases with time and increases as the dimensionless activation energy number increases.

Figure 4.39 displays the graph of volume fraction of dry organic substance $\psi_1(x, t)$ against distance x and time t for different values of dimensionless activation energy

number $(\in)$. It is observed that the volume fraction of dry organic substance increases but later decreases along the distance. It decreases with time and increases as the dimensionless activation energy number increases.

Figure 4.40 depicts the graph of volume fraction of moisture $\psi_2(x, t)$ against distance x for different values of dimensionless activation energy number $(\in)$. It is observed that the volume fraction of moisture increases but later decreases along the distance and decreases as dimensionless activation energy number increases.

Figure 4.41 displays the graph of volume fraction of moisture $\psi_2(x, t)$against time t for different values of dimensionless activation energy number $(\in)$. It is observed that the volume fraction of moisture decreases with time and decreases as the dimensionless activation energy number increases.

Figure 4.42 depicts the graph of volume fraction of moisture $\psi_2(x, t)$against distance x and time t for different values of dimensionless activation energy number $(\in)$. It is observed that the volume fraction of moisture increases but later decreases along the distance. It decreases with time and decreases as the dimensionless activation energy number increases.

Figure 4.43 depicts the graph of volume fraction of coke $\psi_3(x, t)$ against distance x for different values of dimensionless activation energy number $(\in)$. It is observed that the volume fraction of coke decreases but later increases along the distance and decreases as the dimensionless activation energy number increases.

Figure 4.44 displays the graph of volume fraction of coke $\psi_3(x, t)$ against time t for different values of dimensionless activation energy number $(\in)$. It is observed that the volume fraction of coke increases with time and decreases as the dimensionless activation energy number increases.

Figure 4.45 depicts the graph of volume fraction of coke $\psi_3(x, t)$ against distance x and time t for different values of dimensionless activation energy number $(\in)$. It is observed that the volume fraction of coke decreases but later increases along the distance. It increases with time and decreases as the dimensionless activation energy number increases.

Figure 4.46 depicts the graph of oxygen concentration $\phi(x, t)$ against distance x for different values of equilibrium wind velocity (v). It is observed that the oxygen concentration oscillates along the distance and maximum concentration increases as the equilibrium wind velocity increases.

CHAPTER FIVE

5.0 CONCLUSION AND RECOMENDATION

5.1 Conclusion

For a high activation energy situation (i.e. as $\in \to 0$), we have solved the equations governing fire spread in a real-time coupled atmospheric-Wildland fire using direct integration and eigenfunction expansion technique. The effects of the dimensionless parameters as shown on the graph were analyzed. From the result obtained, we can conclude that:

(i) Frank-Kamenetskii number reduces the transient temperature.

(ii) Radiation number reduces the transient temperature, oxygen concentration and volume fraction of coke while it enhances volume fractions of dry organic substance and moisture.

(iii) Peclet energy number reduces the transient temperature, oxygen concentration and volume fraction of coke while it enhances volume fractions of dry organic substance and moisture.

(iv) Peclet mass number enhances the oxygen concentration.

(v) Activation energy number reduces the transient temperature and volume fraction of coke while it enhances volume fractions of organic substance and moisture.

(vi) Equilibrium wind velocity enhances the oxygen concentration.

5.2 Contribution to Knowledge

In this study, the following contributions were made to knowledge:

(i) The thesis established that the Radiation number, R_a , enhances the volume fractions of dry organic substance and moisture while it reduces the temperature, oxygen concentration and volume fraction of coke. The volume fractions of dry organic substance and moisture are at maximum value $\left(\psi_1(x,t) = \psi_2(x,t) \approx 1\right)$ when $x = 0.5$

while the temperature and volume fraction of coke are at minimum value $\left(\theta(x,t) = \psi_3(x,t) \approx 0.0001\right)$ when $x = 0.5$

(ii) The present extends the work of Perminov (2018) by incorporating diffussion term in fire spread process.

(iii) Wildland fire model is solved analytically using eigenfunction expansion technique.

5.3 Recommendations

Further work can be carried out on wildland fire model using other analytical methods to ascertain how best the results can be obtained.

REFERENCES

Albini, F. A. & Reinhardt, E. D. (1985). Modeling ignition and burning rate of large woody natural fuels. *International Journal of Wildland Fire,* 5(2), *81–91.*

Albini, F. A. (1996). Iterative solution of the radiation transport equations governing spread of fire in wildland fuel. *Fizika Goreniya I Zvryva, 32(5): 71–82.*

Andrews, P. L. (2007). BehavePlus fire modeling system: past, present, and future, Paper J2.1, 7th Symposium on Fire and Forest Meteorology, http://ams.confex.com /ams/pdfpapers/126669.pdf.

Anne, G., Andrea, C., Marielle, J., Jesus, S. M. A., Marlene, L., & Corinne, L. (2012). A review of the main driving factors of forest fires ignition over europe. environmental management. *International Journal of Wildland Fire,* 9(4): 841–850.

Ayeni, R. O. (1978). Thermal Runaway.- Ph. D Thesis Cornell Unversity USA.

Barovik, D. & Taranchuk V. (2010). Mathematical modelling of running crown forest fires. *Mathematical Modelling and Analysis,* 15(2), 161–174.

Beer, T. (1990). The australian national bushfire model project. *Mathematical and Computer Modelling,* 13(12), 49–56.

Carlos, B. S. (2014). A comprehensive methodology to predict forest fires behavior using complementary models. PhD thesis, Universitat Autonoma de Barcelona.

Clark, T. L., Coen, J. & Latham, D. (2004). Description of a coupled atmosphere-fire model. *International Journal of Wildland Fire,* 13, 49–64.

Clark, T. L., Jenkins, M. A., Coen, J. L. & Packham, D. R. (1996b). A coupled atmosphere-fire model:24 role of the convective froude number and dynamic fingering at the fireline. *International Journal of Wildland Fire,* 6, 177–190.

Clark, T. L., Jenkins, M. A., Coen, J. & Packham, D. (1996a). A coupled atmospheric-fire model: convective feedback on fire line dynamics. *Journal of Applied Meteorology*, 35, 875–901.

Cruz, M. G., Alexander, M. E. & Wakemoto, R. H. (2002). Predicting crown fire behaviour to support forest fire management decision-making, Proceedings of the IV International conference on forest fire research, Luso-Coimbra, Portugal. (Ed. D. X. Viegas), 11.

Golner, M. J., Miller, C. H., Wei T. & Singh A.V. (2017). The effect of flow and geometry on concurrent flame spread. *Fire Safety Journal*, 91, 68–78.

Grishin, A. M. (1994). Forest Fire Physics. Publishing House of TSU: Tomsk, Russia.

Grishin, A. M. (1997). Mathematical modeling of forest fires and new methods of fighting them. Publishing House of Tomsk State University, Tomsk, Russia, English Translation Edition.

Grishin, A. M. (2002). General mathematical models of forest and peat fires and their applications. *Successes of Mechanics,* 3(4), 41–89.

Grishin, A. M. & Perminov, V. A. (1998). Mathematical modeling of the ignition of tree crowns, combustion, *Explosion and Shock Waves,* 34, *378–386.*

Konev, E. V. (1977). The physical foundation of vegetative materials combustion, Nauka, Novosibirsk, USSR.

Linn, R., Reisner, J., Colman, J. & Winterkamp, J. (2002). Studying wildfire behavior using FIRETEC. *International Journal of Wildland Fire,* 11(1), 233–246.

Lopes, A. M. G., Ribeiro, Viegas, D. X. & Raposo, J. R. (2017). Effect of two-way coupling on the calculation of forest fire spread: model development. *International Journal of Wildland Fire,* 2(6), 829–843.

Mandel, J., Beezley, J. D., Coen, J. L. & Kim, M. (2009). Data assimilation for wildland fires: ensemble kalman filters in coupled atmosphere-surface models. *IEEE Control Systems Magazine,* 29, 47–65.

Mandel, J., Jonathan, D. B. & Adam, K. K. (2018). Coupled Atmosphere-Wildland Fire Modelling with WRF-Fire Version 3.3.

Mandel, J., Bennethum, L. S., Beezley, J. D., Coen, J. L., Douglas, G. C., Kim, M. & Vodacek, A. (2008). A Wildland Fire Model with Data Assimilation. Perprint submitted to Elsevier.

Mell, W., Jenkins, M. A., Gould, J. & Cheney, P. (2007). A physics based approach to modeling grassland fires. *International Journal of Wildland Fire* 16, 1–22.

Mickler, R. A., Welch, D. P. & Bailey, A. D. (2017). Carbon emissions during wildland fire on a north american temperate peatland. *Fire Ecology*, 13, 34–57.

Miphokasap, P. (2017). Spatial Inventory of CO_2 Emissions and removals from land use and land use changes in thailand. *Chemical Engineering Transactions,* 56, 13–18.

Morvan, D. & Dupuy, J. L. (2004). Modelling the propagation of wildfire through a mediterranean shrub using a multiphase formulation, *Combustion and Flame,* 138, 199–210.

Myint-U, T. & Debanth, L. (1987). Partial Differential Equation for Scientists and Engineers. PTR Parentice-Hall Englewood cliffs New Jersey. 5 -14.

Pastor, E., Zarate, L., Planas, E. & Arnaldos, J. (2003). Mathematical models and calculation systems for the study of wildland fire behaviour. *Progress in Energy and Combustion Science*, 29(2), 139–153.

Perminov, V. (2005). Mathematical model of forest fire initiation and spread. Informatics for Environmental Protection - Networking Environmental Information Copyright © Masaryk University Brno. ISBN: 80-210-3780-6.

Perminov, V. A. (2018). Mathematical modelling of wildland fires initiation and spread using a coupled atmospheric-forest fire setting. *The Italian Association of Chemical Engineering*, 70, 1747-1752.

Rothermal, R. C. (1991). Predicting Behaviour and Size of Crown Fires in the Northern Rocky Mountains. In: Res. Pap. INT-438. US Department of Agriculture, Forest Service, Intermountain Forest and Range Experiment Station, 46p, Ogden, UT, United States, DOI: 10.2737/INT-RP-438.

Rothermel, R. C. (1972). A Mathematical Model for Predicting Fire Spread in Wildland Fires, USDA Forest Service Research Paper INT-115, http://www. treesearch.fs.fed.us/pubs/32533.

Scott, A. C. & Glasspool, I. J. (2006). The diversification of paleozoic fire systems and fluctuations in atmospheric oxygen concentration. *Proceedings of National Academy of Sciences*, 103(29), 10861-10865.

Se´ro-Guillaume, O. & Margerit, J. (2002). Modelling forest fires. Part I: a complete set of equations derived by extended irreversible thermodynamics. *International Journal of Heat and Mass Transfer*, 45, 1705–1722.

Skamarock, W. C., Klemp, J. B., Dudhia, J., Gill, D. O., Barker, D. M., Duda, M. G., Huang, X. Y., Wang, W. & Powers, J. G. (2008). A Description of the Advanced Research WRF Version 3, NCAR Technical Note 475, http://www.mmm.ucar.edu/ wrf/users/docs/arw v3.pdf.

Song, J., Huang, X., Liu, N., Li, H. & Zhang, L. (2017). The wind effect on the transport and burning of firebrands, *Fire Technology*, 5(3), 1555-1568.

Sullivan, A. (2007a). A review of wildland fire spread modelling, 1990-present, physical land quasi-physical models. *International Journal of Wildland Fire*, 10(3), 49–60.

Sullivan, A. L. (2009a). Wildland surface fire spread modelling, 1990–2007. physical and quasi-physical models. *International Journal of Wildland Fire*, 18(4), 349–368.

Sullivan, A. L. (2009b). Wildland surface fire spread modelling, 1990–2007. 3. simulation and mathematical analogue models. *International Journal of Wildland Fire*, 18(4), 387–403.

Sullivan, A. L. (2009c). Wildland surface fire spread modelling, 1990–2007. empirical and quasi-empirical models. *International Journal of Wildland Fire*, 18(2), 369–386.

Surawski, N. S., Sullivan, A. L., Meyer, C. P., Roxburgh, S. H. & Polglase, P. J. (2015). Greenhouse gas emissions from laboratory-scale fires in wildland fuels depend on fire spread mode and phase of combustion. *Atmospheric Chemistry and Physics*, 15, 5259–5273.

Van Wagner, C. E. (1977). Conditions for the start and spread of crown fire. *Canadian Journal of Forest Research*, 7(3), 23–34.

Weber, R. (1991). Modelling fire spread through fuel beds. *Progress in Energy Combustion Science*, 17(1), 67–82.